

DESIGN AND IMPLEMENTATION OF A VHF/UHF FRONT-END USING TUNABLE
DUAL BAND FILTERS

A THESIS SUBMITTED TO
THE GRADUATE SCHOOL OF NATURAL AND APPLIED SCIENCES
OF
MIDDLE EAST TECHNICAL UNIVERSITY

BY

FATİH ALACA

IN PARTIAL FULFILLMENT OF THE REQUIREMENTS
FOR
THE DEGREE OF MASTER OF SCIENCE
IN
ELECTRICAL AND ELECTRONICS ENGINEERING

JUNE 2012

Approval of the thesis:

**DESIGN AND IMPLEMENTATION OF A VHF/UHF FRONT-END USING TUNABLE
DUAL BAND FILTERS**

submitted by **FATİH ALACA** in partial fulfillment of the requirements for the degree of
**Master of Science in Electrical and Electronics Engineering Department, Middle East
Technical University** by,

Prof. Dr. Canan Özgen _____
Dean, Graduate School of **Natural and Applied Sciences**

Prof. Dr. İsmet Erkmen _____
Head of Department, **Electrical and Electronics Engineering**

Prof. Dr. Nevzat Yıldırım _____
Supervisor, **Electrical and Electronics Engineering Dept., METU**

Examining Committee Members:

Prof. Dr. Canan Toker _____
Electrical and Electronics Engineering Dept., METU

Prof. Dr. Nevzat Yıldırım _____
Electrical and Electronics Engineering Dept., METU

Prof. Dr. Sencer Koç _____
Electrical and Electronics Engineering Dept., METU

Assoc. Prof. Dr. Şimşek Demir _____
Electrical and Electronics Engineering Dept., METU

Gökhun Selçuk, M.Sc. _____
Senior Specialist Design Engineer, ASELSAN

Date: _____

I hereby declare that all information in this document has been obtained and presented in accordance with academic rules and ethical conduct. I also declare that, as required by these rules and conduct, I have fully cited and referenced all material and results that are not original to this work.

Name, Last Name: FATİH ALACA

Signature :

ABSTRACT

DESIGN AND IMPLEMENTATION OF A VHF/UHF FRONT-END USING TUNABLE DUAL BAND FILTERS

Alaca, Fatih

M.Sc., Department of Electrical and Electronics Engineering

Supervisor : Prof. Dr. Nevzat Yıldırım

June 2012, 89 pages

For the new generation wireless communication systems, there is an increasing demand for devices that covers more than one frequency band. This results in a need for wide-band tunable front-ends. The main objective of this study is to use dual band filters in the design of a multi-band front-end. A wide-band low noise amplifier is also required. To accomplish this project, a fixed frequency bandstop filter, a tunable dual-band filter and a wide-band LNA are designed and implemented successfully. The predefined specifications of this front-end include gain, gain flatness, spurious signal rejection, frequency tuning range, noise figure and linearity. Total power dissipation and number of elements are also taken into consideration. Test results of the manufactured front-end are compared with the results of existing single band front-ends.

In order to design a good tunable wide-band filter, just tuning its center frequency will not be enough. The noise figure of this dual-band filter will be proportional to its insertion loss if it will be used as a pre-selection filter in front of a LNA. Hence its insertion loss will affect the overall noise figure of the system. If it will be used after the LNA, its linearity will be more important. When a bandpass filter is tuned over wide range of frequencies,

its bandwidth varies significantly which leads to a degradation in rejection of the spurious signals. Therefore, there must be a simultaneous control of center frequency, bandwidth and insertion loss while providing enough linearity. In order to accomplish this mission, a filter that has two passbands is designed and implemented. The first passband is tunable between 136MHz and 174MHz while the second one is tunable between 380MHz and 470MHz. Also, the low noise amplifier works properly between 136MHz and 470MHz. As a result, a front-end that covers two bands is obtained.

Keywords: Dual band front-end, dual band lumped filter, tunable filter, wide-band low noise amplifier

ÖZ

AYARLANABİLİR ÇİFT BANTLI SÜZGEÇLER KULLANILARAK VHF/UHF ÖN-UÇ TASARIMI VE UYGULAMASI

Alaca, Fatih

Yüksek Lisans, Elektrik ve Elektronik Mühendisliği Bölümü

Tez Yöneticisi : Prof. Dr. Nevzat Yıldırım

Haziran 2012, 89 sayfa

Yeni nesil kablosuz iletişim sistemlerinde birden fazla frekans bandında çalışabilen cihazlara talep giderek artmaktadır. Bu durum, geniş bantlı, ayarlanabilir ön-uçlara ihtiyaç duyulmasına neden olmaktadır. Çok bantlı bir ön-uç tasarımında çift bantlı süzgeçlerin kullanımı bu tez çalışmasının ana içeriğini oluşturmaktadır. Aynı zamanda geniş bantlı bir düşük gürültülü yükselteci de ihtiyaç duyulmaktadır. Bu çalışmayı başarı ile tamamlayabilmek için sabit frekanslı geniş bantlı bir çentik süzgeç, ayarlanabilir çift bantlı bir filtre ve geniş bantlı bir düşük gürültülü yükselteç tasarlanarak üretilmiştir. Bu ön-ucun sağlanması gereken şartlar kazancı, kazanç düzgünlüğünü, istenmeyen işaret bastırmasını, frekans ayarlama aralığını, gürültü niteliğini ve doğrusallığı içermektedir. Bunlara ek olarak toplam güç tüketimi ve eleman sayısı da dikkate alınmıştır. Üretilen çift bantlı ön-ucun test sonuçları var olan tek bantlı ön-uçları ile karşılaştırılmıştır.

İyi bir ayarlanabilir geniş bantlı süzgeç tasarlayabilmek için sadece merkez frekansını ayarlamak yeterli olmayacaktır. Bu süzgecin gürültü niteliği kaybıyla orantılı olduğu için, bir DGYden önce ön-seçici olarak kullanılması durumunda süzgecin kaybı sistemin genel gürültü niteliğini etkileyecektir. Eğer bir DGYden sonra kullanılırsa da süzgecin doğrusallığı önemli

hale gelecektir. Bir bandgeçiren süzgeç geniş bir bantta ayarlandığı zaman bant genişliği önemli ölçüde değişir ve bu da istenmeyen sinyal bastırmasının bozulmasına neden olur. Bu nedenle, yeterli doğrusallık sağlanırken merkez frekansının, bant genişliğinin ve kaybın eş zamanlı kontrolü gerekir. Bunu başarabilmek için çift bantlı bir filtre tasarlanmıştır. Bu filtrenin ilk bandı 136MHz ve 174MHz arasında ayarlanabilirken ikinci bandı 380MHz ve 470MHz arasında ayarlanabilmektedir. Ayrıca düşük gürültülü, 136MHz ve 470MHz arasında uygun bir şekilde çalışan bir yükselteç tasarlanıp üretilmiştir. Sonuç olarak iki bantlı bir ön-uç başarıyla üretilmiştir.

Anahtar Kelimeler: Çift bantlı ön-uç, çift bantlı süzgeç, ayarlanabilir süzgeç, geniş bantlı düşük gürültülü yükselteç

To My Family

ACKNOWLEDGMENTS

It is my great pleasure to take this opportunity to express my gratitude and deep appreciation to my supervisor Prof. Dr. Nevzat Yıldırım for his guidance, support and valuable recommendations throughout my thesis work. I have benefited from his deep knowledge, constructive comments and suggestions throughout this project.

I am also grateful to Aselsan Electronics Industries Inc. for its support to my graduate study. I also would like to thank my colleagues in Aselsan for their understanding in my hard times.

Finally, I would like to express my deep appreciation to my family for their confidence and endless support which helped me to accomplish this work.

TABLE OF CONTENTS

ABSTRACT	iv
ÖZ	vi
ACKNOWLEDGMENTS	ix
TABLE OF CONTENTS	x
LIST OF TABLES	xiii
LIST OF FIGURES	xiv
CHAPTERS	
1 INTRODUCTION	1
2 BACKGROUND INFORMATION	5
2.1 Low Noise Amplifiers	5
2.2 IP3 Measurement	7
2.3 Classification of Filters	10
2.4 Common Filter Transfer Functions	11
2.4.1 Butterworth Filter	11
2.4.2 Chebyshev Filter	11
2.4.3 Elliptic Filter	12
2.5 Electrically Tunable Filters	12
2.6 Bridge-T Bandstop Filters	13
2.7 Pre-select and Image Reject Filters	15
3 DUAL BAND FILTERS	18
3.1 Introduction	18
3.2 Conversion of a Single Band Filter into a Dual Band Filter	19
3.3 Conversion of Normalized BP Prototype to Dual Band Filter	20
3.4 Analysis of Dual Band Filter Topology	22

4	VHF/UHF DUAL BAND FRONT END DESIGN AND IMPLEMENTATION	25
4.1	Design Constraints	25
4.2	Design of Dual Band Filters	27
4.2.1	Design With Filpro	29
4.2.2	Optimization With ADS	33
4.3	Harmonic Filters	40
4.4	Low Noise Amplifier	43
4.5	Simulation of Front-end	50
4.6	Implementation of Front-end	52
4.7	Test of Front-end	52
4.7.1	Test of Dual-Band Filters	54
4.7.2	Test of Harmonic Filters	55
4.7.3	Test of LNA	55
4.7.4	Test of Dual Band Front-end and Comparison with Single Band Front-ends	60
4.7.5	Performance of the Receiver System With Dual Band Front- end	64
5	DESIGN OF A TRIPLE BAND TUNABLE FILTER AND A WIDE-BAND LNA	70
5.1	Design Constraints	70
5.2	Design of Triple Band Filter	72
5.3	Design of LNA	76
6	CONCLUSION AND THE FUTURE WORK	79
6.1	Future Works	80
	REFERENCES	81
	APPENDICES	
A	LOWPASS PROTOTYPE TO BANDPASS TRANSFORMATION	84
B	MODELS USED IN SIMULATIONS	86
B.1	Model of JDV2S25FS Varactor Diode	86
B.2	Model of JDV2S08FS Varactor Diode	86
B.3	Model of JDV2S07S Varactor Diode	87

B.4	Model of 1SV325 Varactor Diode	88
B.5	Model of BFR340F Bipolar Junction Transistor	89

LIST OF TABLES

TABLES

Table 4.1	Basic Properties of VHF and UHF Receiver Systems	25
Table 4.2	IIP3 Performance of Dual Band Filter	55
Table 4.3	Noise Figure and IIP3 Performance of LNA	57
Table 4.4	Noise Figure and IIP3 Performance of Dual Band Front-end	61
Table 4.5	Performance of Receiver System With Dual Band Front-end	69
Table 5.1	Basic Properties of Triple Band Receiver System	71

LIST OF FIGURES

FIGURES

Figure 1.1	Block Diagram of a Superhetrodyne Receiver System	1
Figure 1.2	Block Diagram of Dual Band Front-end That Covers VHF and UHF Bands	2
Figure 2.1	Noise Figure of Cascaded Circuits	5
Figure 2.2	Measurement Setup for IP3	9
Figure 2.3	Graphical Explanation of IP3	9
Figure 2.4	Typical C-V Curve of a Varactor Diode	13
Figure 2.5	Phase Cancellation [16]	14
Figure 2.6	Bridged All Pass Filter Topology	14
Figure 2.7	Important Spurious Signals	15
Figure 3.1	Conversion of Second Order Resonators into Forth Order Resonators [22] .	19
Figure 3.2	Mapping Between Normalized Bandpass Prototype and Dual Band Filter [22]	21
Figure 3.3	A Simple Dual Band Filter Obtained From A Single Band Filter	22
Figure 3.4	Equivalent Circuits of Dual Band Filter for Each Region	23
Figure 4.1	Block Diagram of Two Parallel Single Band Front-ends	26
Figure 4.2	Block Diagram of Dual Band Front-end	26
Figure 4.3	Response of Fixed Pre-select Filter between 136 MHz and 174 MHz	27
Figure 4.4	Response of Tunable Image Reject Filter at 174 MHz	28
Figure 4.5	Response of UHF Pre-select Filter at 380 MHz	28
Figure 4.6	Response of UHF Image Reject Filter at 380 MHz	29
Figure 4.7	Design Procedure of Single Band Filter in Filpro	30

Figure 4.8 Dual Band Filter Obtained from the Single Band Filter	31
Figure 4.9 Dual Band Filter with Realistic Inductor Values	31
Figure 4.10 Response of Dual Band Filter	31
Figure 4.11 Element Values Required to Tune the Dual Band Filter to Low-ends and High-ends of the Bands	32
Figure 4.12 Response of Dual Band Filter at Low-ends and High-ends	33
Figure 4.13 Capacitor-Varactor Pair Used to Tune Capacitances at Resonators	33
Figure 4.14 Circuit Diagram of Dual Band Filter with Varactor Diodes	35
Figure 4.15 Simulation of Designed Dual Band Filter in ADS with Layout	36
Figure 4.16 Response of Dual Band Filter in ADS	36
Figure 4.17 Designed Dual Band Filter After Optimization in ADS	38
Figure 4.18 Simulation of Dual Band Filter with Layout	39
Figure 4.19 Response of Dual Band Filter	39
Figure 4.20 Bridge Tee Notch Filter Designed in Filpro	41
Figure 4.21 Response of Bridge Tee Notch Filter Designed in Filpro	42
Figure 4.22 VHF Notch Filter Designed in Filpro	42
Figure 4.23 Response of VHF Notch Filter Designed in Filpro	43
Figure 4.24 Simulation Circuit of UHF Harmonic Filter with Layout in ADS	44
Figure 4.25 Simulation Circuit of VHF Harmonic Filter with Layout in ADS	44
Figure 4.26 Simulation Circuit of VHF Notch Filter with Layout in ADS	45
Figure 4.27 Response of VHF Notch Filter in ADS	45
Figure 4.28 Simulation Result of UHF Branch in ADS	46
Figure 4.29 Simulation Result of VHF Branch in ADS	46
Figure 4.30 Circuit Diagram of LNA	48
Figure 4.31 Designed LNA Circuit and Layout	49
Figure 4.32 Response of Designed LNA	49
Figure 4.33 Response of Designed LNA After Optimization Such That It Has Higher Gain at UHF Band	50
Figure 4.34 Block Diagram of Designed Front-end in ADS	50

Figure 4.35 Response of Front-End in ADS When VHF Band is Selected	51
Figure 4.36 Response of Front-End in ADS When UHF Band is Selected	51
Figure 4.37 Layers of Designed PCB	52
Figure 4.38 Component Layer of Designed PCB	53
Figure 4.39 Manufactured Printed Circuit Board	53
Figure 4.40 Measurement Setup	54
Figure 4.41 Response of Dual Band Filter When Tune Voltage is 1 V	56
Figure 4.42 Response of Dual Band Filter When Tune Voltage is 4 V	56
Figure 4.43 Response of VHF Notch Filter	57
Figure 4.44 Response of UHF Branch	58
Figure 4.45 Response of VHF Branch	58
Figure 4.46 Response of LNA	59
Figure 4.47 Circuit of LNA After Optimization	59
Figure 4.48 Response of LNA After Optimization	60
Figure 4.49 Responses of Single Band and Dual Band Front-ends at 136 MHz	63
Figure 4.50 Responses of Single Band and Dual Band Front-ends at 136 MHz	63
Figure 4.51 Comparison of Simulation and Test Results of Front-ends at 136 MHz	64
Figure 4.52 Comparison of Simulation and Test Results of Front-ends at 136 MHz	64
Figure 4.53 Responses of Single Band and Dual Band Front-ends at 174 MHz	65
Figure 4.54 Responses of Single Band and Dual Band Front-ends at 174 MHz	65
Figure 4.55 Comparison of Simulation and Test Results of Front-ends at 174 MHz	65
Figure 4.56 Comparison of Simulation and Test Results of Front-ends at 174 MHz	66
Figure 4.57 Responses of Single Band and Dual Band Front-ends at 380 MHz	66
Figure 4.58 Responses of Single Band and Dual Band Front-ends at 380 MHz	66
Figure 4.59 Comparison of Simulation and Test Results of Front-ends at 380 MHz	67
Figure 4.60 Comparison of Simulation and Test Results of Front-ends at 380 MHz	67
Figure 4.61 Responses of Single Band and Dual Band Front-ends at 470 MHz	67
Figure 4.62 Responses of Single Band and Dual Band Front-ends at 470 MHz	68
Figure 4.63 Comparison of Simulation and Test Results of Front-ends at 470 MHz	68

Figure 4.64 Comparison of Simulation and Test Results of Front-ends at 470 MHz . . .	68
Figure 5.1 Block Diagram of Triple Band Front-end	71
Figure 5.2 Design of Triple Band Filter in Filpro	72
Figure 5.3 Response of Triple Band Filter in Figure 5.2.c	73
Figure 5.4 Response of Triple Band Filter in Figure 5.2.e	74
Figure 5.5 Element Values Required to Tune the Triple Band Filter to Low-ends and High-ends of the Bands	74
Figure 5.6 Circuit Diagram of the Triple Band Filter	75
Figure 5.7 Simulation Result of the Triple Band Filter in ADS	76
Figure 5.8 Circuit Diagram of the Triple Band LNA	77
Figure 5.9 Simulation Result of the Triple Band LNA in ADS	77
Figure A.1 Lowpass Prototype to Banpass Filter Transformation	84
Figure B.1 Model of JDV2S25FS Used in ADS	86
Figure B.2 Model of JDV2S08FS Used in ADS	87
Figure B.3 Model of JDV2S07S Used in ADS	87
Figure B.4 Model of 1SV325 Used in ADS	88
Figure B.5 Model of BFR340F Used in ADS	89

CHAPTER 1

INTRODUCTION

Front-end of a receiver is the part between antenna and the first mixer. In the front-end, input RF signal is put into an appropriate form to be downconverted to intermediate frequencies. The main parts of a superheterodyne receiver system is shown in Figure 1.1 [1].

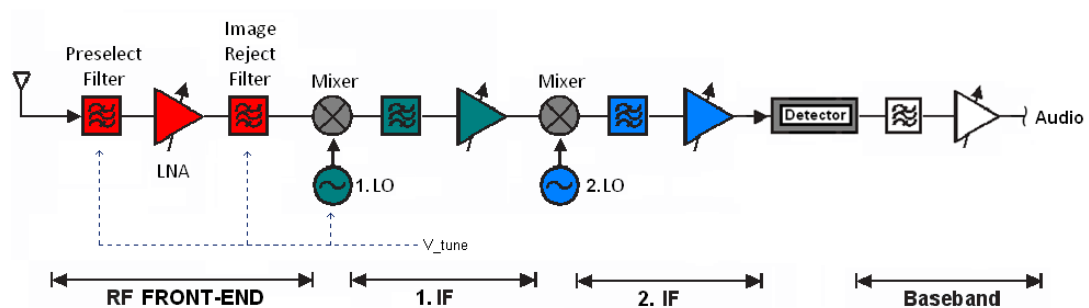


Figure 1.1: Block Diagram of a Superheterodyne Receiver System

In a wide-band transceiver system usually RF front-end and 1st LO sections are tunable. IF sections and 2nd LO are fixed frequencies. In RF front-end, signals at far channels are eliminated while in IF sections signals at adjacent channels are eliminated.

The aim of this thesis is to design and implement a tunable front-end that covers VHF and UHF bands. There exist two single band tunable front-ends: one works at VHF band and the other works at UHF band. VHF band covers the frequencies between 136 MHz and 174 MHz while UHF band covers the frequencies between 380 MHz and 470 MHz. The resultant dual band front-end will present the same performance as the single band front-ends (Figure 1.2). Intermediate frequency (IF) will be 45 MHz.

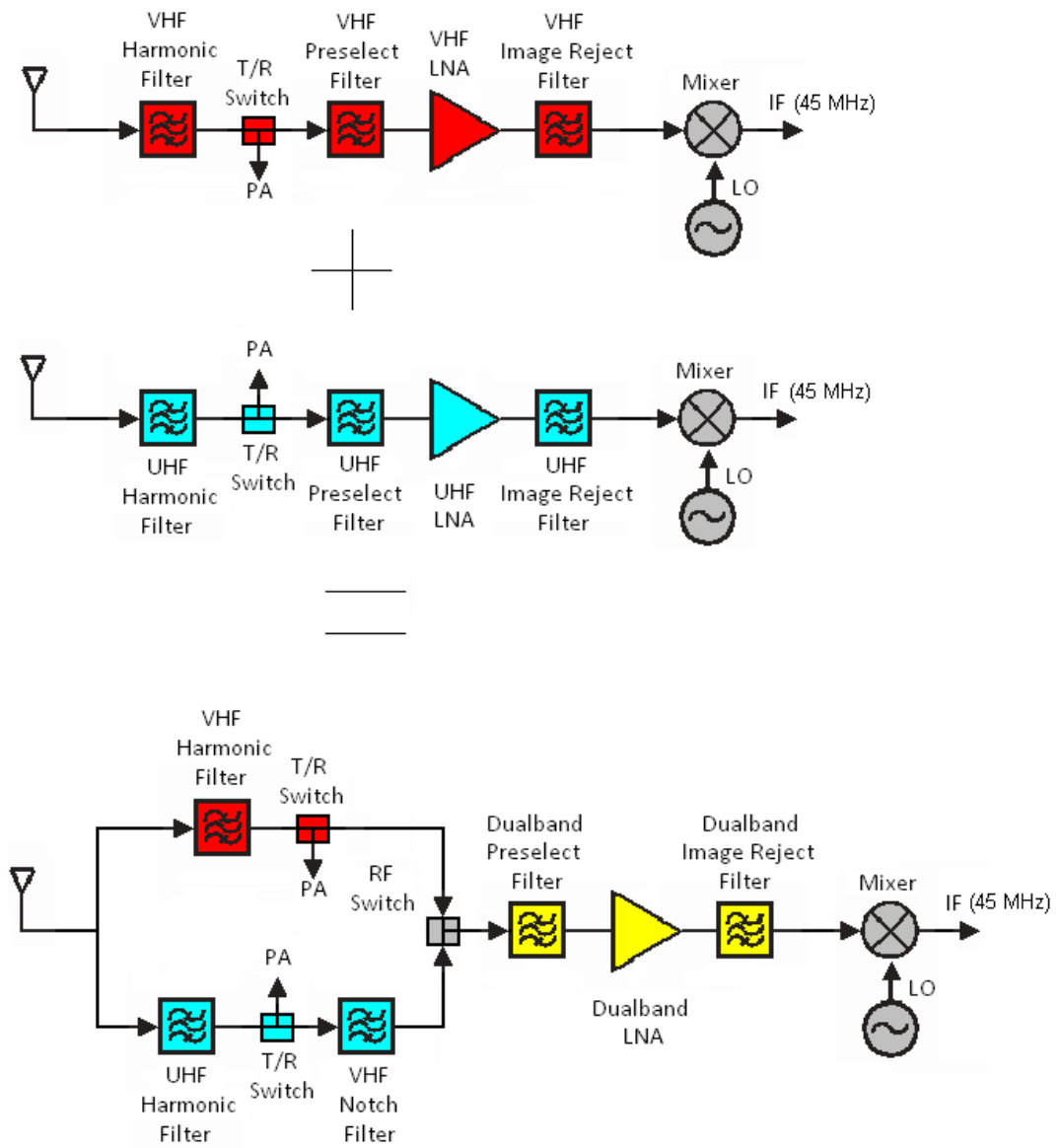


Figure 1.2: Block Diagram of Dual Band Front-end That Covers VHF and UHF Bands

As it can be seen, each single band front-end is composed of a harmonic filter, two RF filters and one low noise amplifier (LNA). On the other hand, dual band front-end has two harmonic filters, a notch filter, two dual band filters and a LNA. Harmonic filters are the only common parts, so they are not designed again and the existing harmonic filters are used. The remaining parts, which are notch filter, dual band filters and LNA are designed in this work. Finally the whole dual band front-end is manufactured and its performance is compared with the single band ones.

The signal at the antenna input of the receiver can contain any frequency components at any amplitude. In other words, there may be some unwanted signals at the antenna input besides the signal at the desired frequency and amplitude of these unwanted signals can be higher or lower than amplitude of the desired signal. If these undesired signals are not attenuated enough, they may appear in the IF frequency after mixing operation and may cause distortion. Therefore, dual-band pre-select and image reject filters are designed to eliminate them. Since there are two filters in the front-end, the filter before LNA is called as pre-select filter and the other one is called as image reject filter throughout this thesis in order to distinguish them easily. The first passband is tunable between 136 MHz and 174 MHz while the second passband is tunable between 380 MHz and 470 MHz. Tuning voltage changes between 1 V and 4 V.

Harmonic filters are used to block the harmonics of the carrier signal appearing at the output of power amplifier when transceiver is in transmitter mode. Since they are located between antenna and mixer, they inevitably affect the performance of front-end. Therefore they are included in this project.

Low noise amplifier is used to amplify the weak input signal at the band of interest and to improve noise performance of the receiver [2]. Design and implementation of a LNA that works between 136 MHz and 470 MHz is also performed during this work.

Additionally, it is required to suppress VHF band when receiver is adjusted to a UHF frequency. Hence, a bandstop filter is designed using bridged topology.

This thesis includes detailed information about design and implementation of the tunable dual band front-end described above. It begins with some theoretical information about the parts that are designed. A chapter is assigned for dual band filters. In Chapter 4, firstly design and

simulation of each circuit will be mentioned. Then, test results of manufactured dual band front-end will be compared with simulation results and single band front-ends performances. In Chapter 5, future works will be defined.

CHAPTER 2

BACKGROUND INFORMATION

2.1 Low Noise Amplifiers

Besides amplifying the weak input signal, a low noise amplifier also improves noise performance of the receiver [2], [3], [4]. Noise figure affects the sensitivity of the receiver. The well known formula for noise figure of a circuit is [5]

$$F = \frac{SNR_{in}}{SNR_{out}} = \frac{S_{in}/N_{in}}{S_{out}/N_{out}} \quad (2.1)$$

$$NF = 10\log(F) = 10\log\left(\frac{SNR_{in}}{SNR_{out}}\right) = SNR_{in,dB} - SNR_{out,dB} \quad (2.2)$$

The noise factor of a system composed of cascaded circuits (Figure 2.1) can be derived as given in Equation 2.3.

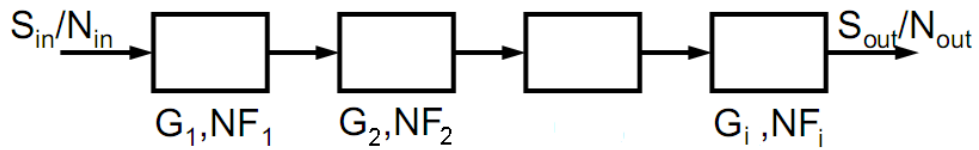


Figure 2.1: Noise Figure of Cascaded Circuits

$$F_{total} = F_1 + \frac{F_2 - 1}{G_1} + \frac{F_3 - 1}{G_1 G_2} + \dots + \frac{F_i - 1}{G_1 G_2 \dots G_{i-1}} \quad (2.3)$$

This equation shows that the contribution of the circuits after an amplifier to the overall noise

figure of the system is inversely proportional to the gain of the amplifier. Therefore, an amplifier is placed always at beginning of the front-end so that the noise figure of the receiver is mainly affected by the noise figure of the amplifier and pre-select filter. The noise figure of this amplifier should be as low as possible since it affects the overall noise figure directly. Also, the gain of this amplifier should be as high as possible to minimize the contribution of later stages to the overall noise figure. However, linearities of the circuits after LNA limit the gain of LNA. If its gain is too high, higher order products may occur in later stages due to non-linearities and consequently distort the signal. Frequency band of LNA can be wide or narrow depending on the application. In this thesis, LNA works between 136 MHz and 470 MHz.

3 dB is an important value for noise figure of an LNA [6]. SNR_{out} can also be expressed as follows:

$$SNR_{out} = \frac{S_{out}}{N_{out}} = \frac{G \cdot S_{in}}{G \cdot N_{in} + N_{LNA}} \quad (2.4)$$

where G is gain of the LNA and N_{LNA} is noise added by the LNA. If noise added by LNA is equal to noise at the input amplified by the LNA, then;

$$G \cdot N_{in} = N_{LNA} \Rightarrow SNR_{out} = \frac{G \cdot S_{in}}{2G \cdot N_{in}} = \frac{S_{in}}{2N_{in}} \quad (2.5)$$

In such a case, noise figure of LNA can be calculated using Equation 2.2 as follows:

$$NF = 10 \log\left(\frac{SNR_{in}}{SNR_{out}}\right) = 10 \log\left(\frac{S_{in}/N_{in}}{S_{in}/2N_{in}}\right) = 3dB \quad (2.6)$$

Equation 2.6 states that if noise power added by LNA to the system will be less than the noise at the input amplified by the LNA, noise figure of the LNA should be lower than 3 dB. Noise figure of a front-end limits the smallest signal level that can be detected by the receiver and affects the sensitivity of the receiver.

2.2 IP3 Measurement

If the output of a system can not be expressed as a linear combination of responses of individual inputs, that system is called nonlinear. Linearity of a system limits the largest signal level that can be input to it without distorting the output signal. This largest signal level affects the dynamic range of that system.

Output of a system can be affected by nonlinearities in a few ways such as harmonic generation, gain suppression, desensitization, cross modulation and intermodulation. In this thesis, intermodulation measurements will be performed to see how linear the front-end is.

Assume that $x_1(t)$ and $x_2(t)$ are inputs to a non-linear system whose input-output relationship is given in Equation 2.8 [5].

$$x_1(t) = A_1 \cos(w_1 t); \quad x_2(t) = A_2 \cos(w_2 t) \quad (2.7)$$

$$y(t) = a_1 x(t) + a_2 x(t)^2 + a_3 x(t)^3 \quad (2.8)$$

Then, due to mixing of x_1 and x_2 , some components appear at the output:

$$y(t) = a_1(A_1 \cos(w_1 t) + A_2 \cos(w_2 t)) + a_2(A_1 \cos(w_1 t) + A_2 \cos(w_2 t))^2 + a_3(A_1 \cos(w_1 t) + A_2 \cos(w_2 t))^3 \quad (2.9)$$

$$\begin{aligned} \Rightarrow y(t) &= a_1 A_1 \cos(w_1 t) + a_1 A_2 \cos(w_2 t) \\ &+ a_2 A_1^2 \cos(w_1 t)^2 + 2a_2 A_1 A_2 \cos(w_1 t) \cos(w_2 t) + a_2 A_2^2 \cos(w_2 t)^2 \\ &+ a_3 A_1^3 \cos(w_1 t)^3 + 3a_3 A_1^2 A_2 \cos(w_1 t)^2 \cos(w_2 t) + 3a_3 A_1 A_2^2 \cos(w_1 t) \cos(w_2 t)^2 + a_3 A_2^3 \cos(w_2 t)^3 \end{aligned} \quad (2.10)$$

By using the following trigonometric identities, Equation 2.10 can be written as given in Equation 2.14.

$$\cos^2\alpha = \frac{1}{2}(1 + \cos 2\alpha) \quad (2.11)$$

$$\cos^3\alpha = \frac{1}{4}(3\cos\alpha + \cos 3\alpha) \quad (2.12)$$

$$\cos(\alpha)\cos(\beta) = \frac{1}{2}(\cos(\alpha + \beta) + \cos(\alpha - \beta)) \quad (2.13)$$

$$\begin{aligned} \Rightarrow y(t) = & [a_1A_1 + \frac{3}{4}a_3A_1^3 + \frac{3}{2}a_3A_1A_2^2]\cos(w_1t) \\ & + [a_1A_2 + \frac{3}{4}a_3A_2^3 + \frac{3}{2}a_3A_2A_1^2]\cos(w_2t) \\ & + \frac{a_2A_1^2}{2} + \frac{a_2A_2^2}{2} \\ & + \frac{a_2A_1^2}{2}\cos(2w_1t) + \frac{a_2A_2^2}{2}\cos(2w_2t) + \frac{a_3A_1^3}{4}\cos(3w_1t) + \frac{a_3A_2^3}{4}\cos(3w_2t) \\ & + a_2A_1A_2\cos((w_1 + w_2)t) + a_2A_1A_2\cos((w_1 - w_2)t) \\ & + \frac{3}{4}a_3A_1^2A_2\cos((2w_1 + w_2)t) + \frac{3}{4}a_3A_1A_2^2\cos((w_1 + 2w_2)t) \\ & + \frac{3}{4}a_3A_1^2A_2\cos((2w_1 - w_2)t) + \frac{3}{4}a_3A_1A_2^2\cos((2w_2 - w_1)t) \end{aligned} \quad (2.14)$$

Note that harmonics and dc components can be filtered out easily since they are far from w_1 and w_2 . However, if w_1 and w_2 are close to each other, intermodulation components at $2w_1 - w_2$ and $2w_2 - w_1$ will appear close to w_1 and w_2 , so they can not be filtered. As a result, these components inevitably cause a distortion at the output.

The traditional approach to measure IMD is third order intercept point, IP_3 . Consider the case $A_1 = A_2 = A$. It can be seen from Equation 2.14 that when A is increased, amplitude of third order products increase proportional to A^3 while amplitude of fundamental signals increase proportional to A. Third order intercept point is the power level at which amplitude of fundamentals become equal to amplitude of third order products (Figure 2.3). The most common way to measure IP_3 is to apply two signals at different frequencies to the nonlinear system and observe the fundamentals and third order products at the output of the system using a spectrum analyzer. If power levels of fundamentals and intermodulation products are known, IIP_3 can be found using Equation 2.15.

$$IIP_3|_{dBm} = \frac{\Delta P|_{dB}}{2} + P_{in}|_{dBm} \quad (2.15)$$

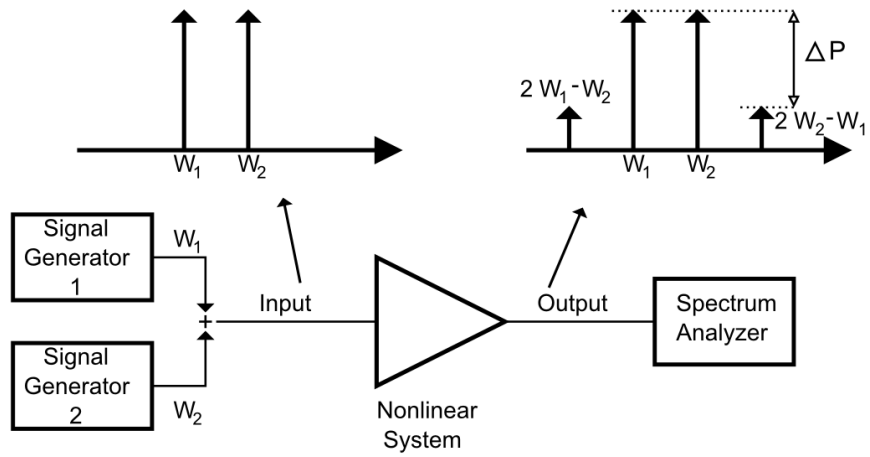


Figure 2.2: Measurement Setup for IP3

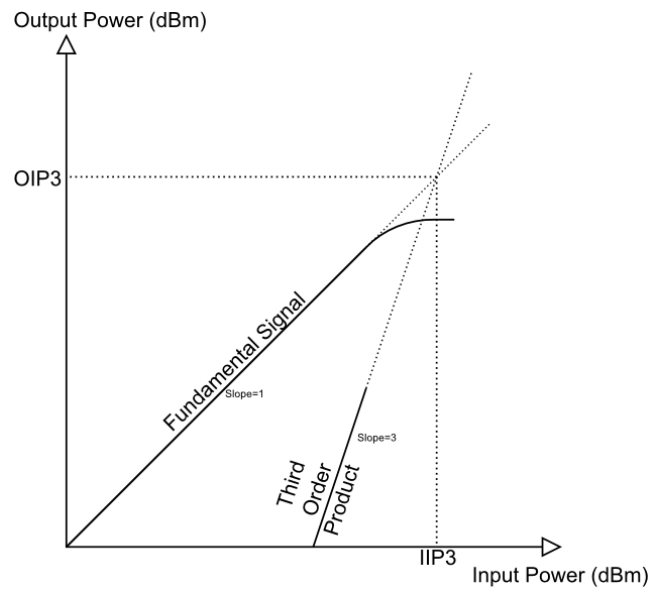


Figure 2.3: Graphical Explanation of IP3

If a system is composed of cascaded circuits whose input IP_3 's are known, total IIP_3 can be calculated as follows [5]:

$$\frac{1}{iip_{3,total}} = \frac{1}{iip_{3,1}} + \frac{G_1}{iip_{3,2}} + \frac{G_1G_2}{iip_{3,3}} + \dots \quad (2.16)$$

where $IIP_{3,i} = 10\log(iip_{3,i})$ and G_i is gain of i^{th} stage.

As stated in [7], if IP_3 , sensitivity (S) and co-channel rejection (C) of a receiver are known, intermodulation distortion performance of it can be calculated from

$$IMD|_{dB} = \frac{2IP3|_{dBm} - 2S|_{dBm} - C|_{dB}}{3} \quad (2.17)$$

IMD performance of the designed receiver is required to be better than 75 dB. Assuming that its sensitivity will be -120 dBm and co-channel rejection ratio will be 7 dB, minimum IP_3 can be calculated as

$$IP3|_{dBm} = \frac{3IMD|_{dB} + 2S|_{dBm} + C|_{dB}}{2} = \frac{3 \times 75 + 2 \times (-120) + 7}{2} = -4dBm \quad (2.18)$$

Although -4 dBm IP_3 is enough for 75 dB IMD, it is preferred to have 0 dBm IIP_3 in order to have a margin to 75 dB IMD. 0 dBm IP_3 refers to 77 dB IMD.

2.3 Classification of Filters

Filters can be classified as lowpass, highpass, bandpass, bandstop and allpass filters with respect to their transfer functions. Transfer function is the mathematical representation of the relation between input and output of a filter.

A lowpass filter transmits all the frequencies below the cut-off frequency and stops all those above the cut-off frequency.

A highpass filter transmits all the frequencies above the cut-off frequency and stops all those below the cut-off frequency

A bandpass filter has two cut-off frequencies. It stops the frequencies below the lower cut-off

and above the higher cut-off, and transmits a particular band of frequencies between two cut of frequencies.

A bandstop filter stops frequencies within the band specified by two cut-off frequencies and transmit all the frequencies out of this band.

An allpass filter transmits all of the frequencies without any attenuation. This type of filters are usually used to alter the phase of input signal.

2.4 Common Filter Transfer Functions

The most important constraint of filter design is the behavior of its magnitude response at passband and stopband. There are three main transfer functions according to the ripple at passband and attenuation at stopband [8]. Practically, there is no ideal filter. Realistic filters have non-zero attenuation at passbands and finite attenuation at stopbands. Hence, before starting the design, the appropriate filter transfer function type should be decided according to the design constraints.

2.4.1 Butterworth Filter

Butterworth filter, which is also called as maximally-flat filter, exhibits a nearly flat passband. It has no ripple in passband or stopband at the expense of smooth transition from passband to stopband. If a sharper transition is required, the order of filter should be increased but its cost will be higher number of elements used. Butterworth filters have good phase response.

2.4.2 Chebyshev Filter

A Chebyshev filter has a steeper cut-off slope than the same order Butterworth filter. The ripple in the passband or stopband is the drawback of this filter. As the ripple increases the transition becomes sharper. Usually it is desired to have sharper roll-off while having fewer ripples in the passband. Therefore a trade off should be made in order to fulfill both passband and stopband requirements. There are two types of Chebyshev filters. Type-1 Chebyshev filters have ripple only at passband while Type-2 Chebyshev filters have ripple only at stopband.

Phase response of Chebyshev filters is worse than that of Butterworth filters.

2.4.3 Elliptic Filter

Among these four filter types, elliptic filter is the one that has the sharpest transition from passband to stopband. On the other hand, its amplitude response has ripples at both passband and stopband. Phase response of Elliptic filters is very non-linear.

2.5 Electrically Tunable Filters

In modern wireless communication systems, there is an increasing demand for devices that cover different communication standards. This results in the need for wide-band and multi-band radios. On the other hand, in order to use the spectrum efficiently, channel bandwidths should be as narrow as possible. These two requirements cannot be accomplished by using a fixed frequency filter. Only a filter whose bandwidth is narrow and center frequency can be changed to scan the full band can achieve this job. Therefore, tunable filters are essential for such devices.

A tunable filter can be obtained by changing the resonance frequency of a fixed frequency filter. There are many methods to control the resonance frequency electrically.

The approach used in this thesis is to change capacitance of the resonator. There are some devices that are used for this purpose such as PIN diodes, varactor diodes [9], [10], [11] and BST (Barium Strontium Titanate) varactors [12], [13]. When a reverse bias voltage is applied on a varactor diode, it acts as a capacitor. The capacitance of the depletion layer of a p-n junction varies continuously with respect to the reverse bias voltage as shown in Figure 2.4. If a reverse biased varactor diode is placed instead of the capacitor in resonator of a filter, the change of bias voltage yields in the tuning of the center frequency. They are small, light and cheap devices. Their tuning speed is high and they consume only a little amount of power since they are reverse biased. They provide octave bandwidth tuning. On the other hand, they have the disadvantage of low power handling, non-linear behavior and lower Q-factor. Similarly, PIN diodes, which contains a thick intrinsic semiconductor layer between p-n junction, can be used to tune the center frequency discretely. The contribution of PIN

diodes to the non-linear characteristics of the circuit is less than the contribution of varactor diodes [14]. If the dc bias current is sufficient, a nearly linear behavior will be displayed by PIN diodes. BST ferroelectric thin-film varactors have relatively higher power handling capability [15]. Permittivity of ferroelectric varactor depends on the applied DC electric field. Hence, as bias voltage changes, capacitance value of BST varactor varies which results in the change in resonance frequency. All of these approaches change the resonance frequency by varying the capacitance in the resonators while inductance remains constant. This causes L/C ratio to change. Thus as center frequency is tuned to higher frequencies, bandwidth of filter increases. This may cause a degradation in the suppression of unwanted signals near the passband.

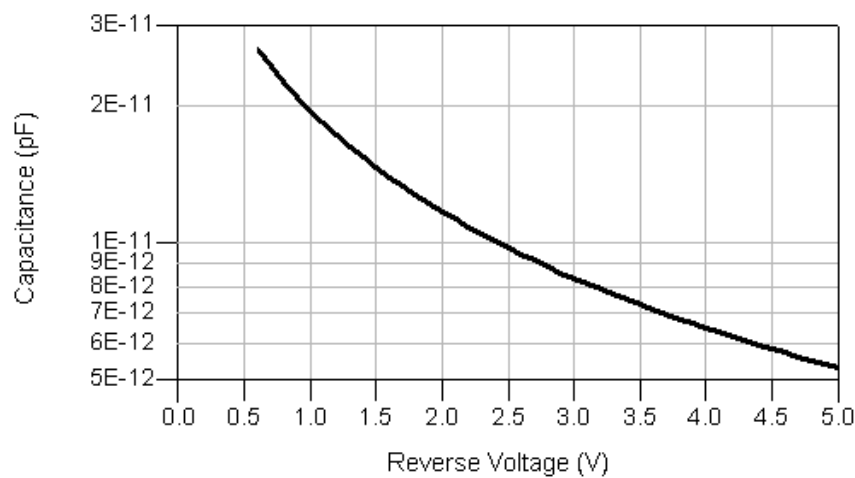


Figure 2.4: Typical C-V Curve of a Varactor Diode

In this thesis, varactor diodes will be used due to their compact sizes, continuous tuning, high tuning speed and low power consumption.

2.6 Bridge-T Bandstop Filters

As mentioned before, bandstop filters are used to block a certain band of signals while passing the signals out of this band. Narrow band bandstop filters are usually called as notch filters. There are various methods to implement a notch filter. The one that will be discussed in this section is bridged topology [16].

This method is based on the phase cancellation approach. Usual notch filters have low atten-

uation at stopbands due to low Q of resonators. In order to increase its rejection levels, its degree can be increased. However, number of elements used will also increase which is an undesired situation. An alternative way to increase the rejection levels is to add another path between input and output of filter. As shown in Figure 2.5, the input signal is split in two paths. One of these branches is a notch filter at a certain frequency (f_0) and the other branch is a delay line. Some part of input signal passes through the delay line and the remaining part passes through the notch filter branch. At the desired frequency, delays and attenuations in each branch should be adjusted so that the signals at the outputs of these branches become same in amplitude and there is a 180 degree phase difference between them. Then, these two signals will cancel each other at the output.

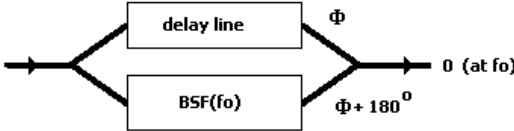


Figure 2.5: Phase Cancellation [16]

A bridged all pass filter can be converted to a bridged notch filter by using the approach explained above. Firstly a bridged all pass filter is designed by bridging a band stop filter as shown in Figure 2.6. Then, some element values are tuned such that there is 180 degree phase difference between the signals passing through BSF path and bridge path at a certain frequency. As a result, these two signals cancel each other.

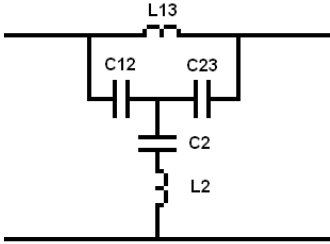


Figure 2.6: Bridged All Pass Filter Topology

The resultant notch filter can easily be converted to a tunable notch filter by placing varactor diodes instead of capacitors. However, in this thesis, notch filter is used to suppress VHF band when channel is adjusted to a frequency in UHF band. Therefore, design of a fixed frequency bandstop filter that attenuates VHF band will be discussed in the next chapters.

2.7 Pre-select and Image Reject Filters

Since pre-select filter is placed before LNA, its noise figure is directly added to the overall noise figure. For a passive circuit, noise factor is equal to its attenuation [5]. Therefore, the insertion loss of pre-select filter at passband should be minimum. This limits the degree of the filter. On the other hand, the higher the degree of the filter is, the higher the attenuation in the stopband is. Hence there is a trade-off between spurious attenuation and noise figure performance for pre-select filter.

Image reject filter is placed after LNA, i.e. its contribution to the overall noise performance is very small. Higher insertion loss can be allowed as a consequence of this. Hence its degree can be higher than the pre-select filter in order to suppress spurious signals. However, since the input signal will be amplified before image reject filter, its input IP3 should be higher than pre-select filter in order not to degrade system performance for high input levels, which affect the dynamic range of the receiver.

The filters' bandwidths will be much larger than the channel bandwidth so more than one channel can pass through the filters. The aim of using filters in the front-end is to suppress spurious signals, not to suppress adjacent channel. Channel filtering will be done in IF stages. The most important spurious signals are at the image frequency, 1/2 IF frequency and 1/3 IF frequency as illustrated in Figure 2.7 [1]. If not suppressed, these signals can appear in IF frequency after mixing operation as explained in Equations 2.19 to 2.22:

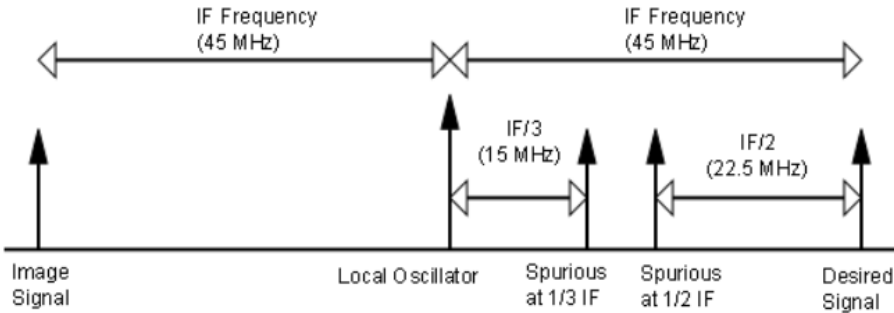


Figure 2.7: Important Spurious Signals

Desired RF Signal: $w_{RF} = w_{LO} + w_{IF}$

Image Signal: $w_{IM} = w_{LO} - w_{IF} = w_{RF} - 2w_{IF}$

1/2 IF Spurious Signal: $w_{1/2IF} = w_{LO} + \frac{w_{IF}}{2} = w_{RF} - \frac{w_{IF}}{2}$

1/3 IF Spurious Signal: $w_{1/3IF} = w_{LO} + \frac{w_{IF}}{3} = w_{RF} - \frac{2w_{IF}}{3}$

When wanted RF signal is multiplied with local oscillator signal in the mixer, it will be down-converted to IF frequency successfully:

$$\begin{aligned} 2\cos(w_{RF}t)\cos(w_{LO}t) &= \cos([w_{RF} - w_{LO}]t) + \text{HigherOrderTerm} \\ &= \cos(w_{IF}t) + \text{H.O.T.} \end{aligned} \tag{2.19}$$

If the image signal is not attenuated, it will be multiplied with LO signal and will be downconverted to IF frequency as shown in Equation 2.20. Assuming the conversion loss of the mixer is same for the whole band, image frequency will not encounter any additional attenuation in mixing procedure.

$$\begin{aligned} 2\cos(w_{IM}t)\cos(w_{LO}t) &= \cos([w_{IM} - w_{LO}]t) + \text{H.O.T.} \\ &= \cos(w_{IF}t) + \text{H.O.T.} \end{aligned} \tag{2.20}$$

If 1/2 IF spurious signal is not suppressed, it will be downconverted to IF frequency due to the non-linear behaviors of front-end section, LO section and mixer. If second harmonic of this spurious signal appears at the RF input of mixer and if second harmonic of LO exists at the LO input of mixer, they will be multiplied and consequently the unwanted signal will be downconverted to IF frequency as shown in Equation 2.21. Since usually amplitude of the harmonics are less than the main signal, attenuation of front-end filters at 1/2 IF frequency can be less than attenuation at image frequency.

$$\begin{aligned}
2\cos(2w_{1/2IF}t)\cos(2w_{LO}t) &= 2\cos(2[w_{LO} + \frac{w_{IF}}{2}]t)\cos(2w_{LO}t) \\
&= \cos(2w_{LO} + w_{IF} - 2w_{LO}) + H.O.T. \\
&= \cos(w_{IF}t) + H.O.T.
\end{aligned}
\tag{2.21}$$

Similarly, if third harmonic of the spurious at 1/3 IF frequency is multiplied with third harmonic of LO, an unwanted signal will appear in the IF frequency as shown in Equation 2.22.

$$\begin{aligned}
2\cos(3w_{1/2IF}t)\cos(3w_{LO}t) &= 2\cos(3[w_{LO} + \frac{w_{IF}}{3}]t)\cos(3w_{LO}t) \\
&= \cos(3w_{LO} + w_{IF} - 3w_{LO}) + H.O.T. \\
&= \cos(w_{IF}t) + H.O.T.
\end{aligned}
\tag{2.22}$$

The signals that are IF/2 and IF/3 higher than LO are discussed above. Similarly, the signals that are IF/2 and IF/3 lower than LO can also distort IF signal if they are not attenuated. However, note that they are more far away from passband and bandpass filters attenuate far points better. In other words, these signals will be attenuated more by the filters. Therefore, IF/2 and IF/3 that are closer to desired RF signal will be considered as spurious signals and the others will not be taken into account.

If spurious signals are downconverted to IF frequency, they will be added to the desired IF frequency and the desired message signal will be distorted. Once these unwanted signals are downconverted to exact IF frequency, it will be impossible to eliminate them in later stages. Therefore, best section to eliminate unwanted signals is the front-end stage.

To sum up, filters in front-end should be designed to attenuate spurious signals as much as possible without degrading other performances of the receiver. In this thesis, dual band filters are used as pre-select and image reject filters.

CHAPTER 3

DUAL BAND FILTERS

3.1 Introduction

As mentioned in previous chapters, the targeted front-end will cover VHF and UHF bands. This results in a need for an RF filter that covers both bands which are 136 MHz - 174 MHz and 380 MHz - 470 MHz. In order to provide enough attenuation for spurious signals, these filters should be tunable according to the selected channel frequency. Varactor diodes will be used in order to change the capacitances in resonators, consequently the center frequency of the filter. However, if a single band filter is tried to be tuned from 136 MHz to 470 MHz, there will be a great degradation in bandwidth of the filter. Also, it will be hard to find a varactor diode whose capacitance ratio is high enough to provide a tuning between 136 MHz and 470 MHz for a tuning voltage changing from 1 V to 4 V. Using dual band filters ease the design of RF filters in this front-end. Since the channel frequency can be as low as 136 MHz, lumped elements are used in the front-end. Therefore, design of lumped dual band filters will be focused in this chapter.

The simplest way to construct a filter which covers two bands is to combine two distinct filters in parallel such that they do not affect each other [17]. However, there is a more compact approach in which a single set of lumped elements is used. Dual band filters has the advantage of combining two filters in a more compact physical filter [18], [19], [20], [21]. This results in a reduction in the total size of the filter. As described in [22], there are various techniques to form a lumped element dual band filter. A simple way is cascading a bandstop filter with a broadband bandpass filter. Then, the response can be optimized by tuning the element values. Another way is to convert a normalized single passband BP prototype filter

into a dual band BP filter by applying LP prototype to BP transformations. This is an exact synthesis technique and no optimization is required to reshape the response. The third method is to convert the LC resonators of a single band BP filter into fourth order resonators to obtain a dual band filter. Last two techniques will be described in the following sections.

3.2 Conversion of a Single Band Filter into a Dual Band Filter

A lumped element single band BP filter can be converted into a dual passband filter by applying some transformations on its LC resonators. The transformations are illustrated in Figure 3.1.

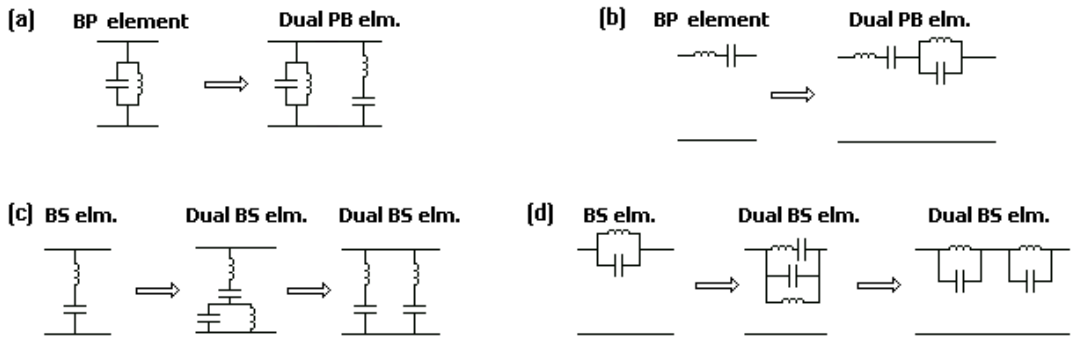


Figure 3.1: Conversion of Second Order Resonators into Forth Order Resonators [22]

These transformations can be applied to the single band BP filters which have transmission zeros only at zero and infinity. In other words, it should not have any finite transmission zeros (FTZs). Also, number of transmission zeros at zero should be equal to the number of transmission zeros at infinity. On the other hand, this method brings the advantage of adjusting the bandwidth of each band. The resultant dualband filter will have two passbands and one stopband created by a finite transmission zero between these passbands. Relative bandwidths of two passbands depend on the location of the FTZ. FTZ will come out to be closer to the narrower passband. Therefore, if the relative bandwidths of two passbands are predefined, it will not be possible to adjust the location of FTZ to obtain a desired stopband response. All the FTZs appear to be at the same frequency.

3.3 Conversion of Normalized BP Prototype to Dual Band Filter

By applying the classical LP prototype to BP transformations on a magnitude and frequency normalized single passband BP prototype filter, a dual band filter can be obtained. In contrary to the previous method, this technique brings the benefit of placing the FTZ to desired locations in order to shape up the stopband response. Locations of the resultant FTZs and edge frequencies of two passbands come out to be geometrically symmetric with respect to the stopband center. Therefore, this approach does not allow us to set widths of two passbands independently.

Firstly a normalized lowpass filter is designed such that $w'_p=1$ and $R_S=R_L=1$. The mapping function used to obtain a bandpass filter from a LP prototype is

$$w' = \left(\frac{w_0}{B}\right)\left(\frac{w}{w_0} - \frac{w_0}{w}\right) \quad (3.1)$$

where w' is the normalized frequency, w_0 and B are respectively the center frequency and bandwidth of the resultant bandpass filter.

If the same mapping is applied to a normalized bandpass prototype filter, a dual band bandpass filter can be obtained. Consider the normalized BP prototype shown in Figure 3.2, whose upper band edge is $w'_2=1$ and lower band edge is w'_1 . This prototype will be transformed to a dual band filter whose lower band is between w_{1a} and w_{2a} , and upper band is between w_{1b} and w_{2b} which satisfy

$$w_{1a}w_{2b} = w_{2a}w_{1b} = w_0^2 \quad (3.2)$$

Here, $w'=0$ is mapped to w_0 , w'_1 is mapped to w_{2a} and w_{1b} , w'_2 is mapped to w_{1a} and w_{2b} , $w'=\infty$ is mapped to $w=0$ and $w=\infty$.

The design of the prototype filter starts by selecting the passband edge frequencies of the desired dual band filter. Note that, it is enough to select only three of them. The fourth edge frequency can be found using Equation 3.2. Then, B_S and B can be calculated using equations below:

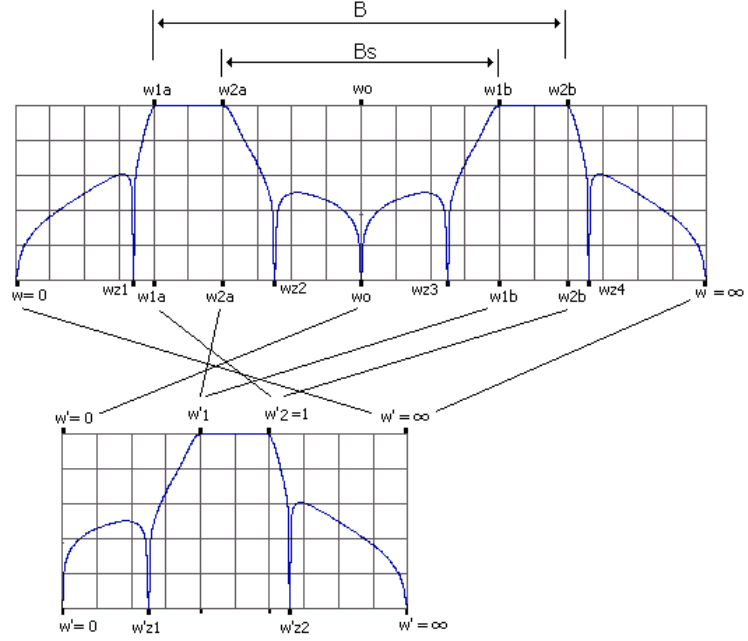


Figure 3.2: Mapping Between Normalized Bandpass Prototype and Dual Band Filter [22]

$$B_s = w_{1b} - w_{2a} \quad (3.3)$$

$$B = w_{2b} - w_{1a} \quad (3.4)$$

Finally w'_1 can be found using Equation 3.5.

$$w'_1 = \frac{B_s}{B} = \frac{w_{1b} - w_{2a}}{w_{2b} - w_{1a}} \quad (3.5)$$

By knowing w'_1 and w'_2 , a normalized bandpass filter can be synthesized using Filpro easily. While designing the prototype, R'_S and R'_L must be selected as 1. Then, the classical LP-to-BP mapping which is explained in Appendix A can be applied to this normalized prototype to obtain a dual band BP filter.

3.4 Analysis of Dual Band Filter Topology

A lumped element dual band filter obtained from a single resonator bandpass filter is indicated in Figure 3.3. The dual band filter is composed of two resonators; a parallel LC resonator in the shunt arm and a series LC resonator in the shunt arm. The parallel LC resonator creates a passband at a certain frequency at which both L'_1 and C'_1 shows a high impedance. On the other hand, the series LC branch acts as a short circuit at the resonance frequency so that a notch is created at that frequency. Then, how is the second passband created and which element affect the center frequency of each passband? Since the dual band filters used in this thesis will be tunable, these issues should be investigated.

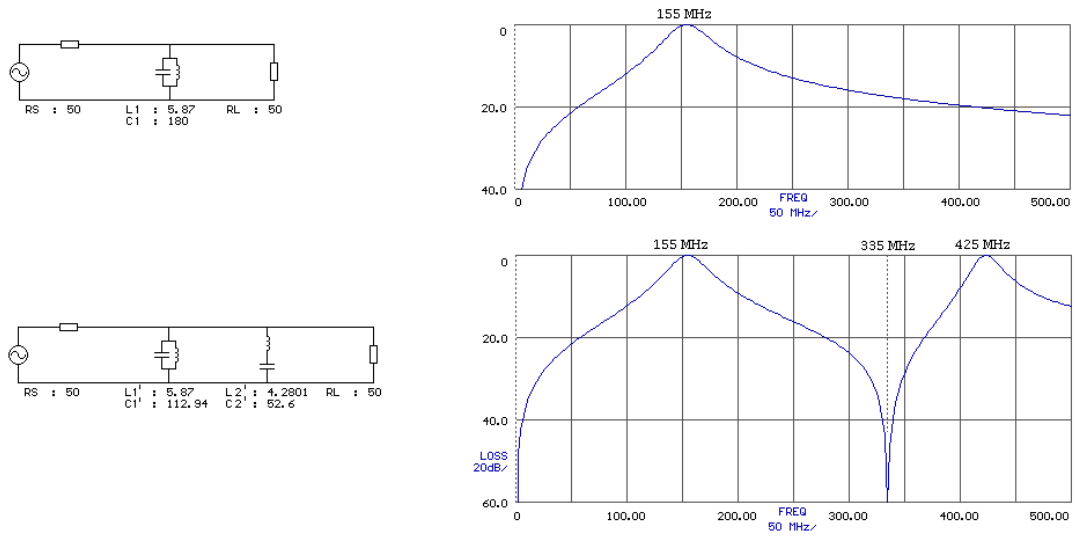


Figure 3.3: A Simple Dual Band Filter Obtained From A Single Band Filter

Consider the resonator containing L'_1 and C'_1 whose resonance frequency is about 155 MHz. Equivalent impedance of this resonator is as shown in Equation 3.6. At the frequencies lower than 155 MHz, L'_1 branch will represent a low impedance to ground so the signal is attenuated. Also, the equivalent impedance of the resonator will be inductive. Similarly, the signals whose frequencies are higher than 155 MHz will be attenuated since C'_1 branch will represent a low impedance to ground and the equivalent impedance of the whole resonator will be capacitive for high frequencies.

$$Z'_{eq1} = \frac{1}{j\omega C'_1 + \frac{1}{j\omega L'_1}} = \frac{j\omega L'_1}{1 - \omega^2 C'_1 L'_1} \quad (3.6)$$

If we investigate the notch resonator whose equivalent impedance is given in Equation 3.7 we see that for the signals lower than resonance frequency, the resonator represents capacitive impedance and for signals higher than resonance frequency, the resonator represents an inductive impedance.

$$Z'_{eq2} = j\omega L'_2 + \frac{1}{j\omega C'_2} = j \frac{\omega^2 C'_2 L'_2 - 1}{\omega C'_2} \quad (3.7)$$

Now, let us divide the frequency spectrum into three regions as shown in Figure 3.4.d. In region-1 and region-2, the equivalent impedance of the notch resonator will be capacitive, thus it will affect the center frequency of the first passband. In the example shown in Figure 3.3, single band filter resonates at 155 MHz. When it is converted to a dual band filter, a notch resonator is added in the shunt arm and the capacitance value of bandpass resonator is changed; i.e, C_1 is 67 pF lower than C'_1 . Note that around 155 MHz, the equivalent capacitance of the notch arm is equal to 66.86 pF as indicated in Equation 3.8. In other words, after addition of the notch resonator, the equivalent circuit becomes as shown in Figure 3.4.a and in order to adjust the first passband again to 155 MHz, value of C_1 should be decreased by an amount equal to the equivalent capacitance of notch resonator. To conclude, values of L_2 and C_2 also affect the center frequency of the first passband.

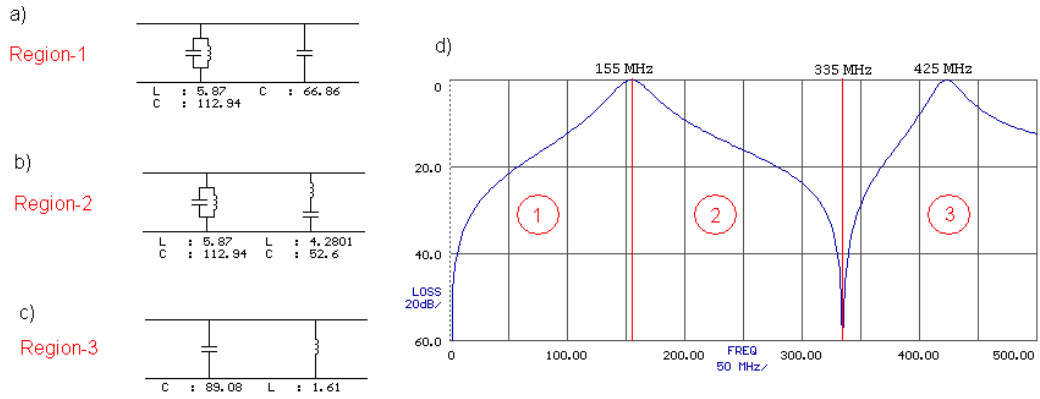


Figure 3.4: Equivalent Circuits of Dual Band Filter for Each Region

$$Z_{eq2}|_{\omega=155MHz} = j\omega L_2 + \frac{1}{j\omega C_2} = j4.166 - j19.53 = -j15.364 = \frac{1}{j\omega C_{eq2}} \quad (3.8)$$

$$\Rightarrow C_{eq2}=66.86 \text{ pF}$$

After the first resonance, equivalent impedance of the bandpass resonator becomes capacitive (Figure 3.4.b). However, it does not affect the notch frequency since it is in parallel with the notch resonator. Notch frequency depends only on L_2 and C_2 .

For the frequencies higher than the notch frequency, the bandpass resonator represents a capacitive impedance and the bandstop resonator represents an inductive impedance as indicated in Figure 3.4.c. This capacitor-inductor pair creates another resonance which yields the second passband. Therefore, the second passband is affected by L_1 , C_1 , L_2 and C_2 .

For example, in the dual band filter shown in Figure 3.3, at 425 MHz equivalent capacitance represented by bandpass resonator can be found to be 89.08 pF as follows:

$$Z_{eq1}|_{\omega=425MHz} = \frac{j\omega L_1}{1 - \omega^2 C_1 L_1} = \frac{j15.66703}{-3.725} = -j4.206 = -j \frac{1}{\omega C_{eq1}} \quad (3.9)$$

$$\Rightarrow C_{eq1} = 89.08 \text{ pF}$$

Similarly equivalent inductance of bandstop resonator can be calculated at 425 MHz as 1.61 nH.

$$Z_{eq2}|_{\omega=425MHz} = j \frac{1 - \omega^2 C_2 L_2}{\omega C_2} = j4.302 = j\omega L_{eq2} \quad (3.10)$$

$$\Rightarrow L_{eq2} = 1.61 \text{ nH}$$

And the resonance frequency of C_{eq1} and L_{eq2} appears at 420 MHz which is so close to the second passband.

CHAPTER 4

VHF/UHF DUAL BAND FRONT END DESIGN AND IMPLEMENTATION

The demand for wide-band and multi-band systems in communication sector is increasing day by day. To fulfill this requirement, receivers covering more than one band should be designed. In this chapter, an example for the usage of dual band filters will be illustrated and implementation of a dual band receiver front-end will be explained. The circuits in the front-end, such as pre-select filter, low noise amplifier, and image reject filter are successfully designed, implemented and tested. At the end of this chapter, the performance of this front-end will be compared to existent single band front-ends.

4.1 Design Constraints

There are two separate single band systems. Properties of these systems are given in Table 4.1. The aim is to design a front-end that works in both bands with same properties as the single band front-ends.

Table 4.1: Basic Properties of VHF and UHF Receiver Systems

	VHF Receiver	UHF Receiver
RF Input Frequency Range (MHz)	136-174	380-470
LO Frequency Range (MHz)	181-219	335-425
IF Frequency (MHz)	45	45
Channel Bandwidth (kHz)	25	25

As it can be seen, for VHF receiver LO frequency is higher than RF input signal; that is,

significant spurious frequencies are higher than desired RF signal. Hence, filters must have higher attenuation at upper stopband. On the other hand, for UHF receiver LO frequency is lower than RF input signal, so the spurious frequencies will also be lower than desired RF signal. Therefore filters must have higher attenuation at lower stopband.

Block diagram of a dual band receiver composed of two single band front-ends is shown in Figure 4.1. Also, block diagram of the targeted dual band front-end is given in Figure 4.2. Design of each part will be discussed in the next sections.

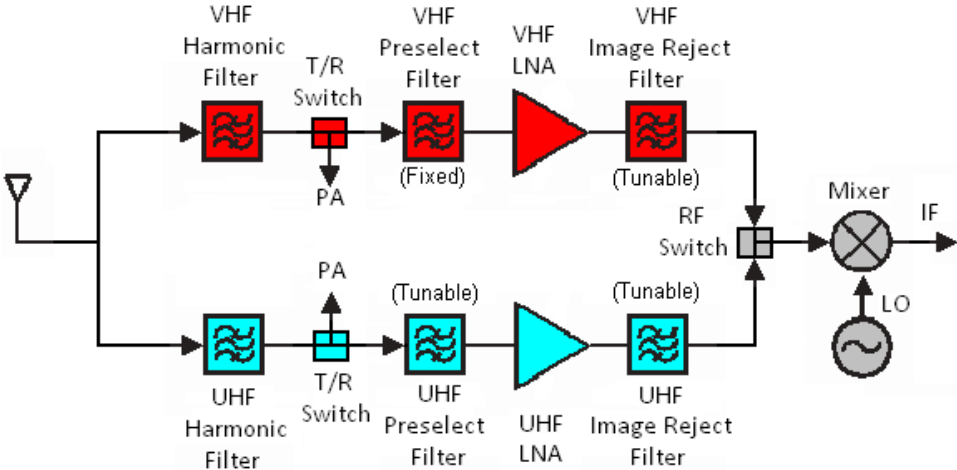


Figure 4.1: Block Diagram of Two Parallel Single Band Front-ends

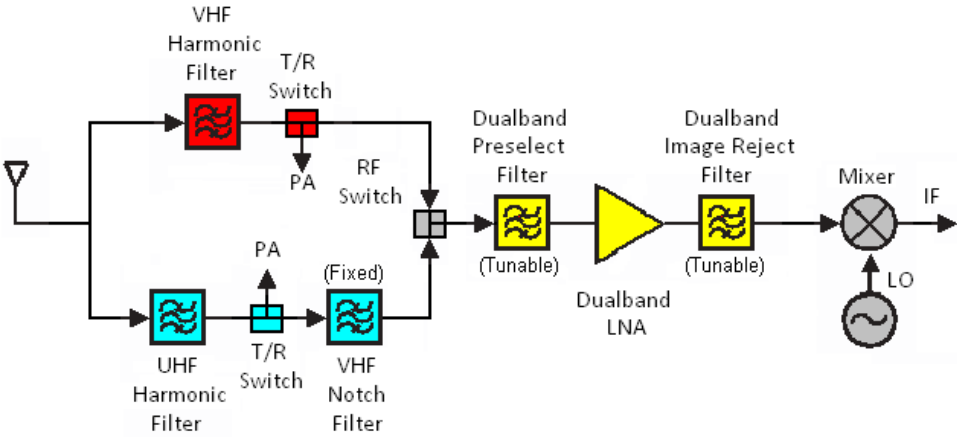


Figure 4.2: Block Diagram of Dual Band Front-end

Design constraints include overall front-end gain, noise figure, linearity, spurious rejection, current consumption and number of elements used. The receiver will be used in a mobile

communication device.

4.2 Design of Dual Band Filters

For VHF band, we have a fixed bandpass filter as pre-select filter and a tunable bandpass filter as image reject filter in the traditional front-end shown in Figure 4.1. Responses of these filters are given in Figure 4.3 and Figure 4.4.

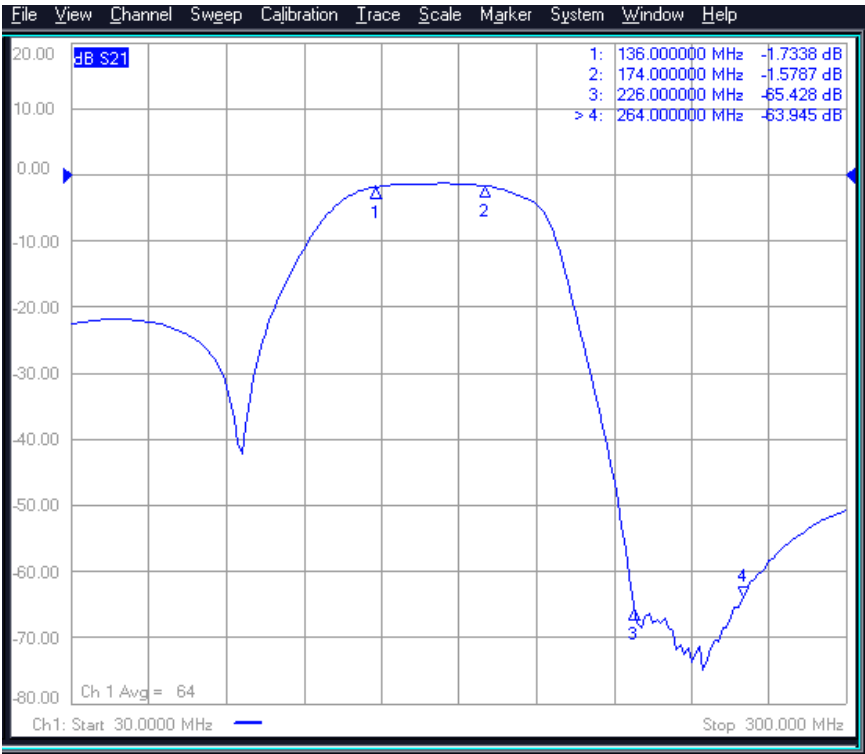


Figure 4.3: Response of Fixed Pre-select Filter between 136 MHz and 174 MHz

For UHF band, we have two tunable bandpass filters. The filter before LNA has a notch in the stopband while the filter after LNA does not have any notch. Both of them have two resonators. Responses of these filters are given in Figure 4.5 and Figure 4.6.

All filters are tuned using varactor diodes at resonators. Tuning voltage, which comes from the charge pump in frequency synthesizer, changes between 1 V and 4 V with respect to the frequency of selected channel. Tunable filters have bandwidth about 20 MHz. In this thesis, attenuation of spurious signals will be considered rather than bandwidth.



Figure 4.4: Response of Tunable Image Reject Filter at 174 MHz



Figure 4.5: Response of UHF Pre-select Filter at 380 MHz



Figure 4.6: Response of UHF Image Reject Filter at 380 MHz

The aim is to design dual band filters that cover both bands with similar insertion losses at passbands and stopbands. Tuning voltage will again change between 1 V and 4 V.

4.2.1 Design With Filpro

The design process started using Filpro. Firstly, a single band bandpass filter is designed at 155 MHz, which is the arithmetic mean of VHF band. After that, this filter is converted to a dual band filter such that its second passband appears at 425 MHz, which is the mean of UHF band. Then, element values are tuned in order to adjust two passbands to 136 MHz and 380 MHz. Finally, element values are retuned such that passbands will be adjusted to 174 MHz and 470 MHz.

Design of the single band bandpass filter is performed using synthesis approach in the following steps:

- Filter Type is selected as lumped, bandpass, equiripple, doubly terminated and type-B.
- Passband ripple is selected as 0.3 dB, two cut-off frequencies are placed to 150 MHz and 160 MHz, termination impedances are typed in as 50 ohms.

- Three TZ's at zero and one TZ at infinity are placed and extracted in the following order: Zero-Zero-Inf-Zero.

As a result, the circuit shown in Figure 4.7.a is obtained.

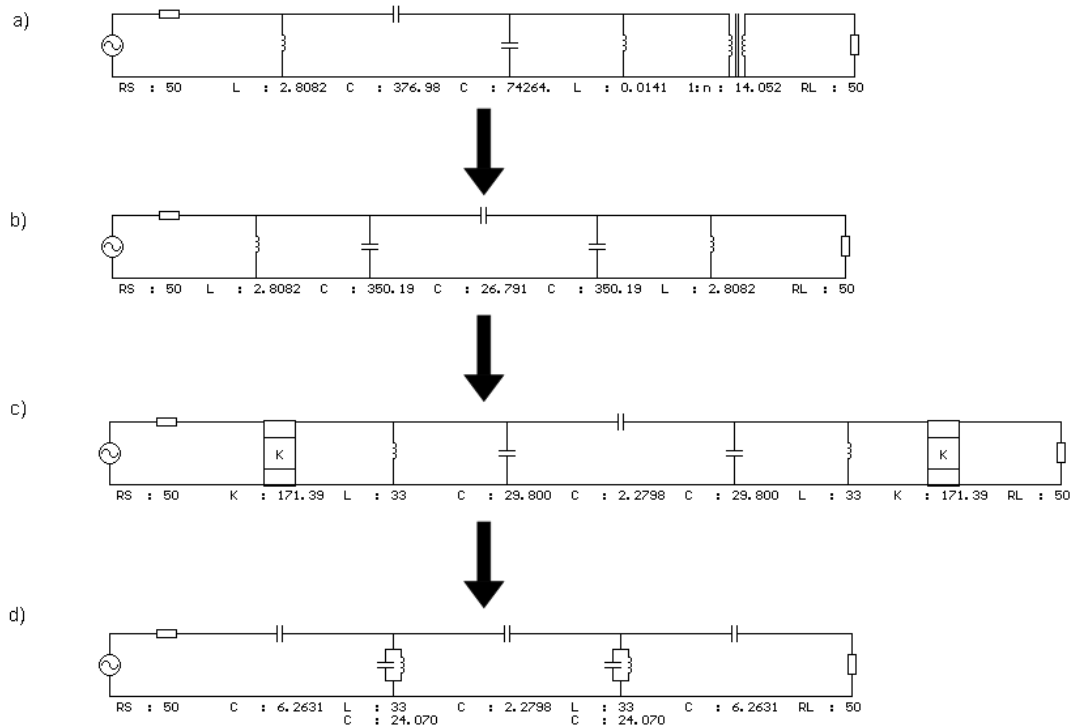


Figure 4.7: Design Procedure of Single Band Filter in Filpro

Then, L-left capacitor pair is transformed into symmetrical pi capacitor pair (Figure 4.7.b). Since the circuit becomes symmetrical and transformer value became very close to 1, the transformer is deleted.

The inductances are scaled to 33nH by placing two inverters at the beginning and at end of the circuit as shown in Figure 4.7.c.

After that the end inverters are replaced by capacitive L sections at 155 MHz. Shunt capacitors came out to be negative but this is not a problem since there are positive capacitances in parallel with those negative ones. After simplifying the circuit, filter given in Figure 4.7.d is obtained. The equivalent shunt capacitor values are positive.

Then, second order resonators are converted to forth order resonators such that the second

passband occurs at 425 MHz which is the mean of UHF band and the dual band filter given in Figure 4.8 is obtained. As it can be seen, inductors and capacitors do not have standard values. Since capacitors in the resonators will be realized using varactor diodes, they do not need to have standard values. Therefore, inductor values are tuned to standard values while the resonance frequencies remain the same. The resultant circuit is obtained as shown in Figure 4.9 and its frequency response is given in Figure 4.10.

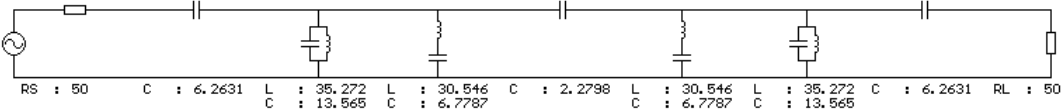


Figure 4.8: Dual Band Filter Obtained from the Single Band Filter

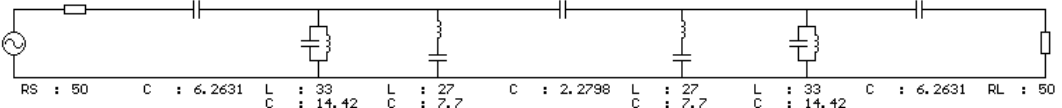


Figure 4.9: Dual Band Filter with Realistic Inductor Values

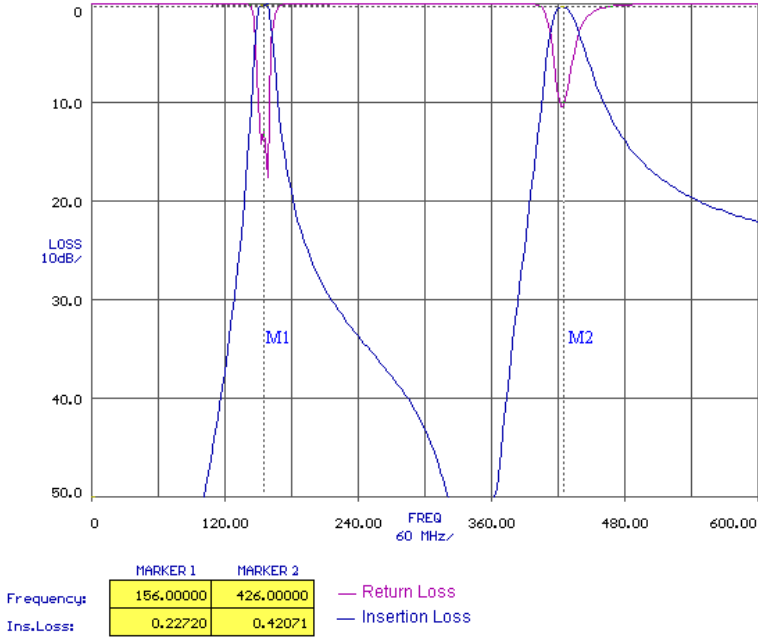


Figure 4.10: Response of Dual Band Filter

Note that while converting the single band filter to dual band filter, series LC resonators are added to circuit and capacitance of parallel LC resonators are decreased to 14.42 pF. If the

circuit is analyzed near 155 MHz, it can be seen that equivalent impedance of series LC resonator is 9.59 pF. Hence the total capacitance seen by 33 nH inductor becomes 24.01 pF so that the resonance again occurs at 155 MHz. This explains why center frequency of first band does not change although the capacitance of parallel LC resonator changes. If same analysis is done at 425 MHz, it can be seen that parallel LC resonator represent an equivalent impedance of 10.17 pF while series LC resonator represent an equivalent impedance of 8.77 nH. Since these equivalent impedances are parallel to each other, they create a new resonance near 425 MHz. Hence, it can be concluded that first and second passbands are affected from both resonators.

Until now, a dual band filter whose passbands are at 155 MHz and 425 MHz has been designed. Its insertion losses at 155 MHz and 425 MHz are about 0.23 dB and 0.42 dB respectively. Also, return losses at the passbands are better than -10 dB. It is required to tune these passbands from 136 MHz to 174 MHz and from 380 MHz to 470 MHz. This filter is optimized so that passbands are located at 136 MHz and 380 MHz by changing the capacitance values in the resonators. Then, it is re-optimized so that passbands are located at 174 MHz and 470 MHz. Values of inductors should remain the same, so this optimization is done by inspection. Element values to adjust the passbands to desired frequencies are as shown in Figure 4.11. The responses of this filter at low-end and high-end of the bands are given in Figure 4.12.

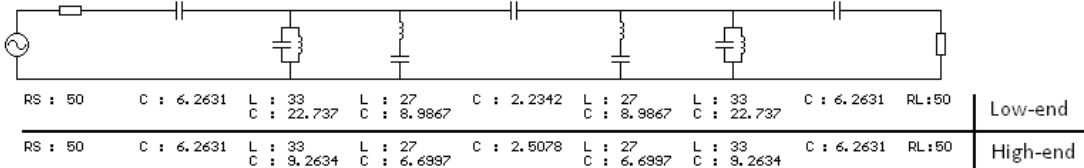


Figure 4.11: Element Values Required to Tune the Dual Band Filter to Low-ends and High-ends of the Bands

Note that inductances remain the same while five capacitances vary as passbands are tuned from low-end to high-end. The bandwidth gets larger at 470 MHz. Insertion losses are very low since ideal elements are used. They are expected to increase when circuit will be implemented.

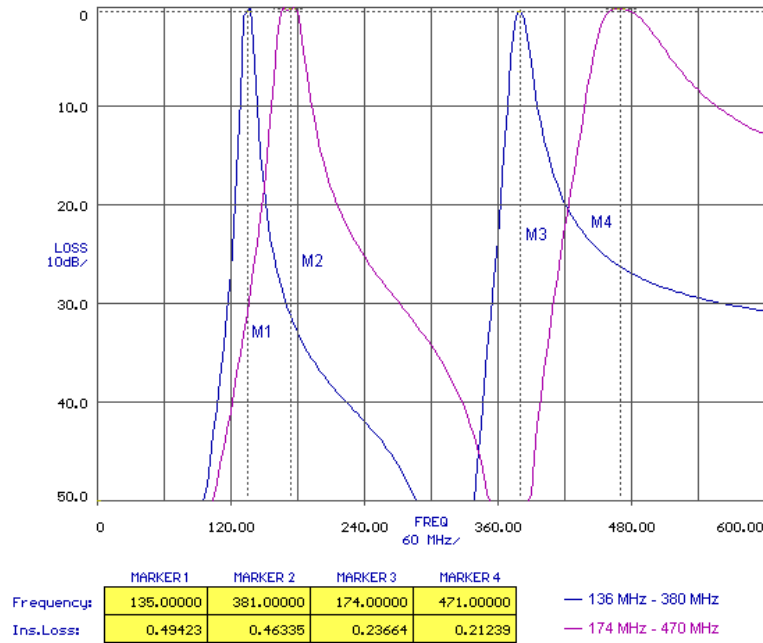


Figure 4.12: Response of Dual Band Filter at Low-ends and High-ends

4.2.2 Optimization With ADS

Until now, the filter has been designed using ideal elements in Filpro. It is simulated in ADS using models of the elements including the effect of layout in order to see more realistic response of it.

Before designing the layout, the packages of elements are decided. All of the capacitances will be 0402 package. The capacitance values at resonators change with respect to the selected frequency so they are realized using capacitor-varactor pairs as shown in Figure 4.13.

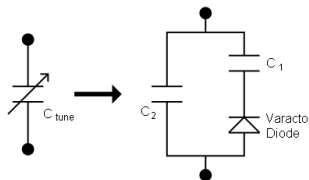


Figure 4.13: Capacitor-Varactor Pair Used to Tune Capacitances at Resonators

The voltage applied to varactors will change from 1 V to 4 V. When 1 V is applied, low-ends of both bands will pass through the filter. When 4 V is applied, high-ends of both bands will

pass. Series resistances of all varactor diodes used in this design are less than 0.5 Ohms.

As it can be seen from Figure 4.11, the capacitances of parallel LC resonators in shunt arm change from 22.737 pF to 9.2634 pF. In order to perform this, 1SV325 varactor diodes can be used. 1SV325 is modeled in ADS using the spice parameters given in its datasheet [23], [24]. When this model is simulated, its capacitance values at 1 V and 4 V come out to be 49 pF and 11 pF respectively. If we place a 39 pF capacitor in series with this varactor and a 1.2 pF capacitor in parallel as shown in Figure 4.13, the equivalent capacitance at 1 V and 4 V becomes 22.92 pF and 9.78 pF which are close to the desired capacitance values.

The capacitances in series LC resonators in shunt arm of the circuit shown in Figure 4.11 change between 9 pF and 6.7 pF. However, when the circuit is simulated in ADS, we observed that it is better if this capacitance changes between 7.5 pF and 5 pF. This capacitance change can be realized using JDV2S25FS varactor diodes. By using the spice parameters given in its datasheet, JDV2S25FS was modeled in ADS [25], [26]. However, simulation results of this model did not fit the data obtained experimentally, so some parameters are changed slightly by inspection. When this model is simulated, its capacitance values at 1 V and 4 V are read as 5.9 pF and 2 pF respectively. Referring to Figure 4.13, if 15 pF capacitor is placed as C1 and 3.3 pF capacitor is placed as C2, equivalent capacitance changes from 7.53 pF to 5.06 pF as the applied voltage changes from 1 V to 4 V.

In this design, inductors of Coilcraft are preferred to be used. Coilcraft already provides models and s-parameters for most of their inductors. 33 nH 0805CS package inductors and 27 nH 0908SQ package inductors of Coilcraft are used. Also, s-parameters for capacitors are also provided by their manufacturers. However, it is seen that using ideal capacitor or model with s-parameters does not affect responses significantly. Therefore, ideal capacitors are used for convenience in optimization process.

The layout is designed via momentum tool of ADS. A two layer card is created. The upper layer is component layer, the lower layer is ground layer and between them Hi-Tg FR4 substrate with thickness of 268 μm is placed. Substrate properties are typed in as $\epsilon_r=4.2$ and $\mu_r=1$ as they are given in datasheet. Conducting metal thickness of the component side is selected as 18 μm . After that, pads of capacitors, inductors and varactors are drawn on layout window and they are connected to each other with microstrip lines having appropriate widths. Inductors that are close to each other were placed perpendicular in order to decrease the cou-

pling between them. Lengths of microstrip lines are as short as possible. Then, this layout is simulated, exported to schematics window and components are placed on the layout as shown in Figure 4.15. The response of this tunable filter is given in Figure 4.16.

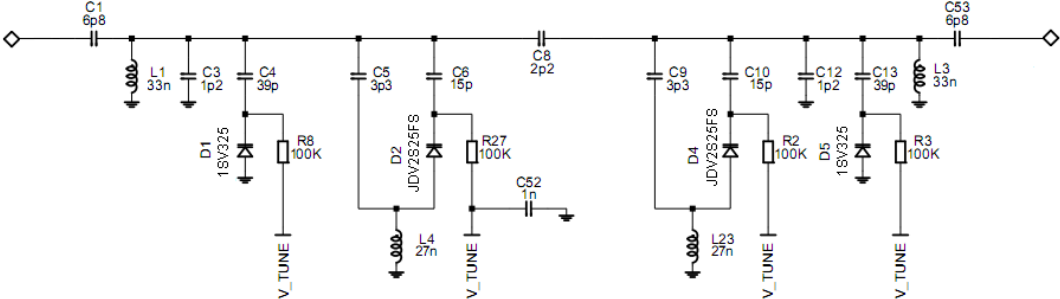


Figure 4.14: Circuit Diagram of Dual Band Filter with Varactor Diodes

As it can be seen, when the filter is simulated using realistic elements and layout, insertion loss increases. Especially the insertion losses at low-ends increased up to 6 dB which is unacceptable. The center frequencies are at the desired frequencies. Also, note that when control voltage is 1 V, the notch appears at 338 MHz which is not an important spurious frequency. In order to attenuate image signal enough, the notch should be moved to the image frequency. Similarly, at high-end response, the notch frequency is 406 MHz and it should also be moved to the image frequency of high-end. As a result, the filter should be optimized to fix the problems mentioned above.

In order to attenuate the image signal sufficiently, we need a notch at the image frequency. Note that there is only one notch between two passbands in the response. However, we need two notches since there are two image frequencies that have to be attenuated; one for VHF band, one for UHF band. For example, when the filter is tuned to low-end, image of 136 MHz will be at 226 MHz and image of 380 MHz will be at 290 MHz. Therefore, both 226 MHz and 290 MHz should be attenuated enough. In order to obtain one more notch, the coupling capacitor is replaced by a parallel LC resonator. Resonance frequency of the coupling resonator is tuned to track the image frequency of VHF band while the resonance frequencies of the shunt notch resonators are tuned to track the image frequency of UHF band. This brings a few more elements to the circuit.

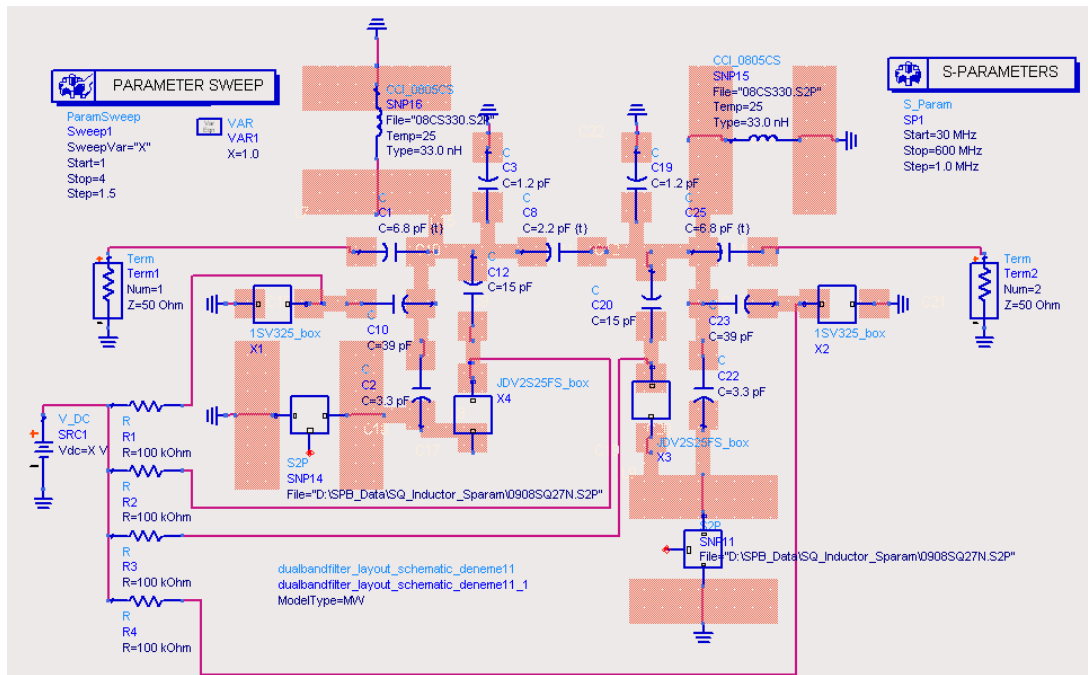


Figure 4.15: Simulation of Designed Dual Band Filter in ADS with Layout

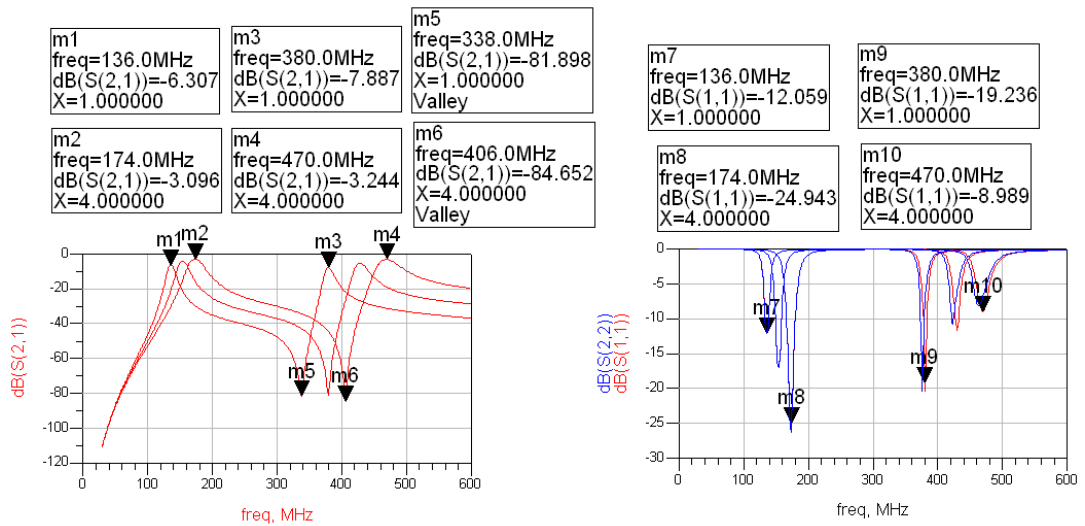


Figure 4.16: Response of Dual Band Filter in ADS

Now, there are five resonators in the circuit. Also, we have two passbands and two notches to be adjusted to the desired frequencies. As mentioned in section 3.4, one resonator can affect more than one constraint of the design. For example, the element values of coupling resonator affect the first notch frequency besides bandwidths and insertions losses of passbands. Similarly, the element values of parallel LC resonators in shunt arms affect the center frequency of both passbands. The element values of series LC resonators in shunt arms affect the frequency of second notch and center frequency of both passbands.

Firstly the resonance frequency of the coupling resonator is decided. When control voltage is 1 V, its resonance frequency should be at 226 MHz. Placing a 68nH inductor in parallel with a 7.3 pF capacitor will create a notch at 226 MHz. When control voltage is 4 V, its resonance frequency should be at 264 MHz. The notch can be tuned to 264 MHz if capacitance is decreased to 5.35 pF while inductance remains 68 nH. Again this capacitance is realized using a capacitor-varactor pair as shown in Figure 4.13. JDV2S07S is used for this purpose. As voltage applied to its terminals change from 1 V to 4 V, its capacitance changes from 4.5 pF to 2 pF respectively [30]. If we select C1 as 4 pF and C2 as 15 pF, equivalent capacitance becomes 7,46 pF for 1 V and 5,76 pF for 4 V. As a result, place of the notch is determined so that image frequencies of VHF band will be attenuated enough by this resonator.

Then, resonance frequencies of the notch resonators in shunt arms are decided. When low-end is selected, their resonance frequencies should be at 290 MHz. In the previous circuit these resonators were composed of a 7.5 pF capacitor in series with a 27 nH inductor and the notch appeared at 338 MHz. In order to tune the notch to 290 MHz, equivalent capacitance in series with 27 nH inductor should be increased to 11 pF. However, if we do this center frequency of second passband will also decrease. Therefore, element values of these resonators should be decided by considering notch frequency and center frequency of second passband simultaneously. This can be done by changing inductance/capacitance ratio of resonator while $L \times C$ product remains constant so that frequency of notch remains at 290 MHz. After a few iterations, appropriate values can be found as 16 nH inductance in series with 19 pF capacitance. Similarly, when high-end is selected, resonance frequency of this resonator should be at 380 MHz. Notch frequency can be tuned to 380 MHz by changing the capacitance to 11 pF while inductance remains as 16 nH. In order to change the capacitance from 19 pF to 11 pF, JDV2S08FS varactor diodes can be used. Its capacitance is 19.5 pF when 1 V is applied to its terminals and this capacitance decreases to 6.5 pF as voltage applied increases to 4 V

[32]. If a 68 pF capacitor is placed in series with JDV2S08FS and a 3.9 pF capacitor is placed in parallel to them as shown in Figure 4.13, the equivalent capacitance changes from 19 pF to 11.3 pF as control voltage changes from 1 V to 4 V.

Next step is to adjust the center frequency of first passband, which is mainly decided by the resonance frequency of the parallel LC resonators in the shunt arm. When low-end is selected, passband should settle at 136 MHz and when high-end is selected, passband should settle at 174 MHz. Suitable element values can be found after making a few iterations. However, note that element values of this resonators also affect the second passband center frequency. Hence, in fact optimization of these resonators is done simultaneously with optimization of notch resonators in the shunt arm. After some iterations it is found that if an inductance of 27 nH is placed in parallel with a capacitance of 14.8pF, center frequency of first passband appears at 136 MHz. For the high end, to tune the first passband to 174 MHz, inductor value should remain as 27 nH and capacitance should be changed to 12 pF. In order to change the capacitance value between 14.8 pF and 12 pF, JDV2S08FS varactor diode can be used. Referring to Figure 4.13, if C_1 is selected as 10 pF and C_2 is selected as 8.2 pF, the equivalent capacitance changes from 14.8 pF to 12.1 pF as control voltage changes from 1 V to 4 V respectively.

Finally, matching is improved in order to decrease insertion losses. To do this, two shunt capacitors are placed at the beginning and at the end of the filter. After a few iterations, final values of the filter elements are obtained as shown in Figure 4.17. Its frequency response is given in Figure 4.19.

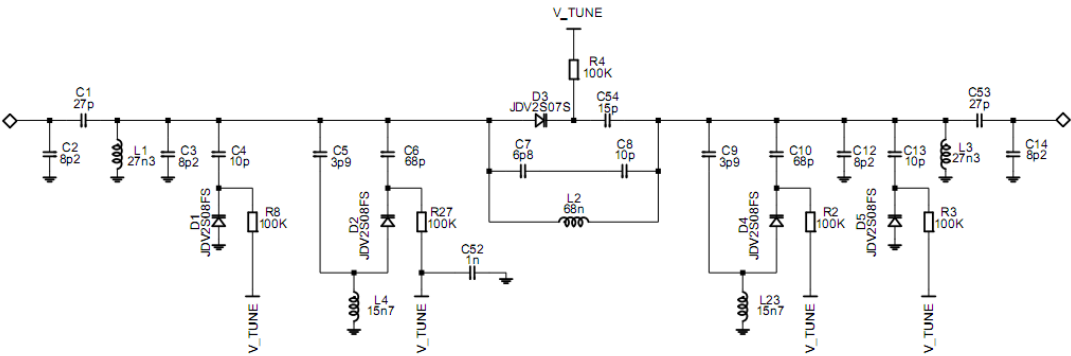


Figure 4.17: Designed Dual Band Filter After Optimization in ADS

Until now, two separate single band filters have been combined as a dual band filter. The

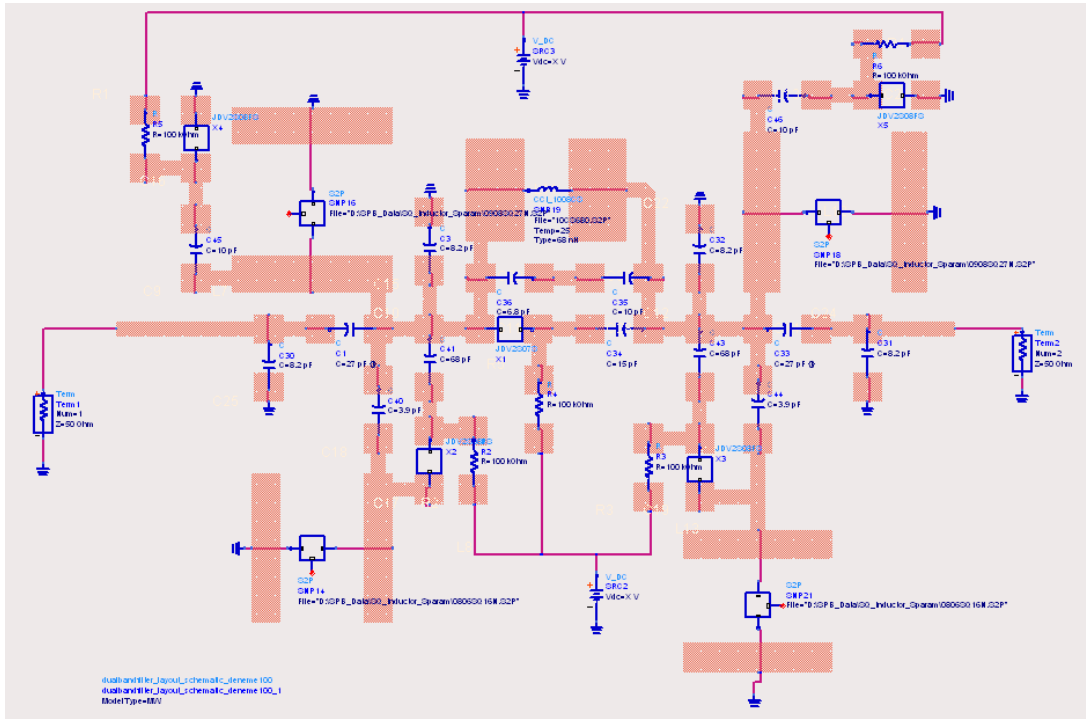


Figure 4.18: Simulation of Dual Band Filter with Layout

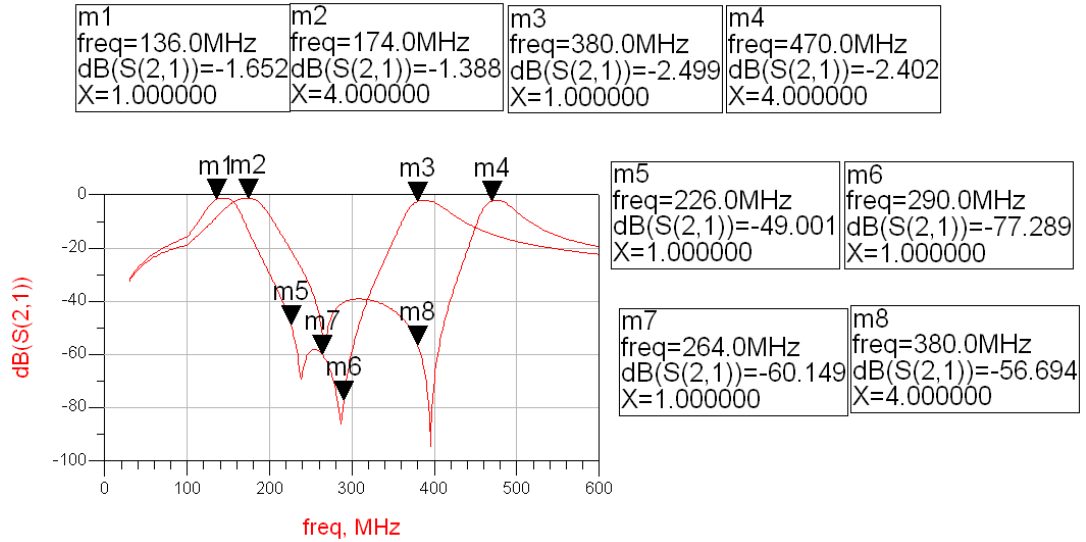


Figure 4.19: Response of Dual Band Filter

disadvantage of this dual band response is that the filter passes both bands. For example when receiver channel is adjusted to 136 MHz, both 136 MHz and 380 MHz will pass through the filter so undesired signals around 380 MHz will not be attenuated at the filter. Hence, the unwanted band should be attenuated such that front-end has only one passband. Solution of this problem will be mentioned in the next sections.

4.3 Harmonic Filters

In a transmitter system, output of the power amplifier (PA) usually passes through a filter so that harmonics of desired signal will be attenuated. Otherwise, harmonics generated by PA can reach to antenna and cause spectral pollution. In our transceiver system, a harmonic filter is used between antenna and T/R switch as shown in Figure 4.1. T/R switch is used to block PA signal to reach receiver side in transmitter mode. When radio is in receiver mode, T/R switch is on and input signal is directed from antenna to receiver. When radio is in transmitter mode, T/R switch is off and PA signal is directed to the antenna. In this thesis, since transmitter circuits is not implemented, only passive elements of T/R switch are included.

Harmonic filter affects the total noise figure of front-end since it is at the beginning of the receiver. Therefore, its insertion loss should be as low as possible for whole band.

Since harmonic filters are important for transmitter part, they can not be implemented as dual-band filters because harmonics of VHF band appears in the UHF band. For instance, when transmitter is adjusted to 150 MHz, its third harmonic at 450 MHz will not be attenuated sufficiently and it will be radiated by antenna if a dual band filter is used as harmonic filters. Therefore, harmonic filters are implemented as two single band filters in a diplexer topology. The antenna is connected to input of this diplexer. The diplexer has two branches: VHF branch and UHF branch. The outputs of these branches are connected to an RF switch whose insertion loss is about 0.3 dB and isolation is better than 50 dB. The output of RF switch is connected to the dual band filter as shown in Figure 4.2.

Also, as mentioned at the end of section 4.2.2, dual band filters pass two bands at the same time. VHF harmonic filter impose a high attenuation at UHF band. When VHF band is selected, VHF Harmonic filter suppress UHF band, so only the desired signal passes through

the front-end without any attenuation. In other words, front-end will have only one passband. However, UHF harmonic filter does not attenuate VHF band significantly. Therefore, when UHF band is selected, both VHF and UHF band signals pass through the front-end. In order to come up with this problem, a notch filter that attenuates VHF band is placed at UHF branch. This VHF notch filter should have very little attenuation at UHF band.

VHF notch filter is designed using Filpro. Firstly, a Bridge-Tee allpass filter is built by inserting elements. All element values are selected as default values. Then, a notch filter is designed from this allpass filter using the principle explained in section 2.6. The elements are tuned to appropriate values. The resultant notch filter and its response are shown in Figure 4.20 and Figure 4.21 respectively.

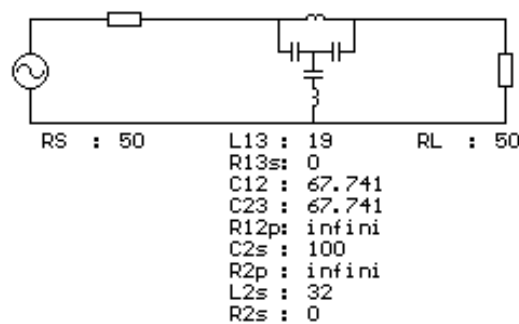


Figure 4.20: Bridge Tee Notch Filter Designed in Filpro

This filter attenuates VHF band more than 20 dB and has insertion loss at UHF band less than 0.14 dB. This amount of suppression at VHF band is not enough, so another notch resonator is cascaded with this filter. The resonance frequency of additional resonator is 174 MHz. After that, element values are changed to realizable values. The final circuit and its response are given in Figure 4.22 and Figure 4.23. As it can be seen, it attenuates VHF band more than 53 dB and its insertion loss at UHF band is less than 0.04 dB. Surely its insertion loss will increase when this filter is simulated using realistic models of elements but this is an acceptable response.

Harmonic filters are not designed again since we can use the harmonic filters that have been used in receiver system shown in Figure 4.1.

As the next step, a simulation including effects of layout and realistic elements is performed using ADS. First of all a suitable layout is designed using momentum tool. For the UHF

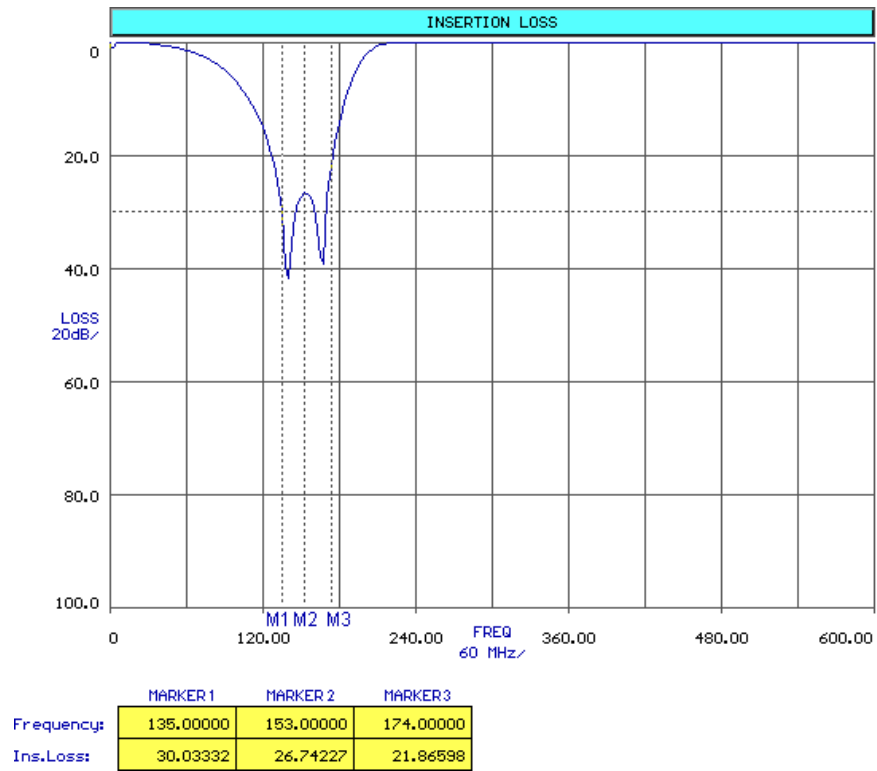


Figure 4.21: Response of Bridge Tee Notch Filter Designed in Filpro

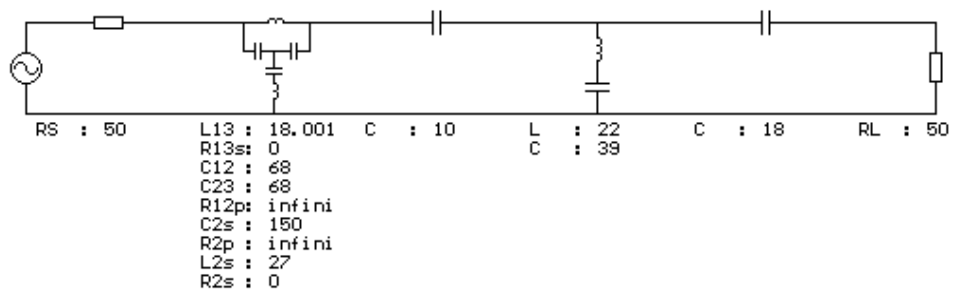


Figure 4.22: VHF Notch Filter Designed in Filpro

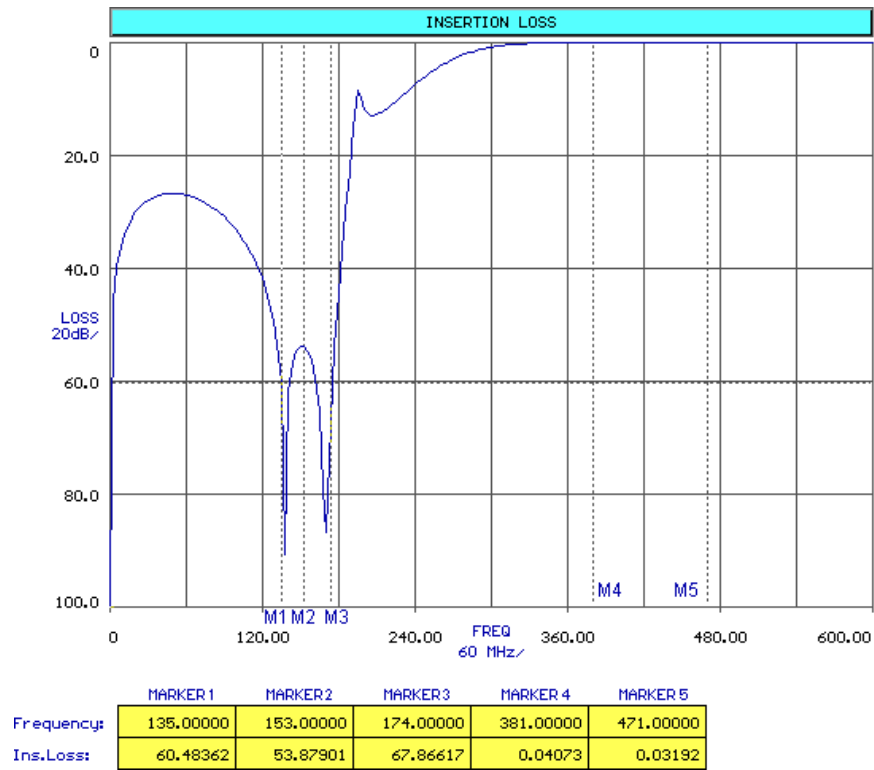


Figure 4.23: Response of VHF Notch Filter Designed in Filpro

harmonic filter, Hi-TG FR4 with thickness of 406 um is used. For VHF harmonic filter and VHF notch filter, substrate thicknesses were set as 268 um. Then, this layout was placed to schematic window and model of each element was located on its pads on the layout. Circuits are shown in Figure 4.24.

Response of VHF notch filter designed in Filpro is shown in Figure 4.27.

Simulation result of UHF branch and VHF branch are given in Figure 4.28 and Figure 4.29 respectively. Affect of RF switch is included in these simulation results.

4.4 Low Noise Amplifier

As mentioned earlier, a low noise amplifier is used in the front-end in order to improve noise performance of the receiver and amplify the input signal. The noise figure of the amplifier should be less than 2.5 dB and a gain of 15 dB will be enough to strengthen the input signal. Total gain of the front-end is expected to be between 10 dB and 11 dB for both bands. Gain

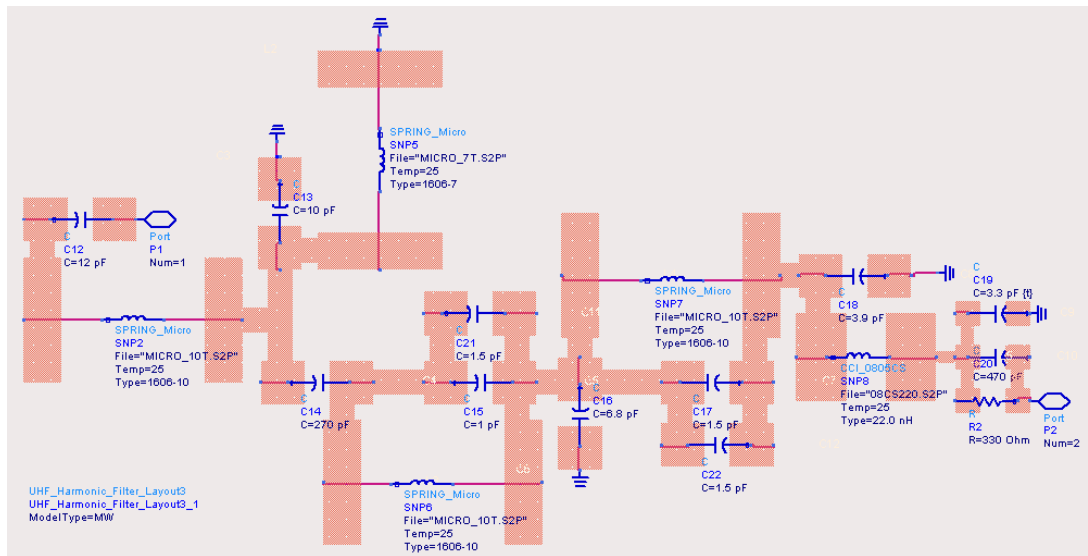


Figure 4.24: Simulation Circuit of UHF Harmonic Filter with Layout in ADS

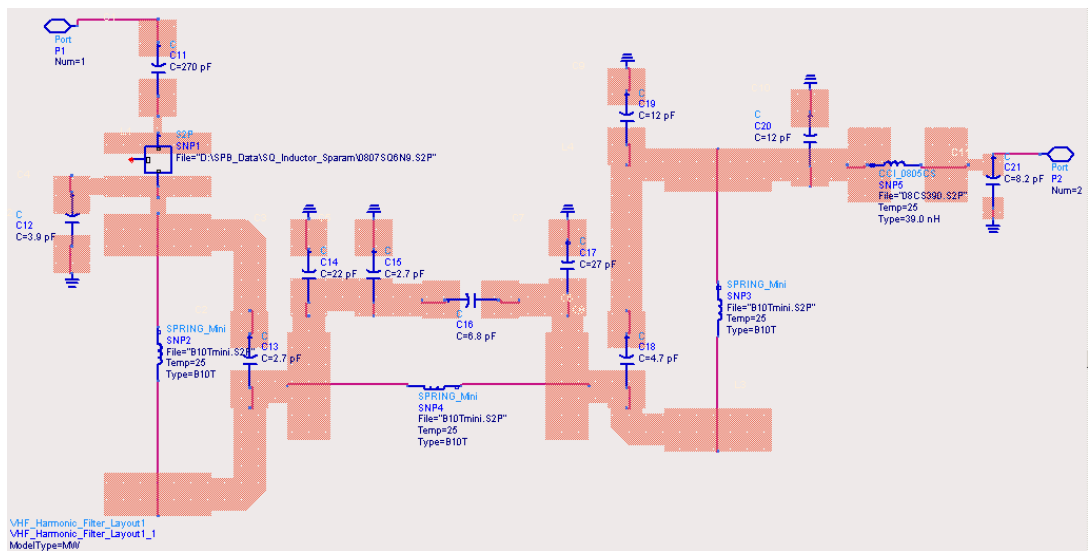


Figure 4.25: Simulation Circuit of VHF Harmonic Filter with Layout in ADS

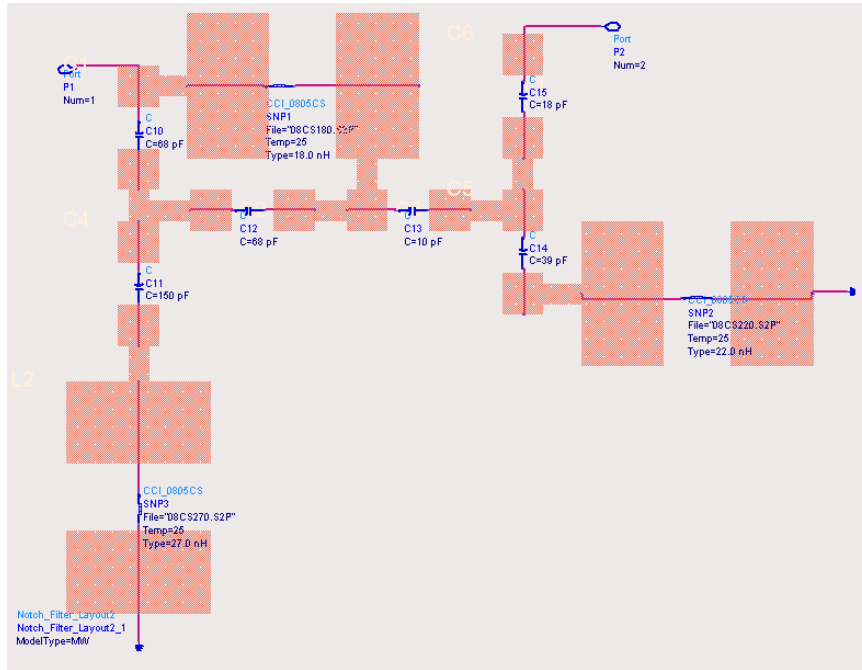


Figure 4.26: Simulation Circuit of VHF Notch Filter with Layout in ADS

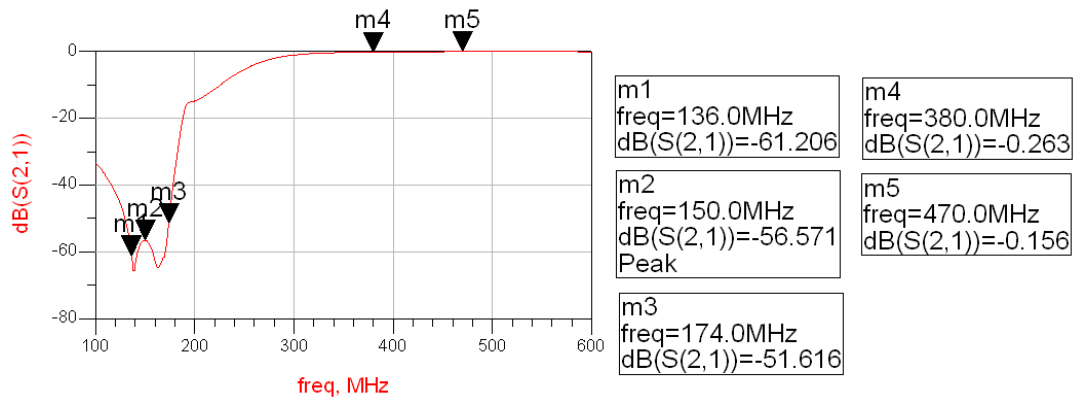


Figure 4.27: Response of VHF Notch Filter in ADS

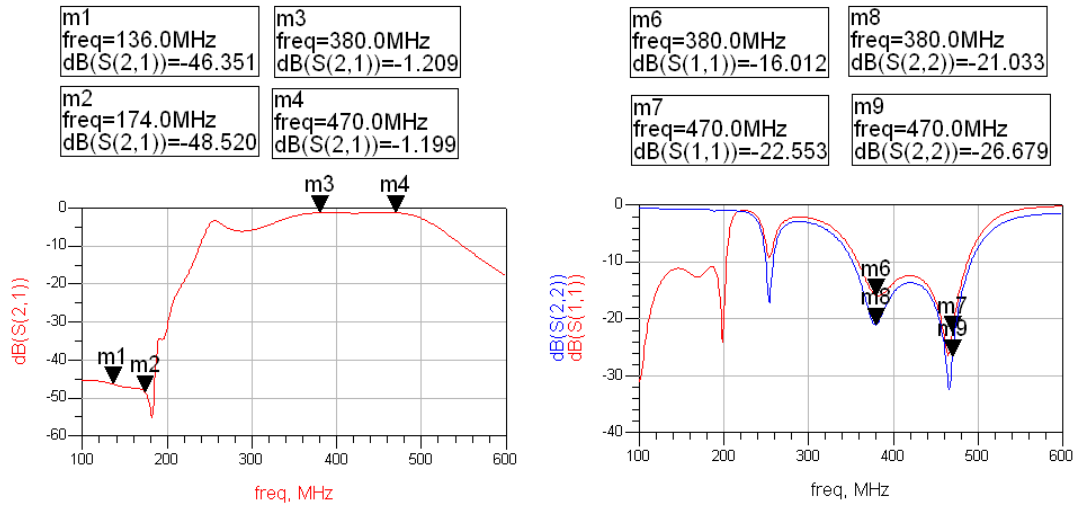


Figure 4.28: Simulation Result of UHF Branch in ADS

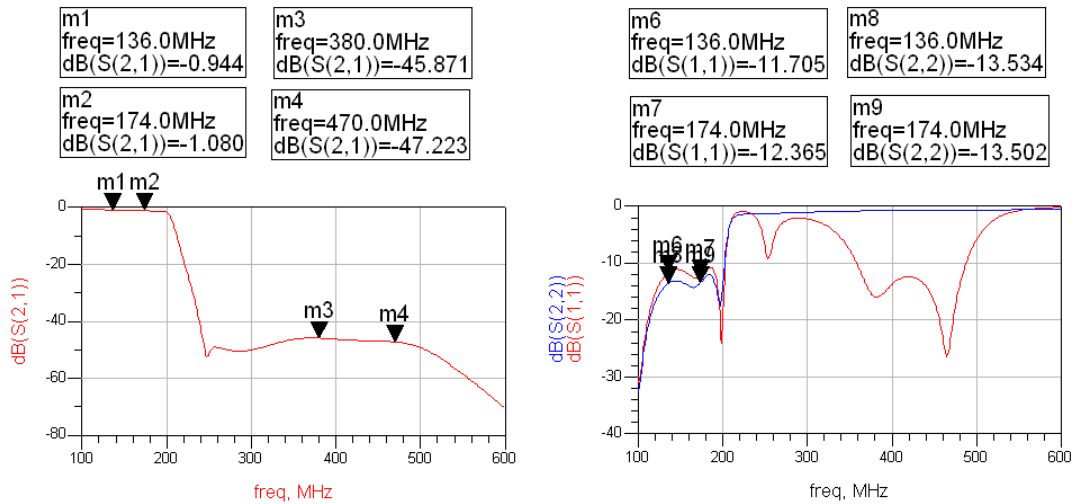


Figure 4.29: Simulation Result of VHF Branch in ADS

flatness is also an important parameter. To ensure same performance for the whole band, gain of LNA should be arranged such that total gain of front-end will not change more than 1 dB with respect to frequency. Another important design constraint is linearity of LNA. Its IIP_3 should be high enough so that IIP_3 of the front-end will be about 0 dBm. Also, S_{11} and S_{22} less than -10 dB are enough for matching. Besides these, amplifier should be stable for the whole spectrum. In order to prevent the amplifier from oscillations, external feedback circuits should be designed carefully since they may lead to instabilities [27].

First of all, LNA is supplied from a 5 V voltage regulator. On the other hand, while deciding current drawn from supply (I_{SS}), a trade-off should be taken into account. According to the rule of thumb given in Equation 4.1, IP_3 can be improved by increasing collector current (I_C) of transistor [28]. Also, gain can be increased by increasing current drawn by LNA. However, noise performance is inversely proportional to current drawn. As I_{SS} increases, noise figure increases too. Also, since this LNA will be used in a mobile receiver system, it will be better to decrease power dissipation as much as possible. Therefore, I_{SS} should be decided in simulation process to satisfy all design constraints. The low noise amplifiers of single band filters draw 6 mA from power supply.

$$OIP_3[dBm] = 10\log(5xV_{ce}xI_c) \quad (4.1)$$

There are some MMIC low noise amplifiers in the market that cover both VHF-UHF bands but their power dissipation are usually too high. RFMD's SGL0363Z RFIC LNA draws nearly 5 mA current from 3.3 V [29]. Its noise figure is very low. Return loss is better than -10 dB. Its gain is given in its datasheet as 20 dB which is too high but an attenuator can be placed after the LNA. Its OIP_3 is given as higher than 13 dB which refers to -7 dB IIP_3 since its gain is about 20 dB. This may be a problem. Another disadvantage of SGL0363Z is that it requires different matching circuits for VHF and UHF bands according to suggested application schematics given in its datasheet. While designing the PCB, a circuit for this RFIC is placed to see whether it works properly after an optimization. However, since there is a risk of failure for SGL0363Z, a discrete LNA is designed using BFR340F and a circuit for it is also placed on the PCB.

Circuit diagram of the designed discrete LNA is given in Figure 4.30. Here, the active bias circuit provides DC bias stability to the LNA. C56 and C65 are used for matching and DC

blocking. L27 and L26 are also used for matching. Besides, they isolate RF signal from the DC bias circuit while not affecting DC biasing. Bypass capacitors are also used to block RF signals since they act as ground at high frequencies. C57, L24 and R1 provide feedback to adjust the gain and gain flatness. R5 is used to improve the stability of LNA, however it degrades the IP_3 performance [28].

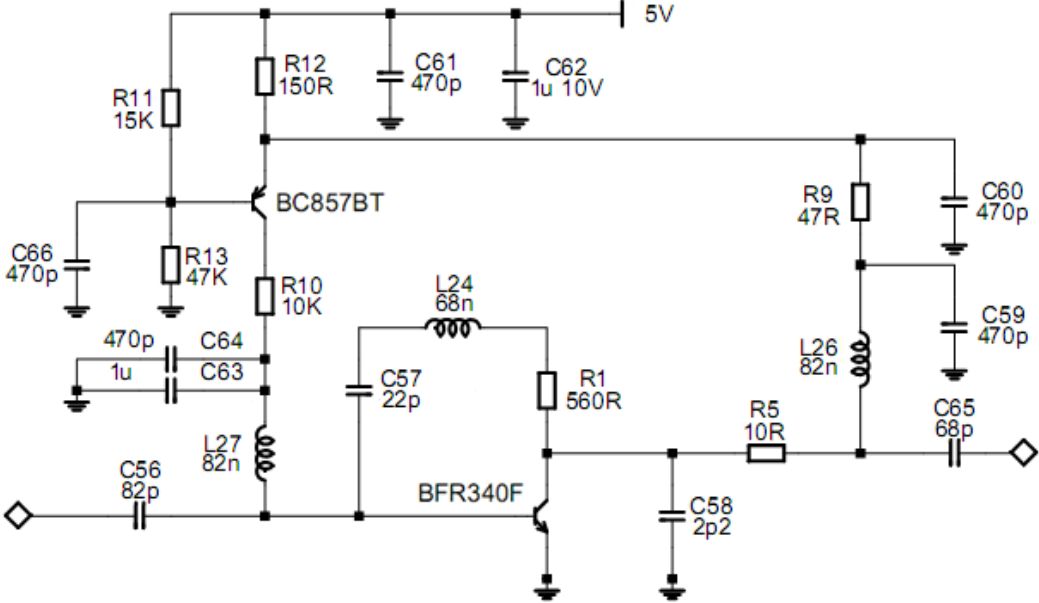


Figure 4.30: Circuit Diagram of LNA

In order to simulate this LNA, a proper layout is designed in ADS as shown in Figure 4.31. The response of the LNA is given in Figure 4.32. As it can be seen, gain of LNA varies between 17.265 dB and 17.530 dB. Gain level and flatness is as desired. S_{11} is lower than -13 dB. On the other hand, highest value of S_{22} is -9.5 dB. These responses are acceptable. However, note that the total losses of filters in UHF band are nearly 1 dB higher than those in VHF band. In practice this difference can be higher. The aim was to have maximum of 1 dB difference in total gain of front-end for the whole band. Therefore, it may be necessary to re-optimize this LNA so that it has higher gain in UHF band.

Referring to the circuit in Figure 4.30, when C56, C57, R1, L26 and C65 are changed to 100 pF, 220 pF, 390 Ohm, 150 nH and 470 pF respectively, gain of LNA becomes higher at UHF than VHF. Response of the circuit with these elements is shown in Figure 4.33. If such a response is needed for LNA in practice, these element values can be used.

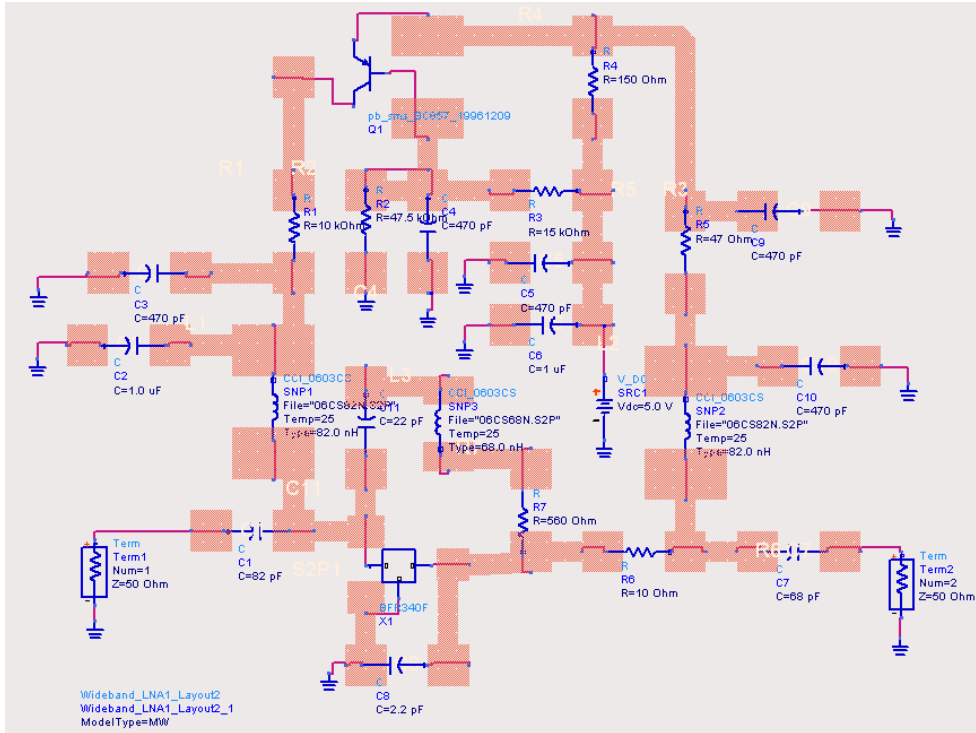


Figure 4.31: Designed LNA Circuit and Layout

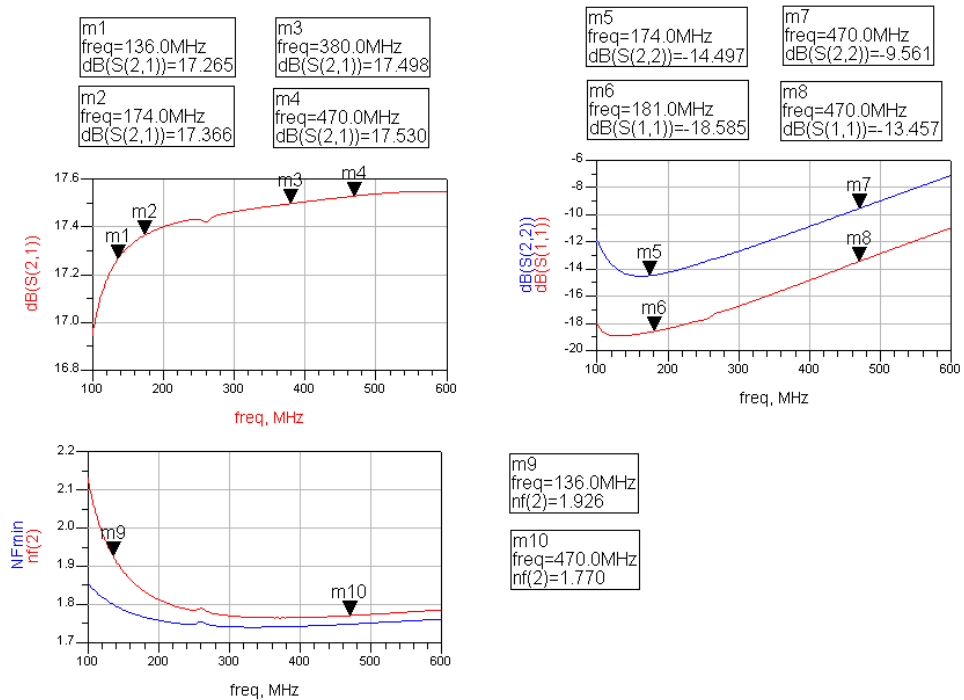


Figure 4.32: Response of Designed LNA

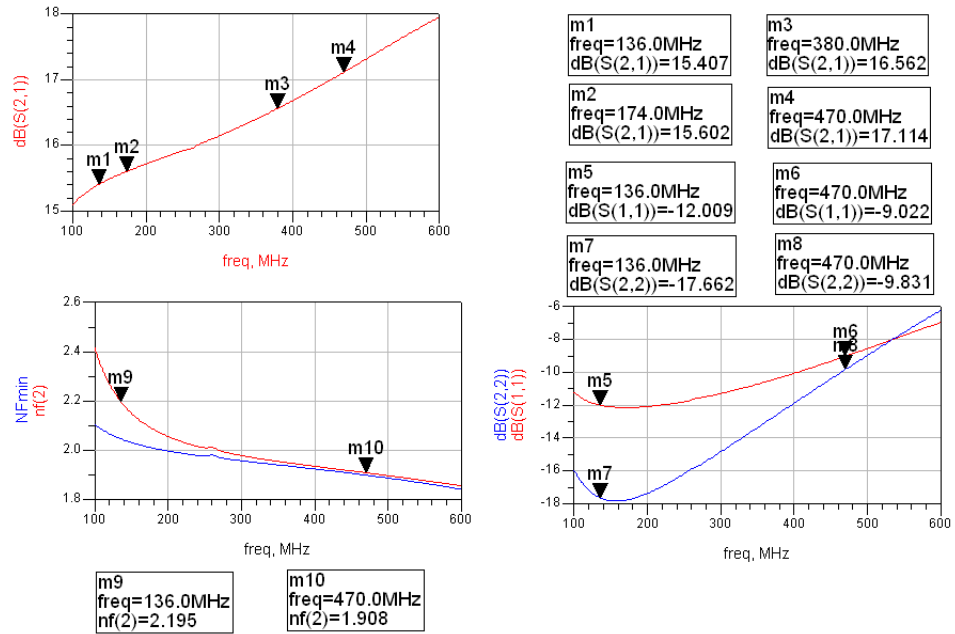


Figure 4.33: Response of Designed LNA After Optimization Such That It Has Higher Gain at UHF Band

4.5 Simulation of Front-end

Until now, each circuit was designed and simulated separately. Now, the performance of all front-end will be investigated by combining the circuits as shown in Figure 4.34. In this figure, V_{tune} is the tuning voltage of dual band filters and $V_{control}$ is the control voltage of RF switch. Receiver frequency can be adjusted via $V_{control}$ and V_{tune} . When $V_{control}$ is low, VHF band is selected and when it is high, UHF band is selected. As V_{tune} is changed between 1 V and 4 V, the selected band changes between low-end and high-end.

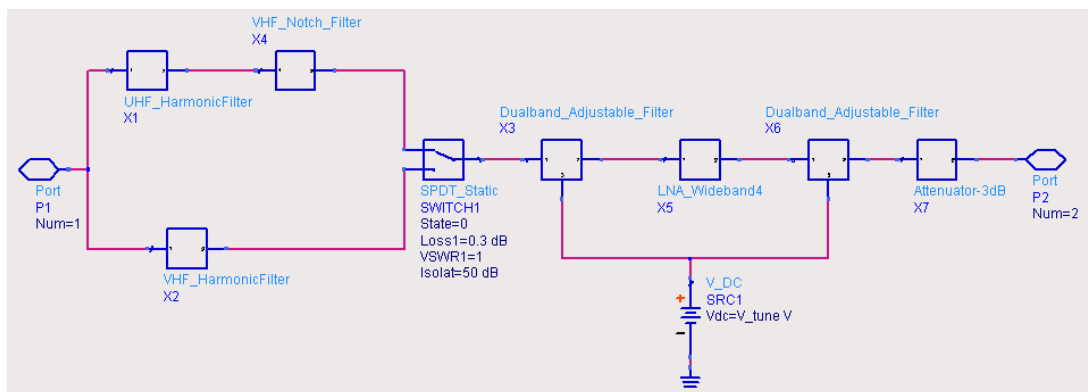


Figure 4.34: Block Diagram of Designed Front-end in ADS

The response of front-end is given in Figure 4.35 and Figure 4.36. As it can be seen, total gain of the front-end changes between 10.3 dB and 10.8 dB for the whole band. Desired gain flatness is achieved. The image frequency is attenuated more than -85 dB. Also, 1/2 IF and 1/3 IF spurious signals are suppressed enough. Besides these, note that when VHF band is selected, UHF band is attenuated about 50 dB and vice versa. These responses are acceptable, so this front-end is implemented.

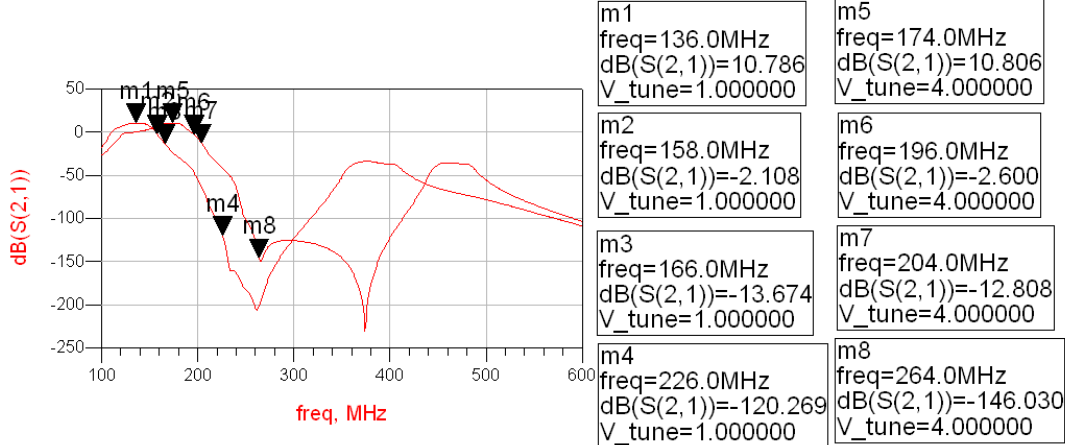


Figure 4.35: Response of Front-End in ADS When VHF Band is Selected

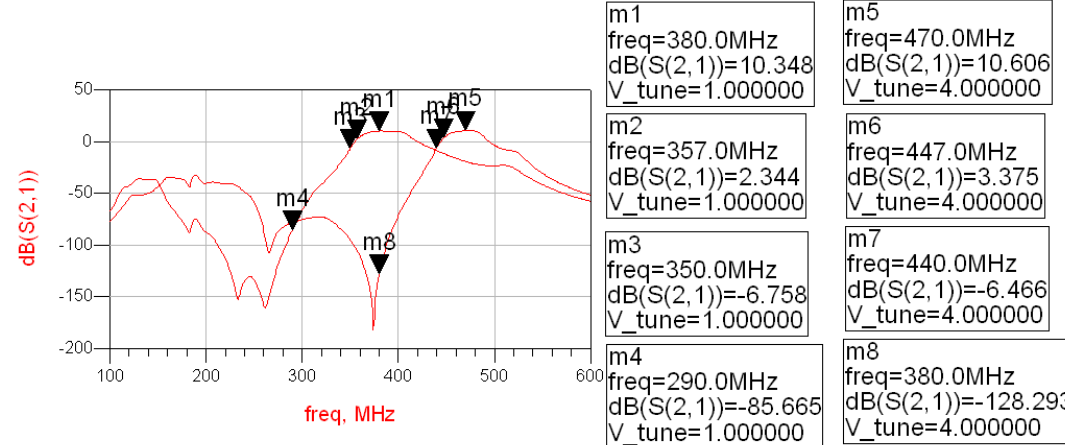


Figure 4.36: Response of Front-End in ADS When UHF Band is Selected

4.6 Implementation of Front-end

In order to test the designed front-end, a printed circuit board is manufactured. While designing and simulating the front-end in ADS, the layout of the circuits, pads of the elements, thickness and properties of substrate were also taken into account. Layout of the PCB is drawn similar to that of simulated circuits as much as possible. PCB is composed of three HI-TG FR4 substrates and four layers as shown in Figure 4.37. The first layer is the component side. Second layer is removed completely. The part of third layer under UHF harmonic filter is removed and the remaining part is set as ground layer. All of the fourth layer is set as ground layer. Paths of DC control voltages are drawn on this layer. As a result, the distance between UHF harmonic filter and ground layer is 406 μm while the distance between other circuits and ground layer is 268 μm . These values are close to the substrate thickness values used in simulations. The component layer of PCB is given in Figure 4.38 and picture of the produced PCB is given in Figure 4.39. As it can be seen, locations of pads of all elements are similar to those in simulated circuits. Also traces are drawn as short as possible. In order to optimize and test each circuit individually, u-fl connectors are located at the beginning and end of each circuit.



Figure 4.37: Layers of Designed PCB

4.7 Test of Front-end

After the PCB is manufactured, measurements of each circuit are performed using Agilent E8801A PNA Network Analyzer, Agilent E3633A DC Power Supply, HP E3620A Dual Out-



Figure 4.38: Component Layer of Designed PCB

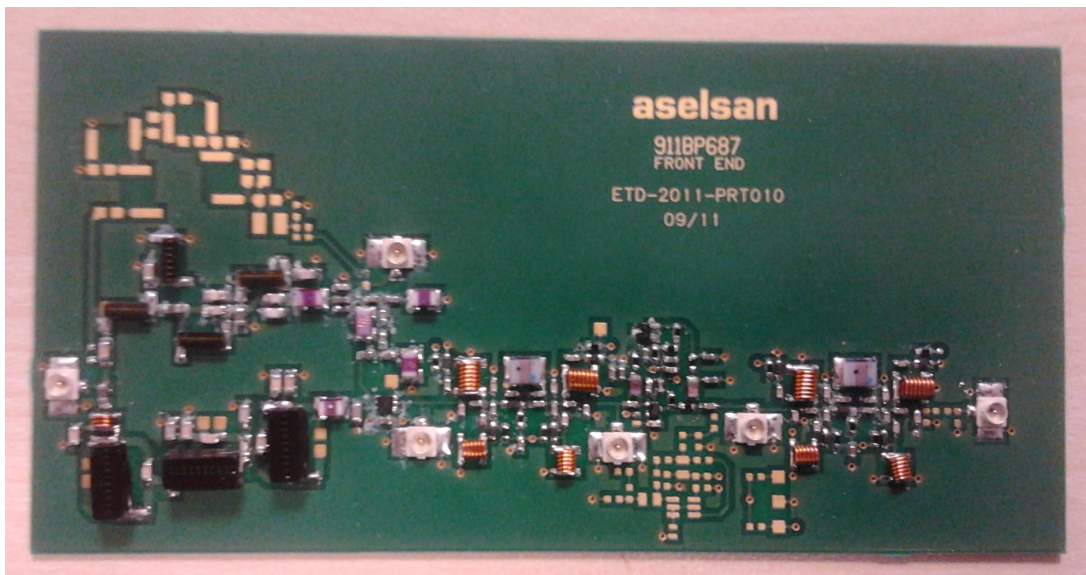


Figure 4.39: Manufactured Printed Circuit Board

put DC Power Supply, HP 8970B Noise Figure Meter, Agilent 346B Noise Source, Agilent E4438C Vector Signal Generator and HP 8590L Spectrum Analyzer. The measurement setup is shown in Figure 4.40.

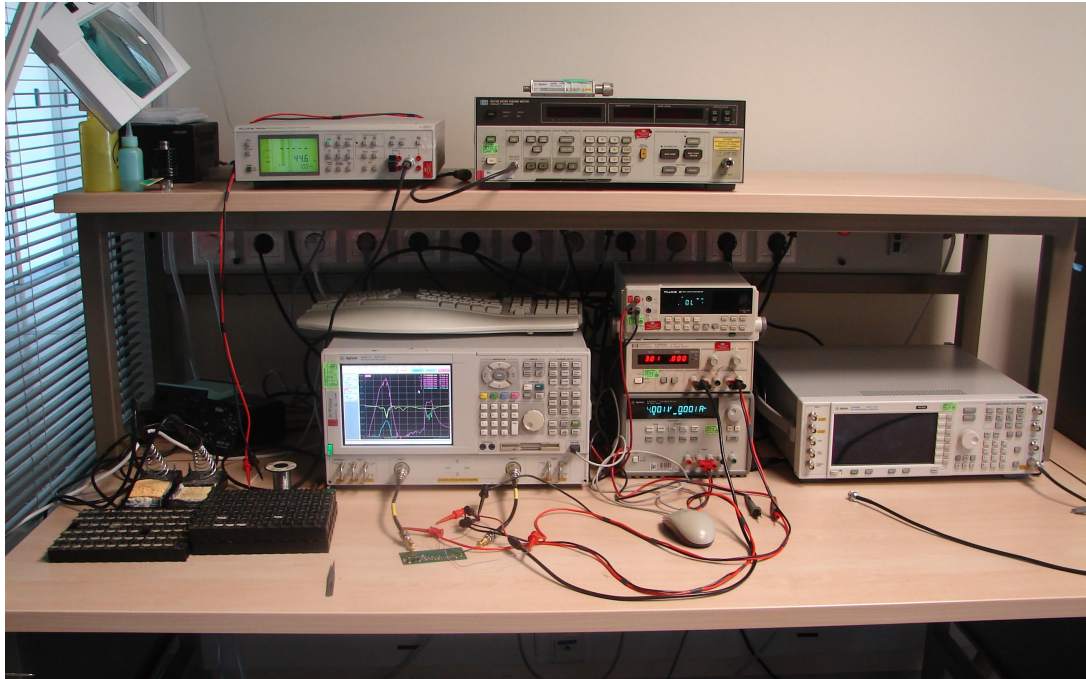


Figure 4.40: Measurement Setup

4.7.1 Test of Dual-Band Filters

First of all, elements of dual band filter are soldered. After testing the filter, it is seen that passbands are at the desired frequencies and attenuations of spurious signals are acceptable. The only problem was that attenuation at UHF is slightly higher than the expected values. This problem is solved by changing the matching capacitances at the input and output of circuit. Referring to Figure 4.17, C2 is changed to 4.7 pF, C53 is changed to 15 pF and C14 is changed to 2.7 pF. Other element values remain the same.

The response of this optimized filter is shown in Figure 4.41 and Figure 4.42. As it can be investigated from these figures, image signals are attenuated more than 40 dB. Also, attenuation levels at other spurious frequencies are enough. Insertion loss at VHF is less than 2 dB while insertion loss at UHF is slightly higher than 2 dB. Besides, return losses are better than -10 dB within the passbands. IIP_3 of this filter is measured as given in Table 4.2. Its

lowest value is +14 dBm at 470 MHz. According to this, pre-select filter do not cause any linearity problem. On the other hand, input signal at antenna is amplified about 12-13 dB until it reaches to image reject filter. Hence, there may be distortion for high input levels at 470 MHz. In short, the filter fits the requirements and it can be used in the front-end.

Table 4.2: IIP3 Performance of Dual Band Filter

Frequency	IIP_3 ($\pm 0.5dB$)
136 MHz	16 dBm
174 MHz	19 dBm
380 MHz	24 dBm
470 MHz	14 dBm

4.7.2 Test of Harmonic Filters

First, elements of VHF notch filter are soldered and its response is observed as shown in Figure 4.43. Its insertion loss at UHF is lower than 0.34 dB and suppression of VHF band is higher than 45 dB. Since this response is acceptable, no optimization is made for this filter.

Then, elements of UHF and VHF Harmonic Filters are placed on the PCB. Insertion loss of UHF branch appeared as 2 dB at 470 MHz. Therefore, element values are slightly tuned until having an acceptable response. Finally, the responses shown in Figure 4.43 and Figure 4.45 are achieved. These responses exclude the effect of RF switch. As it can be seen, insertion loss of UHF branch is lower than 1.37 dB in UHF band while its attenuation in VHF band is more than 33 dB. Insertion loss of VHF branch is lower than 1 dB in VHF band and it suppresses UHF band more than 60 dB. Note that insertion loss of UHF branch is slightly more than that of VHF branch due to the notch filter in UHF branch. IIP_3 of harmonic filter branches were measured better than +28 dBm for all frequencies including the effect of RF switch.

4.7.3 Test of LNA

Then, the elements of LNA are soldered and its response is observed. Excluding S_{22} , it is as expected. By making a few optimizations, the response shown in Figure 4.46 is obtained.



Figure 4.41: Response of Dual Band Filter When Tune Voltage is 1 V



Figure 4.42: Response of Dual Band Filter When Tune Voltage is 4 V

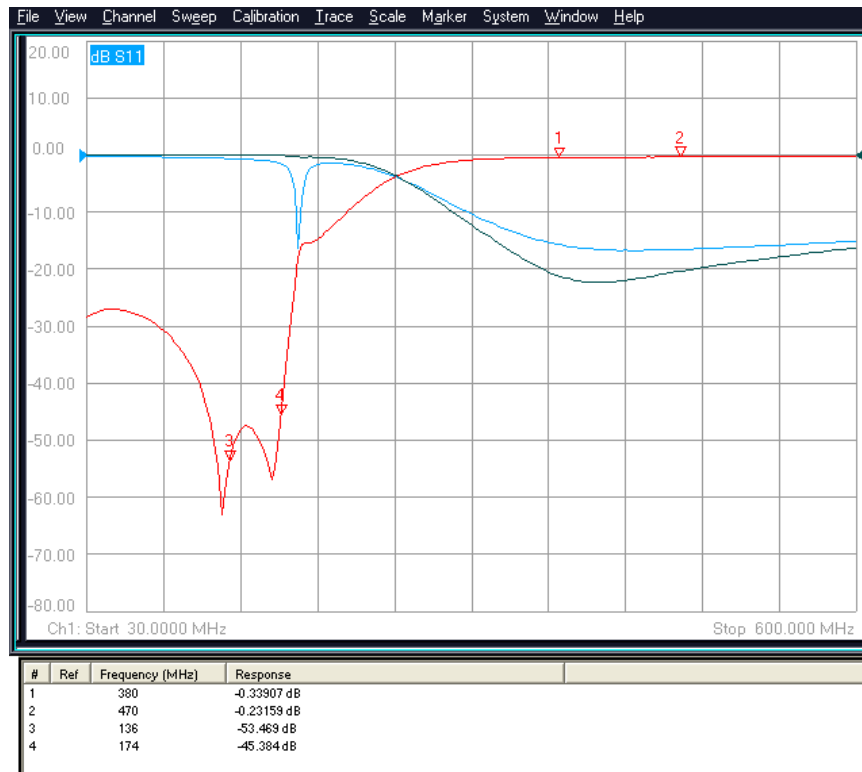


Figure 4.43: Response of VHF Notch Filter

As it can be seen, S_{21} changes between 15.7 dB and 15.4 dB while S_{11} and S_{22} are better than -9.5 dB. Each dual band filter has nearly 0.75 dB higher insertion loss at UHF. Also, insertion loss of UHF harmonic filter is 0.5 dB higher than that of VHF harmonic filter. If this LNA is used, there will be about 2 dB difference between gain of front-end at UHF and VHF. Hence, LNA shown in Figure 4.47 is used in front-end and its response are given in Figure 4.48.

Input IP_3 of this LNA is measured as given in Table 4.3 and its lowest value is -4 dBm at 470 MHz. Also, its noise figure is lower than 2.5 dB for the whole band. This LNA is usable for the front-end.

Table 4.3: Noise Figure and IIP3 Performance of LNA

Frequency	Noise Figure (± 0.2 dB)	IIP_3 (± 0.5 dB)
136 MHz	2.4 dB	0.5 dBm
174 MHz	2.3 dB	0.7 dBm
380 MHz	2.4 dB	-2.5 dBm
470 MHz	2.3 dB	-4.0 dBm

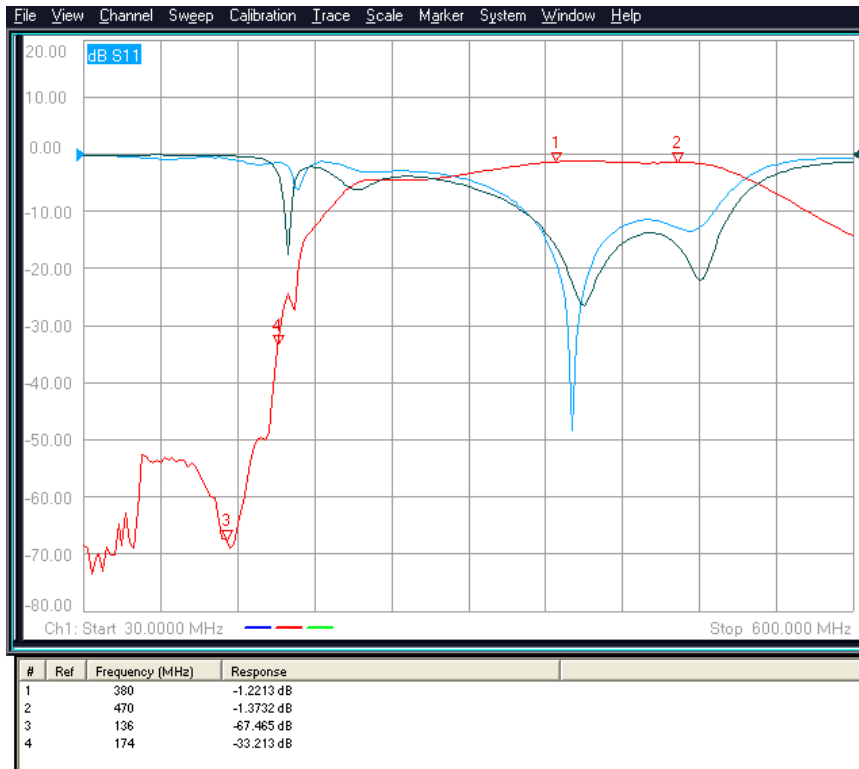


Figure 4.44: Response of UHF Branch

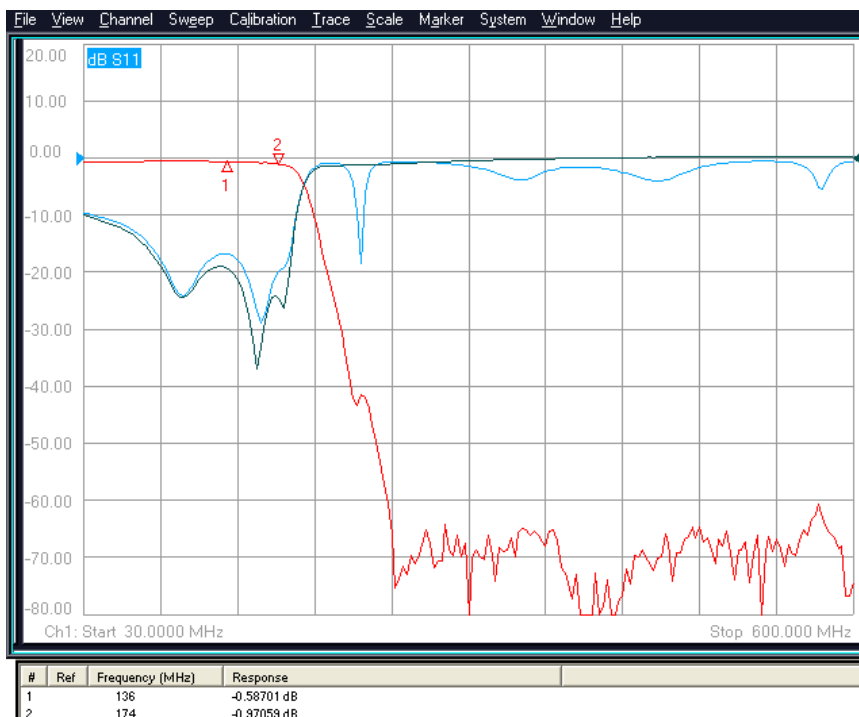


Figure 4.45: Response of VHF Branch

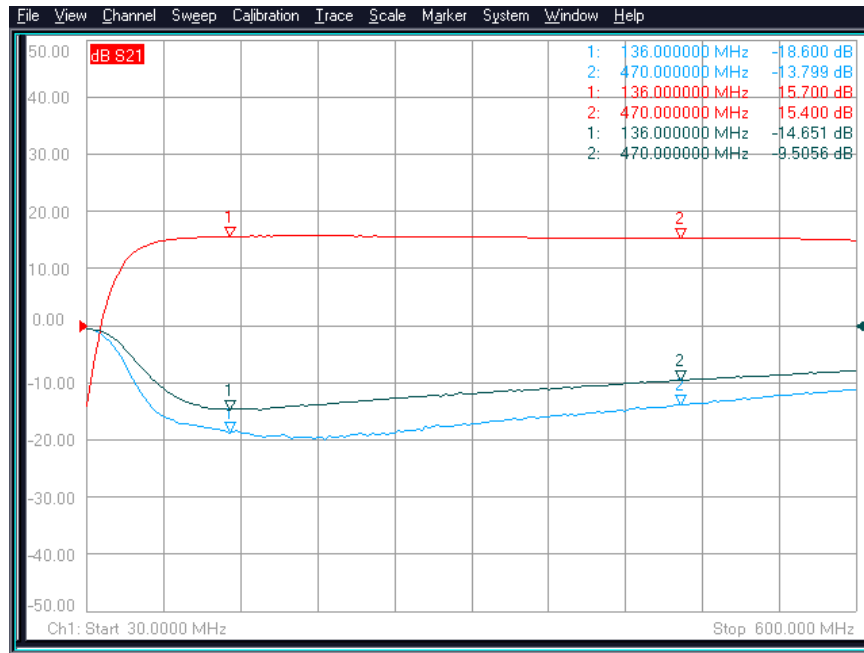


Figure 4.46: Response of LNA

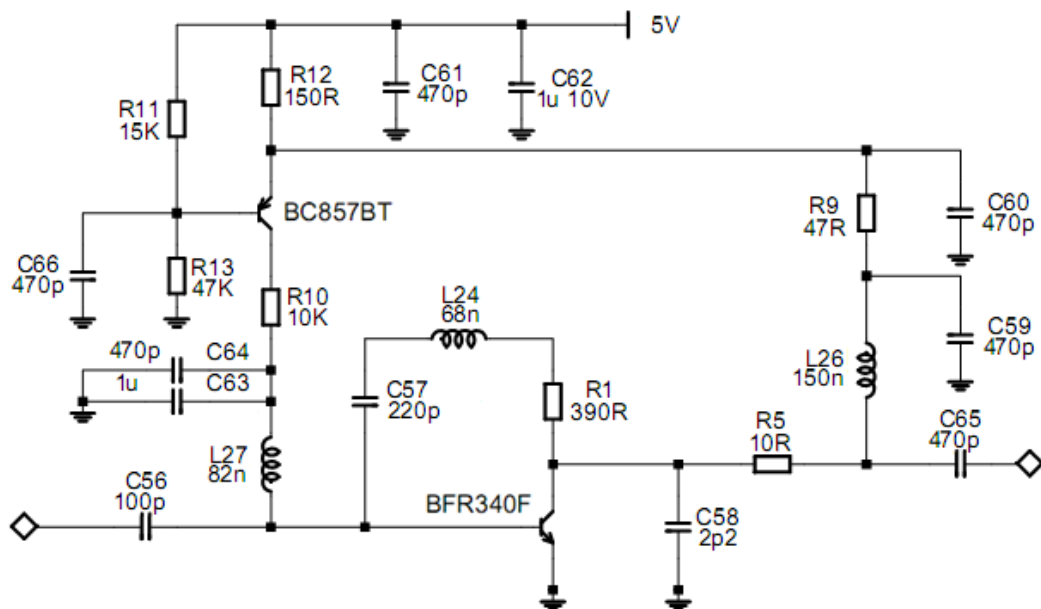


Figure 4.47: Circuit of LNA After Optimization

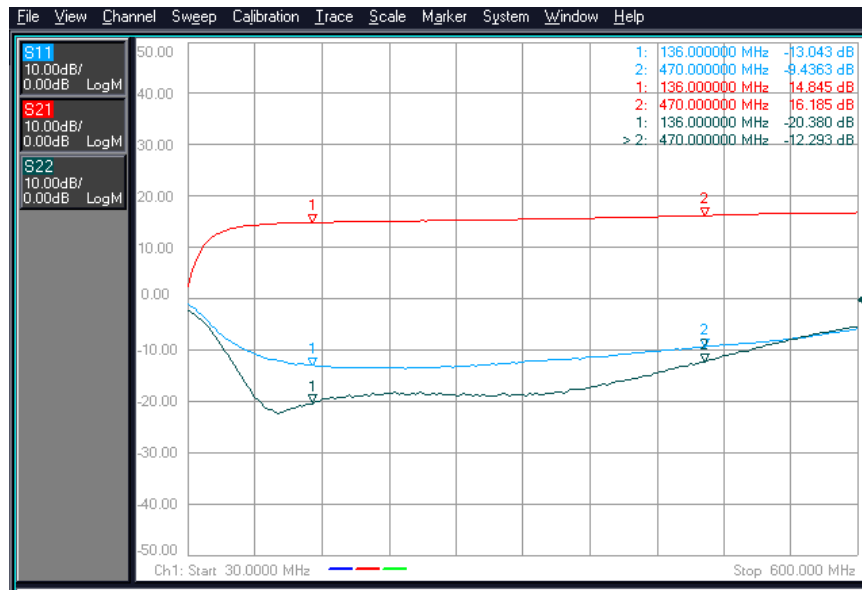


Figure 4.48: Response of LNA After Optimization

4.7.4 Test of Dual Band Front-end and Comparison with Single Band Front-ends

In this section, responses of designed dual band front-end will be discussed and compared to the simulation results and response of traditional single band front-ends. Responses of simulated dual band front-end, manufactured dual band front-end and single band front-ends are illustrated in Figures 4.49 to 4.64. Also, noise figure and IIP_3 of produced dual band front-end are measured as given in Table 4.4.

To begin with, S_{21} of dual band front-end changes between 10.38 dB and 10.82 dB. To adjust the gain level to these values, a 1 dB attenuator is placed at the end of the front-end. Targeted gain level and gain flatness are reached. Besides, S_{11} and S_{22} are lower than -10 dB for whole band as desired.

As illustrated in Table 4.4 noise figure is lower than 6.4 dB and input third order interception point is higher than -3 dBm. Noise figure is observed for the whole band and it does not exceed 6.4 dB which occurs at 470 MHz. The aim was to have a noise figure between 5 dB and 6 dB. This goal was decided by considering the performance of single band front-ends and need for an additional filter was not estimated. However, for UHF band, we had to place a notch filter to suppress VHF band. Since this filter is in front of LNA, its loss at UHF band causes an increase in noise figure. Besides, the loss of RF switch degrades the noise figure

performance, too. Hence, for UHF band, goal can be extended and 6.4 dB noise figure can be accepted. Note that, at VHF band there is no additional filter before the LNA, so the goal for noise figure is reached.

Table 4.4: Noise Figure and IIP₃ Performance of Dual Band Front-end

Frequency	Noise Figure ($\pm 0.2dB$)	IIP ₃ ($\pm 0.5dB$)
136 MHz	5.3 dB	0 dBm
174 MHz	5.6 dB	-0.5 dBm
380 MHz	6.1 dB	-1.5 dBm
470 MHz	6.4 dB	-3.0 dBm

On the other hand, IIP₃ is only measured at four frequencies given in Table 4.4. The lowest value was observed at 470 MHz as -3 dB. The aim for IIP₃ was 0 dBm. Test results are close to the goal. This much of IIP₃ can be accepted since it results in 75.6 dB IMD. If a better IP₃ performance is needed, the cause of degradation in IP₃ should be found and that part should be re-designed. Harmonic filters do not have any active component, so they are not expected to cause a degradation in linearity of front-end. As mentioned in Chapter 1, linearity of the filter after LNA should be higher since it has the highest input signal level. In our design, same dual band filter is used before and after the LNA. The slight difference between test results and goal may be caused by the dual band filter after LNA. IP₃ performance can be improved by using another dual band filter that has higher IIP₃ instead of the dual band filter after LNA. Additionally, the gain of front-end changes actually between 11.4 dB and 11.8 dB. In order to decrease total gain, a 1 dB attenuator was placed at the end of the front-end. If gain of LNA can be decreased 1 dB for the whole band, aimed gain and gain flatness can be reached without a need for an attenuator. By this way, the signal level at the input of second dual band filter will decrease 1 dB and the IIP₃ performance of front-end will be better. This can also be done by placing the 1 dB attenuator between LNA and second dual-band filter instead of placing it at the end of front-end. However, IIP₃ of dual band filter was high enough at 380 MHz. Its lowest value was 14 dBm at 470 MHz. Therefore, the slight difference in IIP₃ at 380 MHz is most probably caused by another circuit. If it is caused by non-linearity of LNA, it should be re-designed such that it has higher IP₃. In order to increase the linearity of LNA, current drawn by it can be increased. However, this may lead to an increase in noise figure and gain of the amplifier. Hence, it may be necessary to re-design the LNA. Since -3 dB IIP₃

is enough for 75 dB IMD performance, no optimization is done for LNA and double band filter.

Actually, by using the formula of IIP_3 for cascaded stages, the guilty of degradation in total IIP_3 can be found as follows:

at 380 MHz \Rightarrow

$$\begin{aligned}\frac{1}{\ddot{u}p_{3,total}} &= \frac{1}{\ddot{u}p_{3,HF}} + \frac{G_{HF}}{\ddot{u}p_{3,DBBPF}} + \frac{G_{HF}G_{DBBPF}}{\ddot{u}p_{3,LNA}} + \frac{G_{HF}G_{DBBPF}G_{LNA}}{\ddot{u}p_{3,DBBPF}} \\ &= \frac{1}{631} + \frac{0.755}{251} + \frac{0.755 \times 0.63}{0.562} + \frac{0.755 \times 0.63 \times 39.81}{251} \\ &\approx 0 + 0.003 + 0.846 + 0.075 = 0.925 \\ &\Rightarrow IIP_{3,total} = 0.34dB\end{aligned}\quad (4.2)$$

In the calculation of total IIP_3 , since IIP_3 of harmonic filter is too high, the first term vanishes. Third term is the highest one (0.846) which corresponds to IIP_3 of LNA. Hence, it can be said that LNA causes degradation in total IIP_3 at 380 MHz. Similar analysis can be performed at 470 MHz.

$$\begin{aligned}\frac{1}{\ddot{u}p_{3,total}} &= \frac{1}{\ddot{u}p_{3,HF}} + \frac{G_{HF}}{\ddot{u}p_{3,DBBPF}} + \frac{G_{HF}G_{DBBPF}}{\ddot{u}p_{3,LNA}} + \frac{G_{HF}G_{DBBPF}G_{LNA}}{\ddot{u}p_{3,DBBPF}} \\ &= \frac{1}{631} + \frac{0.729}{25} + \frac{0.729 \times 0.59}{0.4} + \frac{0.729 \times 0.59 \times 39.81}{25} \\ &\approx 0 + 0.029 + 1.075 + 0.685 = 1.789 \\ &\Rightarrow IIP_{3,total} = -2.5dB\end{aligned}\quad (4.3)$$

Again, the highest term is the third one which corresponds to IIP_3 of LNA. Therefore, if LNA is re-optimized such that it has a higher IIP_3 , total IIP_3 of system can be improved. Image reject filter also affects IIP_3 of front-end. Note that calculated total IIP_3 is very close to the measured one at 470 MHz.

As mentioned before, gain, gain flatness and matching of designed front-end are as desired. In figures below, attenuations of produced dual band front-end are compared with simulated dual band front-end and traditional single band front-ends.

Simulation and test results of dual band front-end fit mostly each other. Usually there is an

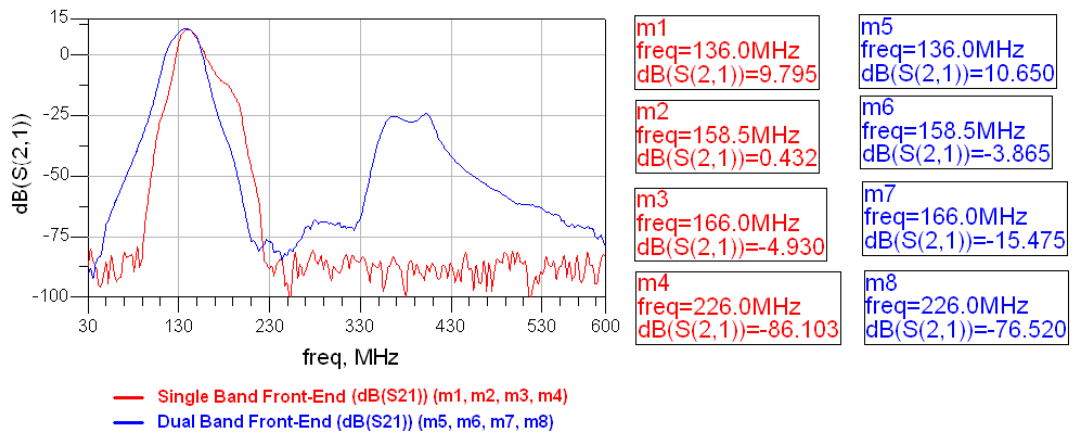


Figure 4.49: Responses of Single Band and Dual Band Front-ends at 136 MHz

incompatibility between attenuations at image frequencies. However, in practice it would be utopic to expect nearly 130 dB attenuation at image frequency. Attenuations at image frequencies seem to be enough. The aim is better than 75 dB attenuation at image frequency. The worst case occurs at 470 MHz as 79.6 dB. At other frequencies, image rejection is better than 80 dB. Also, attenuation levels at 1/2 IF and 1/3 IF spurious frequencies are close to each other for simulation and test results. It is enough to attenuate 1/2 IF spurious signal and 1/3 IF spurious signal for 6 dB and 12 dB respectively. These values base on the responses of single band front-ends. For the whole band, attenuation at 1/2 IF spurious frequency is more than 7 dB and attenuation at 1/3 IF spurious frequency is more than 12.6 dB. Hence, it can be concluded that the dual band front-end blocks the spurious signals enough.

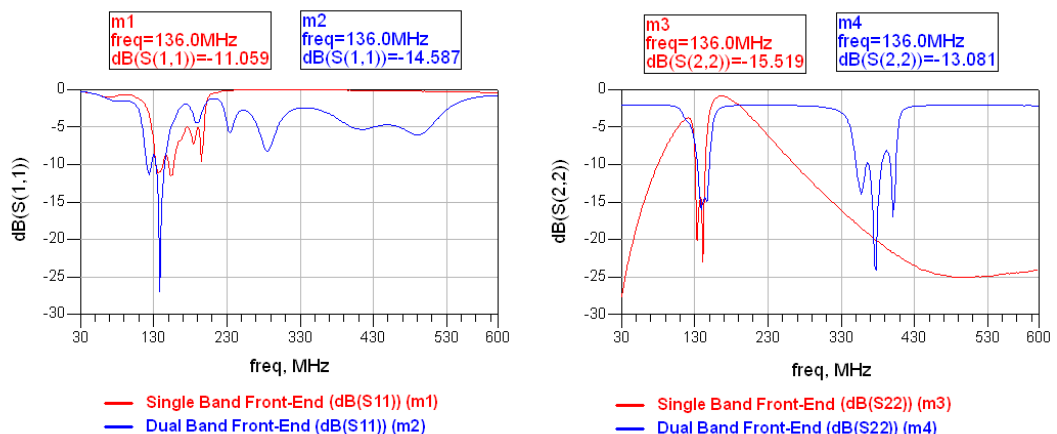


Figure 4.50: Responses of Single Band and Dual Band Front-ends at 136 MHz

Note that all the circuits on fabricated PCB are at the same side and there is no precaution for coupling between them. The performance of implemented front-end can be improved by separating circuits from each other so that couplings are minimized. For this purpose, metal walls can be placed between each circuit. Another method is to place some of the circuits to the backside of PCB and place a ground layer to prevent coupling. However, since these responses were acceptable for us, PCB was not re-designed.

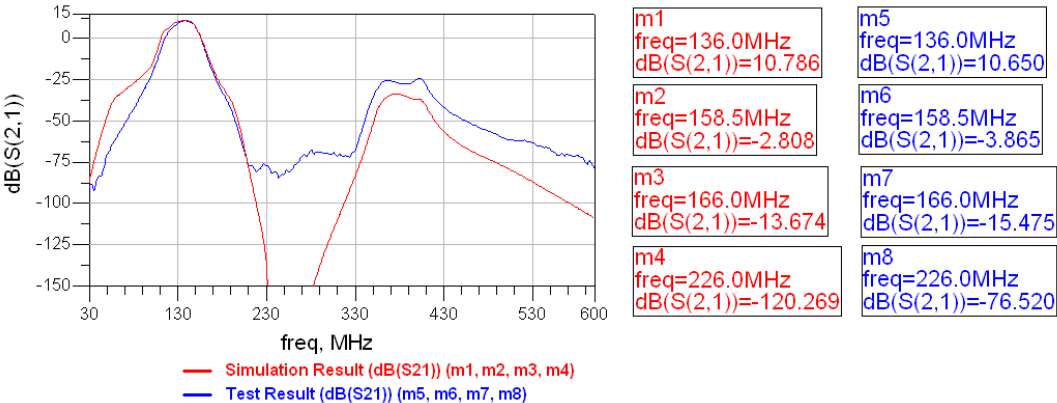


Figure 4.51: Comparison of Simulation and Test Results of Front-ends at 136 MHz

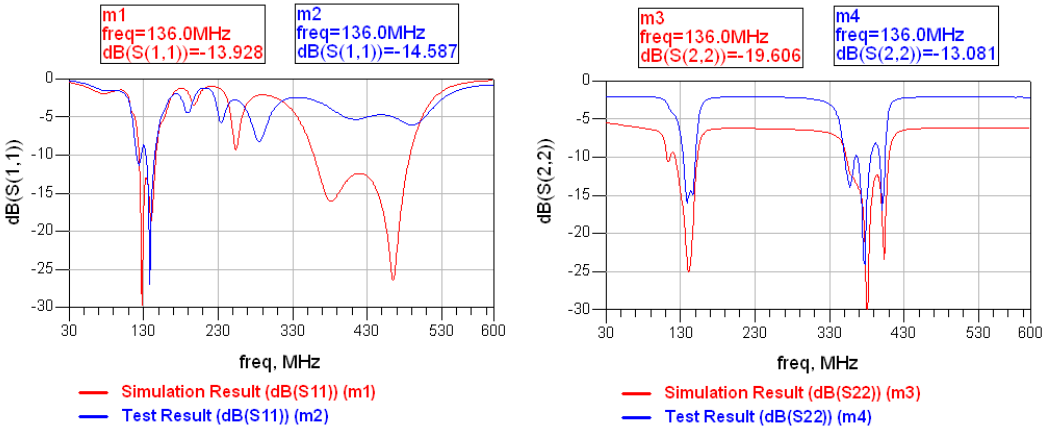


Figure 4.52: Comparison of Simulation and Test Results of Front-ends at 136 MHz

4.7.5 Performance of the Receiver System With Dual Band Front-end

After testing the implemented dual band front-end, we connected output of it to RF input of the mixer in the receiver system by using a coaxial cable. As a result, the performance of the receiver was obtained as given in Table 4.5.

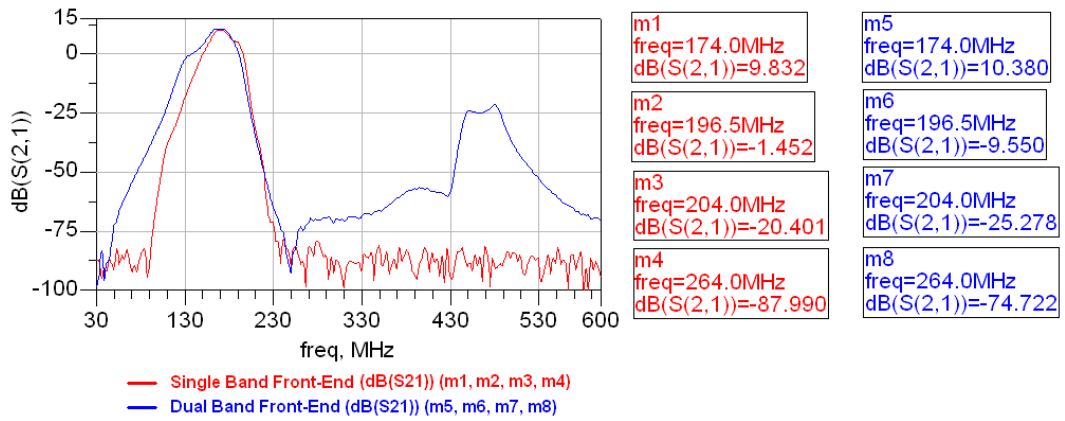


Figure 4.53: Responses of Single Band and Dual Band Front-ends at 174 MHz

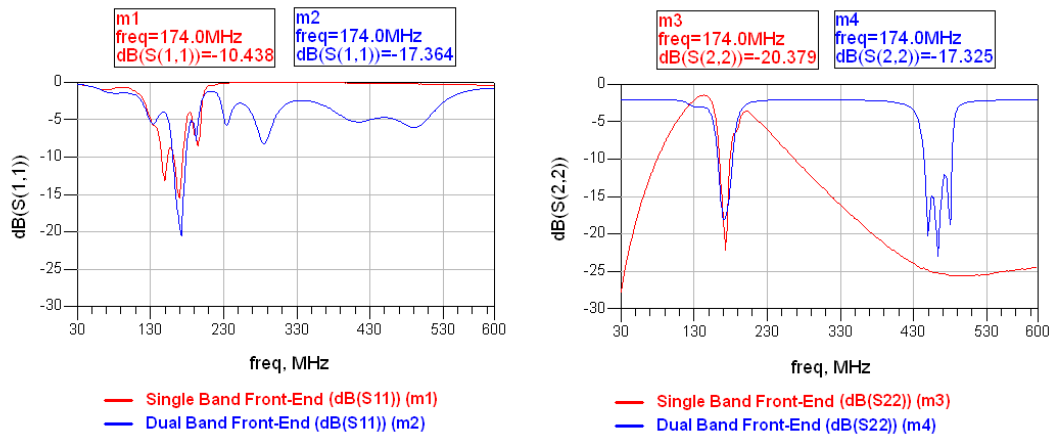


Figure 4.54: Responses of Single Band and Dual Band Front-ends at 174 MHz

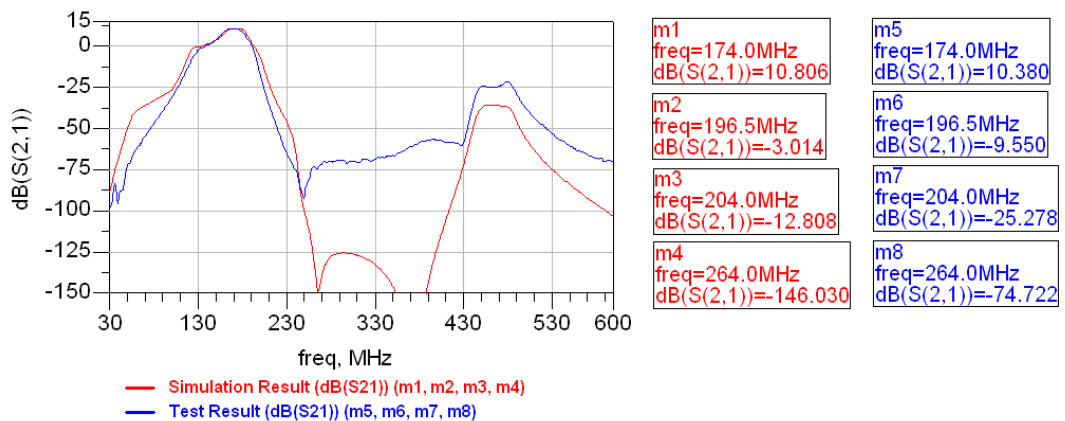


Figure 4.55: Comparison of Simulation and Test Results of Front-ends at 174 MHz

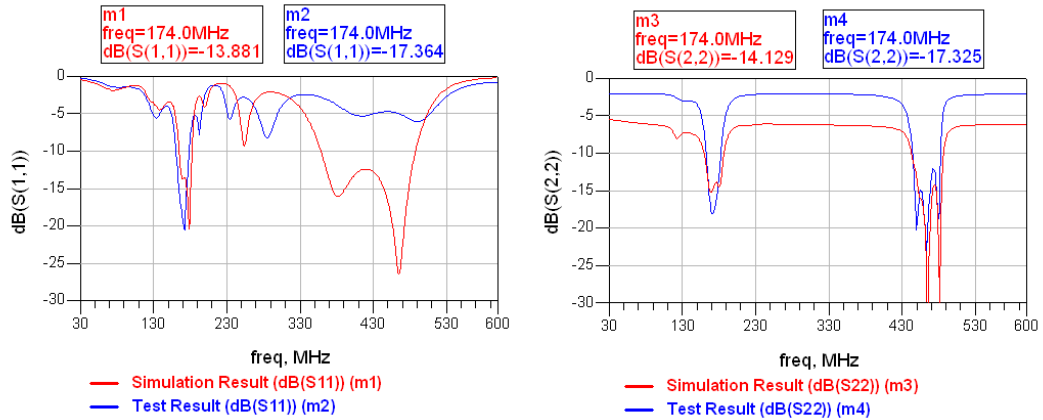


Figure 4.56: Comparison of Simulation and Test Results of Front-ends at 174 MHz

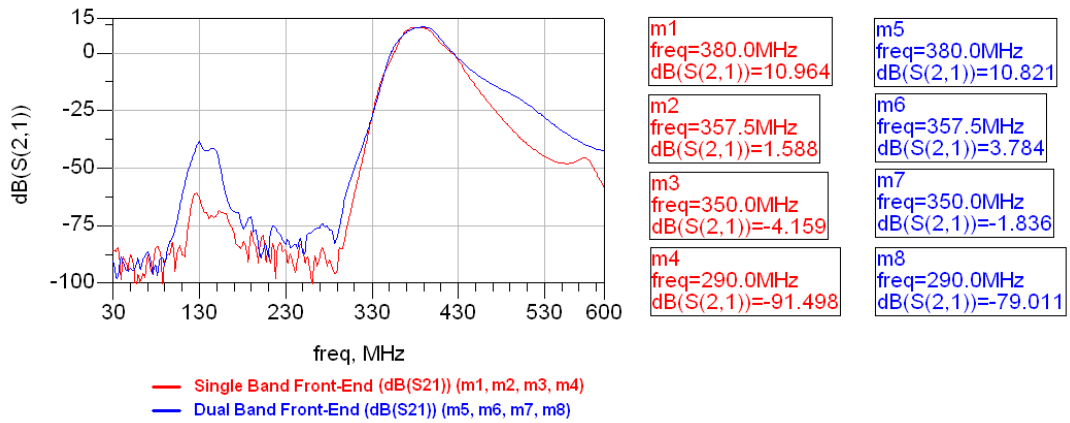


Figure 4.57: Responses of Single Band and Dual Band Front-ends at 380 MHz

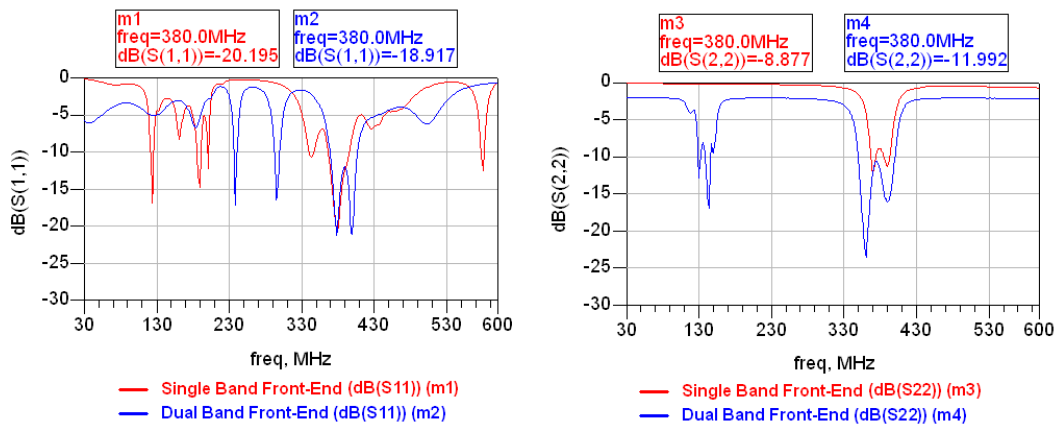


Figure 4.58: Responses of Single Band and Dual Band Front-ends at 380 MHz

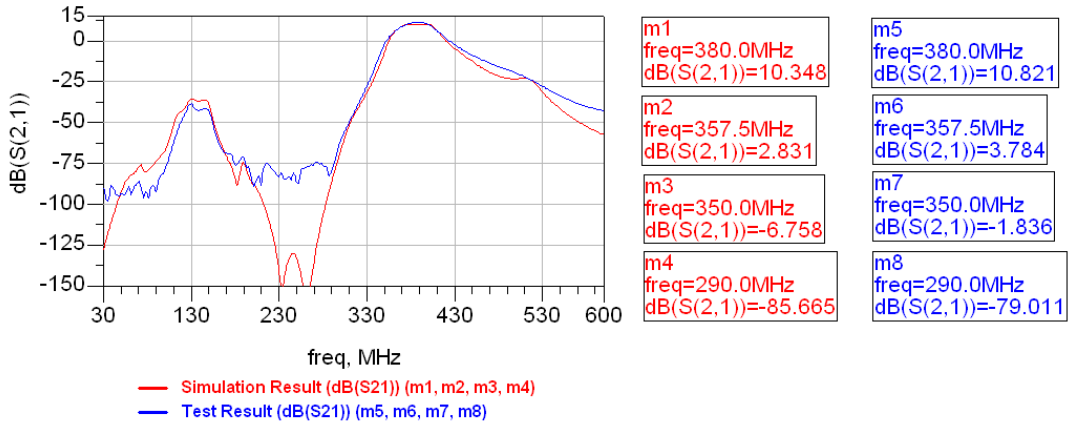


Figure 4.59: Comparison of Simulation and Test Results of Front-ends at 380 MHz

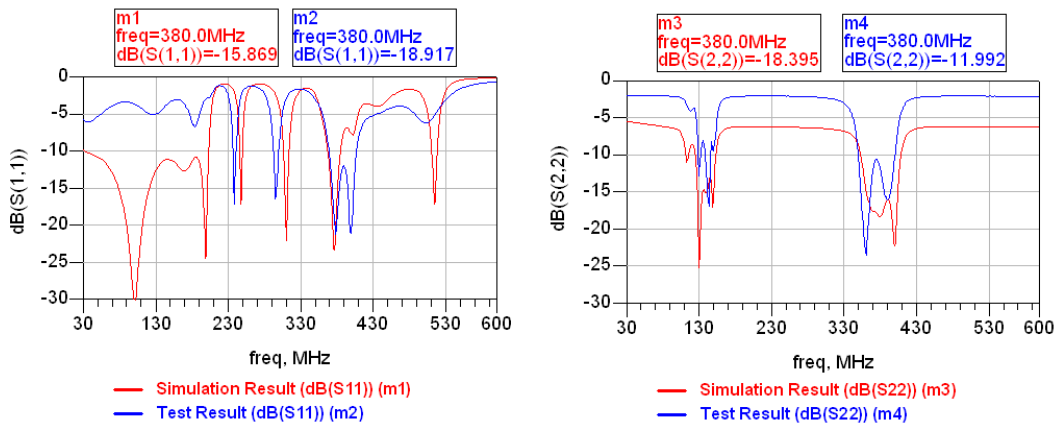


Figure 4.60: Comparison of Simulation and Test Results of Front-ends at 380 MHz

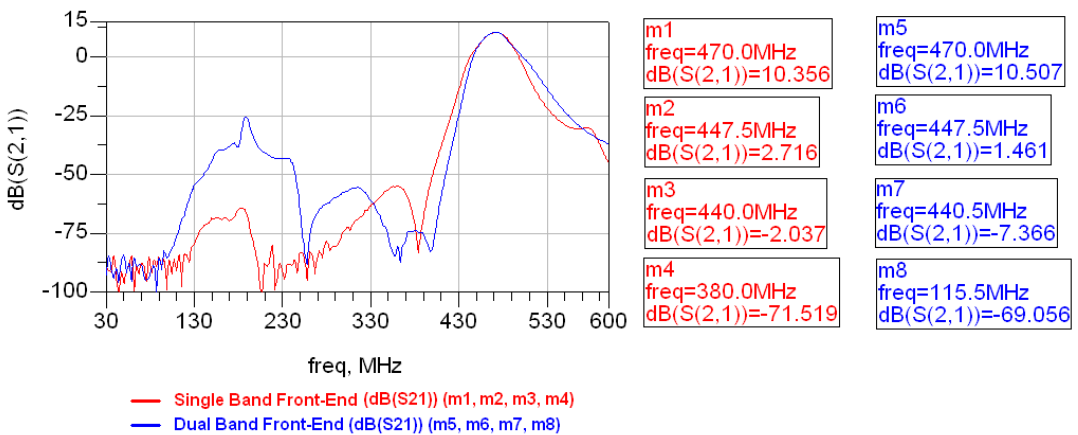


Figure 4.61: Responses of Single Band and Dual Band Front-ends at 470 MHz

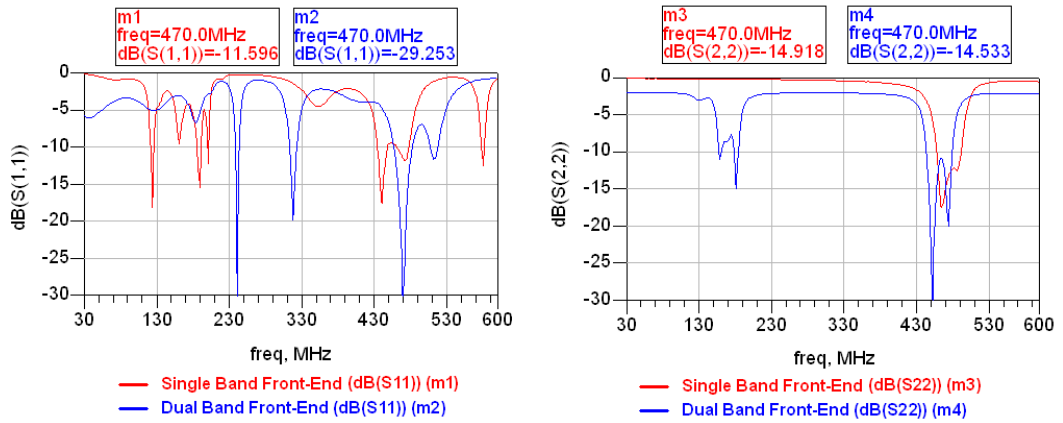


Figure 4.62: Responses of Single Band and Dual Band Front-ends at 470 MHz



Figure 4.63: Comparison of Simulation and Test Results of Front-ends at 470 MHz

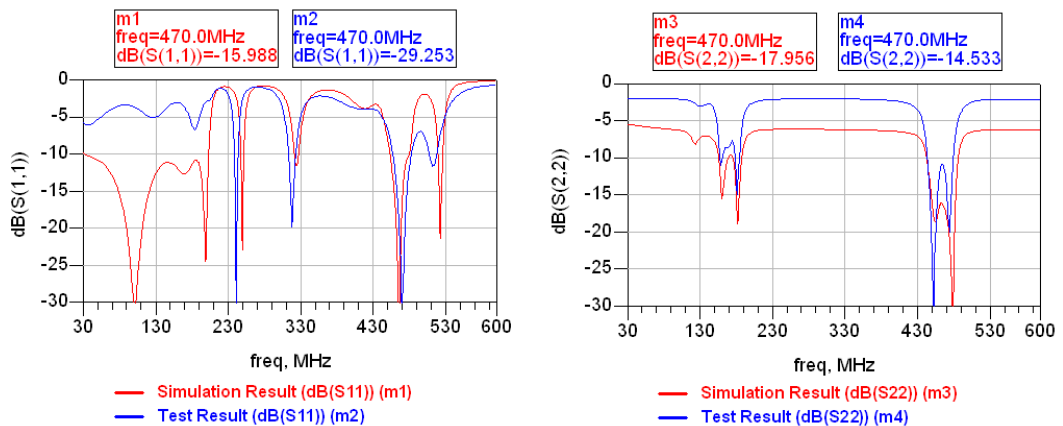


Figure 4.64: Comparison of Simulation and Test Results of Front-ends at 470 MHz

Table 4.5: Performance of Receiver System With Dual Band Front-end

Frequency (MHz)	136	174	380	470	Specification
Sensitivity (dBm)	-119.0	-119.5	-118.5	-119.0	-118.0
IMD (dB)	75	76	73	73	73
1/2 IF Rej. (dB)	94	101	81	82	70
1/3 IF Rej. (dB)	98	101	97	93	70
Image Rej. (dB)	91	73	70	71	70

Sensitivity of the receiver is better than -118 dB. IMD is at the limit but it is still acceptable. IMD is probably limited by the IF circuits since the input signal is amplified further in IF stages. Spurious rejections at 1/2 IF and 1/3 IF frequencies are very good while image rejection is close to the limit value. This may happen due to the coupling between circuits. Note that while measuring this performance, front-end circuits were not in the same PCB with the rest of receiver. If the dual band front-end and rest of receiver are implemented in the same PCB and metal walls are placed between each circuit, image rejection performance may improve. To conclude, receiver system satisfies the specified performance with implemented dual band front-end.

CHAPTER 5

DESIGN OF A TRIPLE BAND TUNABLE FILTER AND A WIDE-BAND LNA

Until now, a dual band front-end has been designed, implemented and tested. The primary object of this thesis is accomplished successfully. Now, it is time to take another step forward. As the future work, we can try to design a triple band tunable front-end. For this purpose, a triple band tunable filter and a low noise amplifier that covers three bands will be needed. Also, there will be three harmonic filters for each band. According to the performances of harmonic filters there may be a need for notch filters in order to suppress the unwanted passbands of triple band filter. Primary object of harmonic filters is to suppress harmonic components that occur at the output of power amplifier in transmitter mode. Design of harmonic filter should be done by taking power amplifier into account. Hence in this chapter only design of triple band filters and wide-band LNA are considered.

5.1 Design Constraints

Assume that a new band is added to the previously designed dual band filter. This additional band will cover the band of frequencies between 700 MHz and 800 MHz. IF frequency will again be 45 MHz, so LO will be 45 MHz lower than the desired RF signal (Table 5.1). Hence, most important spurious signals will be lower than selected channel frequency which yields in need for a notch between second passband and third passband of the triple band filter.

Block diagram of the triple band front-end is shown in Figure 5.1.

Table 5.1: Basic Properties of Triple Band Receiver System

	VHF Receiver	UHF-1 Receiver	UHF-2 Receiver
RF Input Frequency Range (MHz)	136-174	380-470	700-800
LO Frequency Range (MHz)	181-219	335-425	655-755
IF Frequency (MHz)	45	45	45

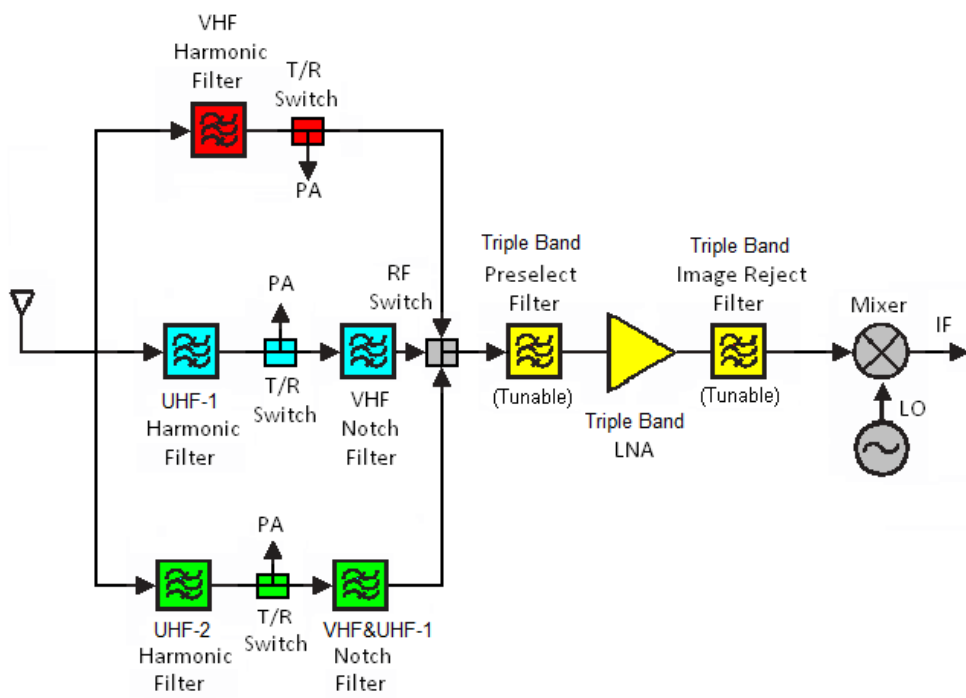


Figure 5.1: Block Diagram of Triple Band Front-end

5.2 Design of Triple Band Filter

Design procedure of triple band filter is same as the dual band one. Starting point is the single band filter shown in Figure 5.2.a. Center frequency of this filter is at 155 MHz. Then, a dual band filter is obtained by converting the second order L-C resonators to fourth order resonators so that its second passband occurs at 425 MHz (Figure 5.2.b). Then comes the step to obtain the triple band filter. Applying the same transformation to the parallel LC resonators again results in addition of another series LC resonator in shunt arm (Figure 5.2.c). This resonator creates a notch near 660 MHz and a passband at 750 MHz. S_{21} response of this filter is given in Figure 5.3.

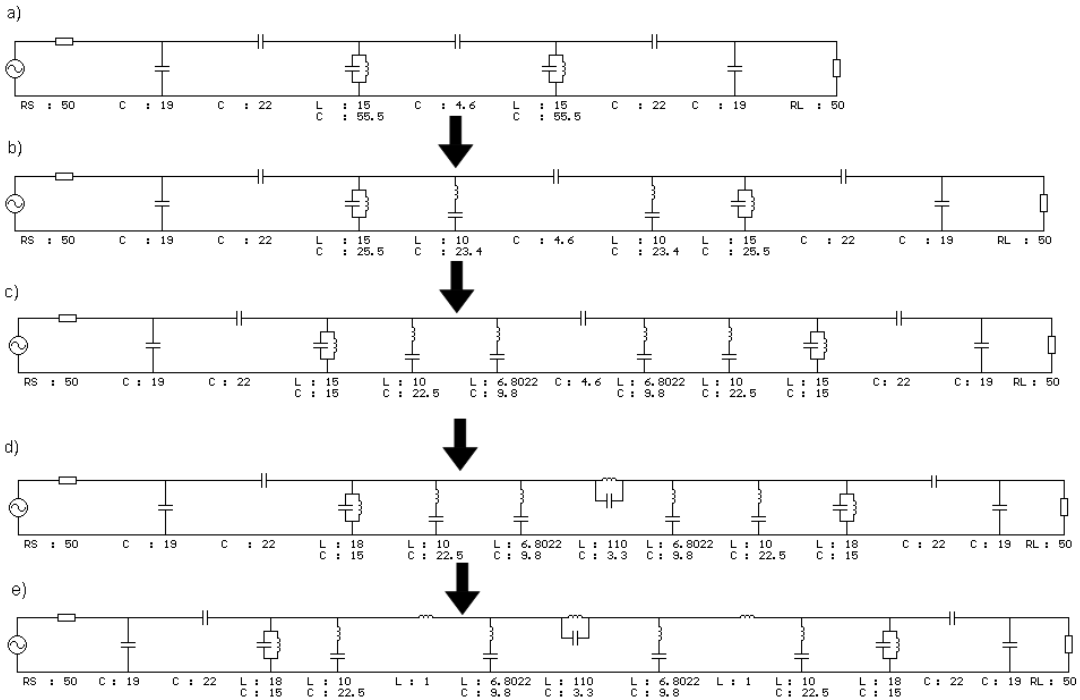


Figure 5.2: Design of Triple Band Filter in Filpro

Optimization of this triple band filter is done by inspection. Response of the circuit in Figure 5.2.c has too much ripple in the third passband. Besides, note that there is only one notch between first and second passbands. In order to attenuate image signals of VHF and UHF signals, we need two notches between first two passbands. Hence the coupling capacitor is replaced by a parallel LC resonator which creates an additional notch to track image signal of VHF band (Figure 5.2.d). Also adding two 1nH coupling inductors between notch resonators decreases the ripple in the third passband. As a result, the triple band filter shown in Figure

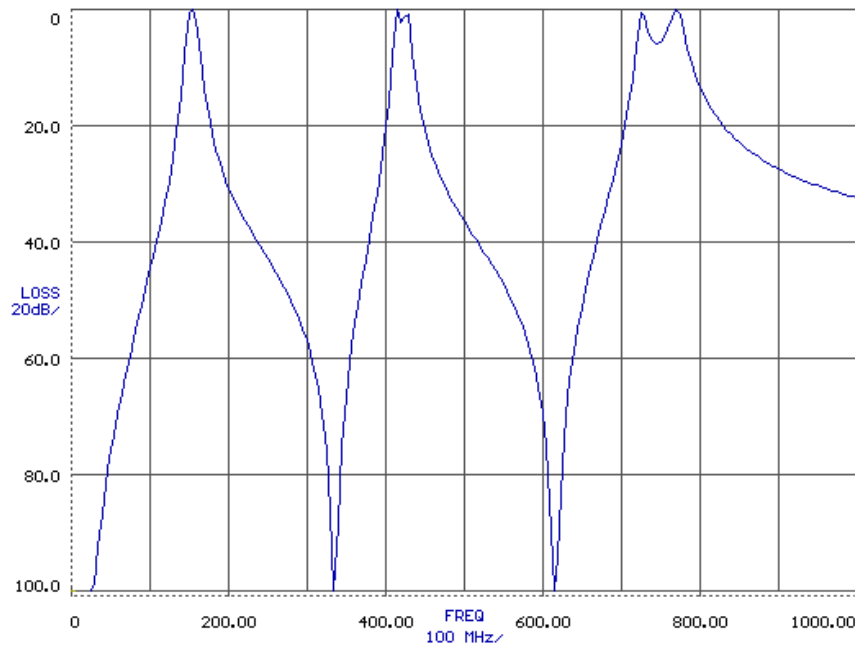


Figure 5.3: Response of Triple Band Filter in Figure 5.2.c

5.2.e is obtained. Its response is given in Figure 5.4.

Finally, element values needed to tune this front-end filter to low-end and high-end of each band are found as given in Figure 5.5. Note that, in order to tune the filter, it is required to tune 9 capacitors. Tuning these capacitors will be performed using varactor diodes. Then, this filter is optimized and simulated in ADS using varactor diodes. During the optimization process, it is seen that tuning all of the matching capacitors yields better response. Matching capacitances in shunt arm need to be changed from 5 pF to 35 pF as tuning voltage changes from 1 V to 4 V. Similarly, matching capacitances in series arm need to be changed from 4 pF to 22 pF for 1 V and 4 V, respectively. Hence, those capacitors are also realized using varactors. Circuit diagram of this filter is given in Figure 5.6 and simulation result of it is given in Figure 5.7.

In the circuit diagram, it can be seen that varactor diodes at input and output of filter are biased from 5 V and V_{tune} . When reverse voltage applied to a varactor diode increases, capacitance of it decreases. As V_{tune} increases, capacitances at resonators need to decrease so that center frequencies can increase. On the other hand, capacitances at the input and output of filter tend to increase as V_{tune} increases. Therefore, 5 V is applied to cathode of these varactors and V_{tune} is applied to anode of them. When V_{tune} is 1 V, reverse voltage applied to these diodes

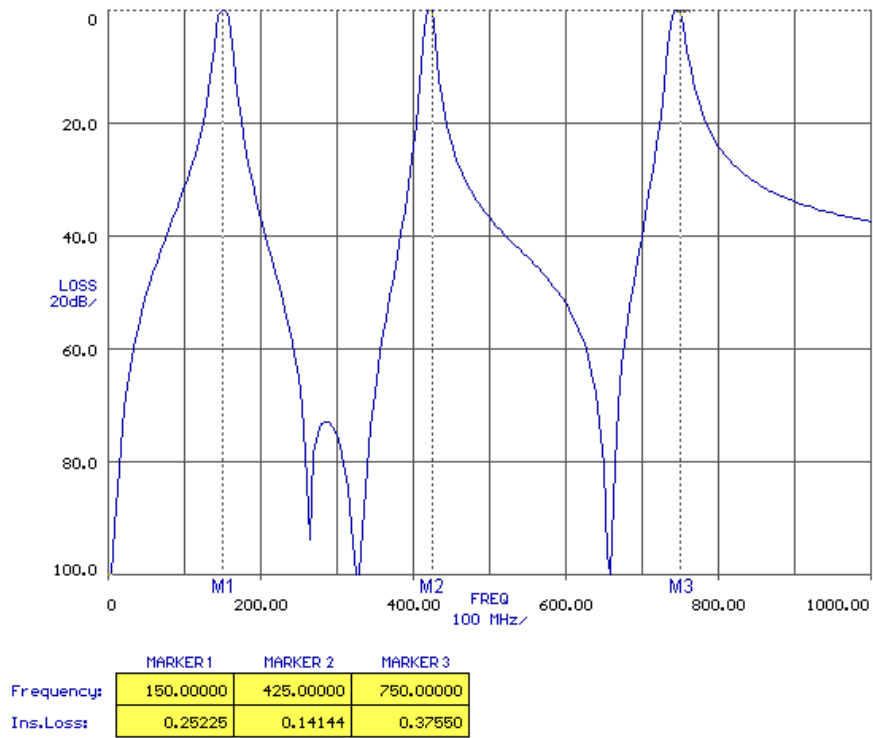


Figure 5.4: Response of Triple Band Filter in Figure 5.2.e

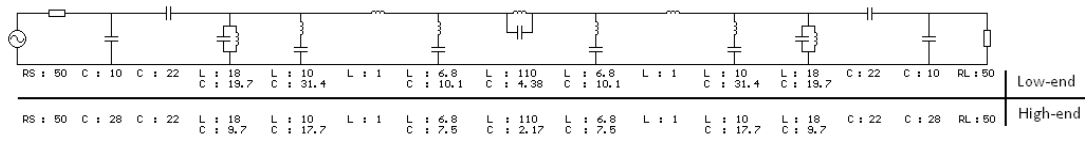


Figure 5.5: Element Values Required to Tune the Triple Band Filter to Low-ends and High-ends of the Bands

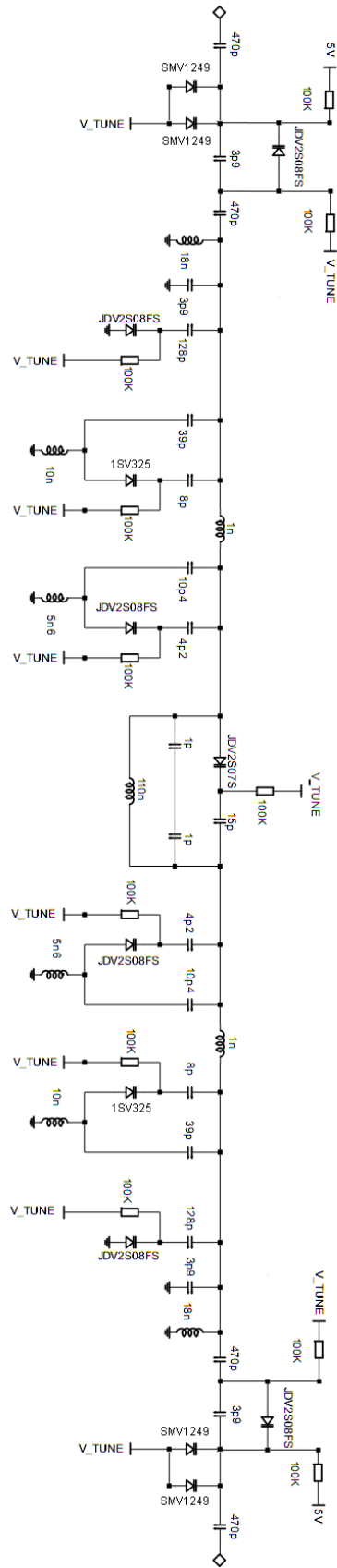


Figure 5.6: Circuit Diagram of the Triple Band Filter

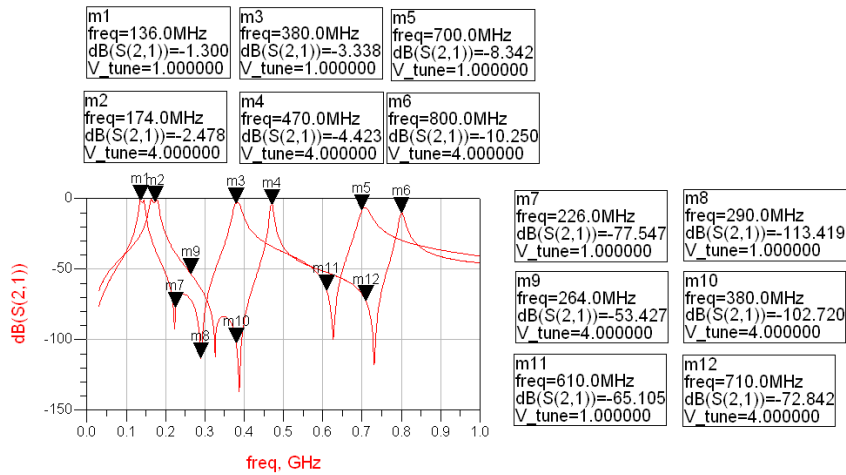


Figure 5.7: Simulation Result of the Triple Band Filter in ADS

becomes 4 V and vice versa.

Loss of filter at VHF band is lower than 2.5 dB. It increases up to 4.5 dB at UHF-1 band. Since there are seven resonators and 13 varactor diodes in the filter, this much of loss is expected. However, this prevents it to be used as pre-select filter since it causes an increase in noise figure of receiver. At UHF-2 loss dramatically increases up to 10 dB. This is unacceptable and should be decreased. Attenuations at image signals are higher than 50 dB for whole bands. This filter can be used in the triple band front-end if its loss at UHF-2 band is decreased below 5 dB.

5.3 Design of LNA

For the dual band front-end, a LNA working between 136 MHz and 470 MHz was designed using BFR340F. This LNA is re-optimized so that its band is extended to 800 MHz. Simulated LNA and its response are illustrated in Figure 5.8 and Figure 5.9, respectively.

Its noise figure is lower than 2.5 dB. S_{11} and S_{22} are better than 10 dB for the whole band. Gain changes between 14.2 dB and 15.3 dB. Assuming that the total loss of other circuits does not change with respect to frequency, this LNA can be used in the triple band filter. However, loss of triple band filter increase as the frequency increases. Therefore, it may be required to optimize this LNA so that its gain increases as frequency increases.

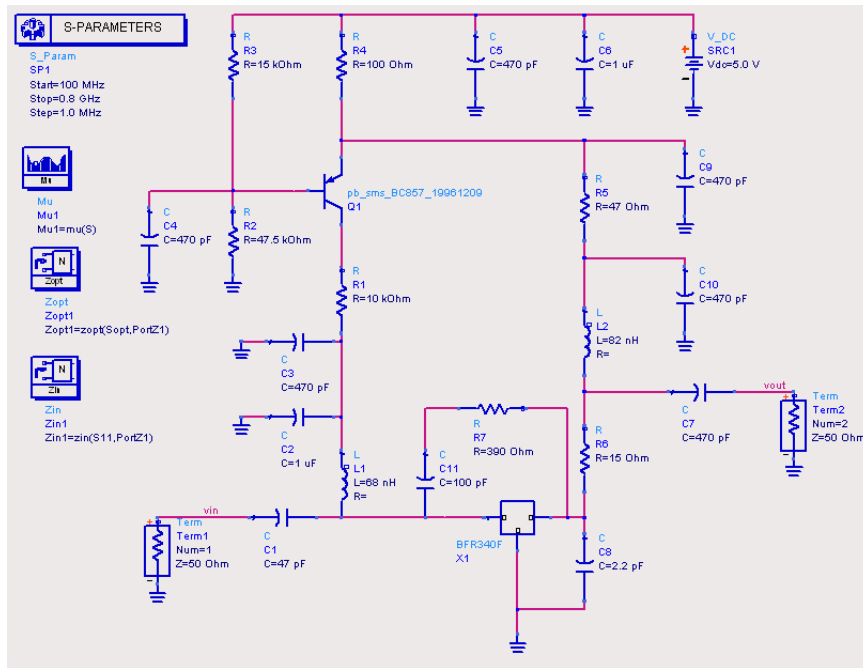


Figure 5.8: Circuit Diagram of the Triple Band LNA

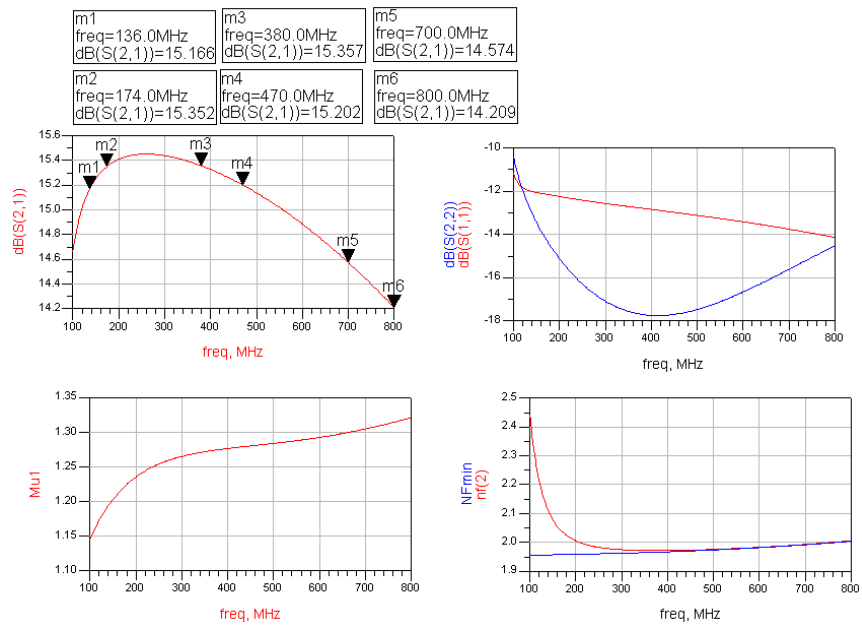


Figure 5.9: Simulation Result of the Triple Band LNA in ADS

This project has not been finished yet. The procedure explained in Chapter 6 should be performed in order to implement the triple band front-end.

CHAPTER 6

CONCLUSION AND THE FUTURE WORK

In this thesis, a tunable dual band front-end which can be used in a V/UHF mobile wireless transceiver system has been designed and implemented successfully. The key feature of this work was the usage of dual band tunable filters. Besides dual-band filter, a wide-band low noise amplifier and a notch filter was designed and implemented to form the front-end. The predefined goals were determined according to the responses of existing single band tunable front-ends. The aim was to design and implement a dual-band front-end that has the same performance as the single band front-ends.

In the design of dual band filter, filter design program FILPRO is used. The resulting circuits are transferred to ADS in order to simulate whole front-end. Simulation and test results fit each other.

The most important characteristics of a front-end are its gain, gain flatness, noise figure, linearity and suppression of spurious signals. Number of elements used and current drawn from supply are also taken into consideration. The gain of the implemented front-end is changing between 10.38 dB and 10.82 dB throughout the whole band. Total noise figure is lower than 6.44 dB. Attenuation levels at spurious frequencies are enough. The only current dissipating component is LNA. Exactly like the single band amplifiers, the LNA of dual-band front-end draws 6 mA current from a 5 V power supply. Number of elements used in dual band front-end is 136 while the total number of elements in single band front-ends is 155.

In summary, the objective was accomplished and it was proved that it is possible to combine two single band front-ends in a dual band front-end containing dual band filters without any significant degradation in the performance.

6.1 Future Works

Future work includes the design of tunable front-ends that cover more than two bands. A triple band front-end can be designed using triple band filters and a wider band LNA. A study that can be an introduction to this future project is explained in Chapter 5. If the procedure described below is followed, a triple band front-end can be obtained:

- Designed triple band filter and LNA should be simulated including affects of realistic models of inductors and layout. In this step, further optimizations may be needed.
- A Harmonic filter should be designed and simulated for UHF-2 band. If attenuation of this filter at VHF and UHF-1 bands becomes low, a notch filter should be placed at the output of it to block those bands when UHF-2 band is selected.
- Whole front-end should be simulated.
- The triple band front-end should be fabricated.
- Optimizations should be done for each circuit until their response fit the simulation results.
- Response of triple band front-end should be observed. It should be compared to the single band front-ends and simulation results.

Similarly a front-end that covers four bands can be designed by using a four-band filter or two dual-band filters. For these works, IF frequencies different than 45 MHz can be selected.

REFERENCES

- [1] J. Laskar, B. Matinpour, S. Chakraborty, *Modern Receiver Front-Ends, Systems, Circuits, and Integration*, Wiley, New Jersey, 2004.
- [2] L. De Xing, S. Shafie, I. A. Halin, S. S. Januar, "Design of Front End of a RF Receiver," *Proceedings of 2009 IEEE Student Conference on Research and Development (SCOReD2009)*, pp. 533-536, Nov. 2009.
- [3] C.-L. Hsiao, Y.-L. Huang, "A Low Supply Voltage Dualband Low Noise Amplifier Design," *IEEE International Symposium on Consumer Electronics*, pp. 339-341, 2009.
- [4] Y. Lu, Q. Tang, W. Li, H. Qi, "Design of a 1GHz 4GHz Ultra-Wide Band Low Noise Amplifier," *IEEE*, 2010.
- [5] B. Razavi, *RF Microelectronics*, Prentice Hall, New Jersey, 1998.
- [6] A. Jajoo, *A Wide-band Low Noise Amplifier Synthesis Methodology*, Master of Science Thesis, Department of Electrical and Computer Engineering, Carnegie Mellon University, Aug. 2005.
- [7] J. J. Carr, *The Technicians's Radio Receiver Handbook*, Butterworth-Heinemann, Woburn, 2001.
- [8] W. A. Davis, K. K. Agarwal, *Radio Frequency Circuit Design*, Wiley, New York, 2001.
- [9] I. C. Hunter and J. D. Rhodes, "Electronically tunable microwave bandpass filters," *IEEE Trans. Microwave Theory Tech.*, vol. 30, no. 9, pp. 1354-1360, Sep. 1982.
- [10] N. Tanzi, "Varactor-Tuned Coupled Resonator Front-End Bandpass Filters for Cognitive Radio Applications," *IEEE*, pp. 155-158, 2006.
- [11] M. A. A. Latip, M. K. M. Salleh, N. Ab Wahab, "Tuning Circuit Based on Varactor for Tunable Filter," *2011 IEEE International RF and Microwave Conference*, pp. 26-28, Dec. 2011.
- [12] A. Tombak, J.-P. Maria, F. T. Ayguavives, Z. Jin, G. T. Stauff, A. I. Kingon, A. Mortazawi, "Voltage-controlled RF filters employing thin-film barium-strontium-titanate tunable capacitors," *IEEE Trans. Microwave Theory Tech.*, vol. 51, no. 2, pp. 462-467, Feb. 2003.
- [13] J. Nath, D. Ghosh, J-P Maria, A. I. Kingon, W. Fathelbab, P. D. Franzon and M. B. Steer, "An Electronically Tunable Microstrip Banpass Filter Using Thin-Film Barium-Strontium-Titanate (BST) Varactors," *IEEE Transactions on Microwave Theory Tech.*, vol. 53, no. 9, pp. 2707-2711, Sept. 2005.
- [14] B. E. Carey-Smith, P. A. Warr, "Distortion Mechanisms in Varactor Diode-Tuned Microwave Filters," *IEEE Transactions on Microwave Theory Tech.*, vol. 54, no. 9, pp. 3492-3499, Sept. 2006.

- [15] G. Sanderson, A. H. Cardona, T. C. Watson, D. Chase, M. Roy, J. N. Paricka, R. A. York, "Tunable IF Filter Using Thin-Film BST Varactors," *IEEE*, pp. 679-682, 2007.
- [16] N. Yıldırım, "Narrowband tunable bandpass and bandstop filters," EE-509 Lecture Notes, METU.
- [17] Y.-X. Guo, L.C. Ong, M. Y. W. Chia and B. Luo., "Dual-Band Bandpass Filter in LTCC," *IEEE MTT-S Int. Microw. Symp. Dig.*, pp. 2219-2222, Jun. 2005.
- [18] H. Joshi, W. J. Chappell, "Dual-Band Lumped-Element Bandpass Filter," *IEEE Transactions on Microwave Theory and Tech.*, vol. 54, no. 12, pp. 4169-4177, Dec. 2006.
- [19] Z. Ma, T. Shimizu, Y. Kobayashi, T. Anada and G. Hagiwara, "Novel Compact Dual-Band Bandpass Filters Using Composite Resonators to Obtain Separately Controllable Passbands," *IEEE Proceedings of Asia-Pacific Microwave Conference*, 2006.
- [20] C.-C. Chen, "Dual-Band Bandpass Filter Using Coupled Resonator Pairs," *IEEE Microwave and Wireless Components Letters*, vol. 15, no. 4, pp. 259-261, Apr. 2005.
- [21] G. Macchiarella, S. Tamiazzo, "A Design Technique for Symmetric Dual Band Filters," *IEEE*, pp. 115-118, 2005.
- [22] N. Yıldırım, *Chapter-16: Dual band filters*, EE-509 Lecture Notes, METU, Available at: <<http://www.eee.metu.edu.tr/nyil/manual/Ch16A-v42-DualBandFilts.zip>> Nov. 2006, [Accessed 08 June 2012].
- [23] Toshiba Corp., *TOSHIBA Diode Silicon Epitaxial Planar Type 1SV325*, Available at: <<http://www.semicon.toshiba.co.jp/openb2b/websearch/productDetails.jsp?partKey=1SV325>> Mar. 2003, [Accessed 08 June 2012].
- [24] Toshiba Corp., *1SV325 Spice Parameter*, Available at: <http://www.semicon.toshiba.co.jp/eng/product/rf/simulation/spice_pdf/1SV325_SP_01.pdf> [Accessed 08 June 2012].
- [25] Toshiba Corp., *TOSHIBA Diode Silicon Epitaxial Planar Type JDV2S25FS*, Available at: <<http://www.semicon.toshiba.co.jp/openb2b/websearch/productDetails.jsp?partKey=JDV2S25FS>> Nov. 2007, [Accessed 08 June 2012].
- [26] Toshiba Corp., *Spice Parameter JDV2S25FS*, Available at: <http://www.semicon.toshiba.co.jp/download/rf_spara/JDV2S25FS_SP_001.txt> [Accessed 08 June 2012].
- [27] L. Wu, M. Yu, "A Wideband Low-Noise-Amplifier With Compact Size and Improved Bandwidth," *IEEE ICMMT 2011 Proceedings*, pp. 653-655, 2010.
- [28] I. Rosu, *LNA Design*, Available at: <<http://www.qsl.net/va3iul/LNA%20design.pdf>> [Accessed 08 June 2012].
- [29] RF Micro Devices, *SGL0363Z 5 MHz to 2000 MHz Low Noise Amplifier Silicon Germanium*, Available at: <<http://www.rfmd.com/CS/Documents/SGL0363ZDS.pdf>> 2006, [Accessed 08 June 2012].
- [30] Toshiba Corp., *TOSHIBA Diode Silicon Epitaxial Planar Type JDV2S07S*, Available at: <http://www.toshiba.com/taec/components2/Datasheet_Sync//273/1413.pdf> Jan. 2002, [Accessed 08 June 2012].

- [31] Toshiba Corp., *JDV2S07S Spice Parameter*, Available at: <http://www.semicon.toshiba.co.jp/eng/product/ef/simulation/spice_pdf/JDV2S07S_SP_01.pdf> [Accessed 08 June 2012].
- [32] Toshiba Corp., *TOSHIBA Diode Silicon Epitaxial Planar Type JDV2S08FS*, Available at: <<http://www.semicon.toshiba.co.jp/openb2b/websearch/productDetails.jsp?partKey=JDV2S08FS>> Nov. 2007, [Accessed 08 June 2012].
- [33] Toshiba Corp., *Spice Parameter JDV2S08FS*, Available at: <http://www.semicon.toshiba.co.jp/download/ef_spara/JDV2S08FS_SP_001.txt> [Accessed 08 June 2012].
- [34] Infineon Technologies AG, *NPN Silicon RF Transistor BFR340F*, Available at: <<http://www.infineon.com/dgdl/bfr340f.pdf?folderId=db3a30431400ef68011425b1354605c1&fileId=db3a30431400ef68011426b5ce300676>> Jul. 2004, [Accessed 08 June 2012].
- [35] K. W. Whites, *Lecture 32: Highpass and Bandpass Microwave Filters. Resonant Stub Filters.*, EE-481 Lecture Notes, SDSMT, Available at: <<http://whites.sdsmt.edu/classes/ee481/notes/481Lecture32.pdf>> 2011, [Accessed 08 June 2012].

APPENDIX A

LOWPASS PROTOTYPE TO BANDPASS TRANSFORMATION

A prototype filter is an electronic filter which is normalized with respect to some design parameters such as cut-off frequency, termination impedance, etc. Usually a lowpass filter with a characteristic impedance $R_o=1$ Ohm and cut-off frequency $w_c=1$ Hz is used as a prototype filter. A lowpass prototype filter can be transformed to another lowpass, highpass, bandpass or bandstop filter by scaling element values of the prototype filter with respect to frequency and impedance [35]. In this section, conversion of a lowpass prototype filter to a bandpass filter will be discussed as illustrated in Figure A.1.

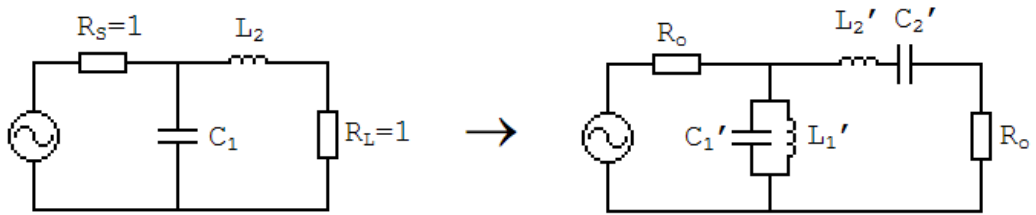


Figure A.1: Lowpass Prototype to Banpass Filter Transformation

In order to transform a lowpass prototype filter to a bandpass filter, by employing the following mapping function:

$$w' \Rightarrow \left(\frac{w_0}{B}\right)\left(\frac{w}{w_0} - \frac{w_0}{w}\right) \quad (\text{A.1})$$

where w_0 is the center frequency and B is the bandwidth of the resultant bandpass filter.

Since the prototype is a lowpass filter, it is composed of inductors in series arms and capacitors in shunt arms. When the mapping function is applied, the impedance of a series inductance

changes as follows:

$$Z_L = j\omega L_2 = j\left(\frac{\omega_0}{B}\right)\left(\frac{\omega}{\omega_0} - \frac{\omega_0}{\omega}\right)L_2 = j\omega\frac{L_2}{B} + \frac{1}{j\omega}\frac{\omega_0^2 L_2}{B} \quad (\text{A.2})$$

As it can be seen, the series inductor is converted into a series LC combination. Including the impedance transformation, values of resultant inductor and capacitor can be calculated using following equations:

$$L'_2 = \frac{L_2 R_o}{B} \quad (\text{A.3})$$

$$C'_2 = \frac{B}{\omega_0^2 L_2 R_o} \quad (\text{A.4})$$

Similarly, a capacitor in shunt arm is converted to a parallel LC combination as follows:

$$Y_C = j\omega C_1 = j\left(\frac{\omega_0}{B}\right)\left(\frac{\omega}{\omega_0} - \frac{\omega_0}{\omega}\right)C_1 = j\omega\frac{C_1}{B} + \frac{1}{j\omega}\frac{\omega_0^2 C_1}{B} \quad (\text{A.5})$$

As a result, a capacitor in the lowpass prototype are transformed to a parallel LC combination with elements

$$C'_1 = \frac{C_1}{B R_o} \quad (\text{A.6})$$

$$L'_1 = \frac{B R_o}{\omega_0^2 L_2} \quad (\text{A.7})$$

APPENDIX B

MODELS USED IN SIMULATIONS

B.1 Model of JDV2S25FS Varactor Diode

Spice parameters of JDV2S25FS is provided in its datasheet [25][26]. However, simulation results of this model did not fit the data obtained experimentally, so some parameters were changed slightly by inspection. The model used in simulations is given in Figure B.1.

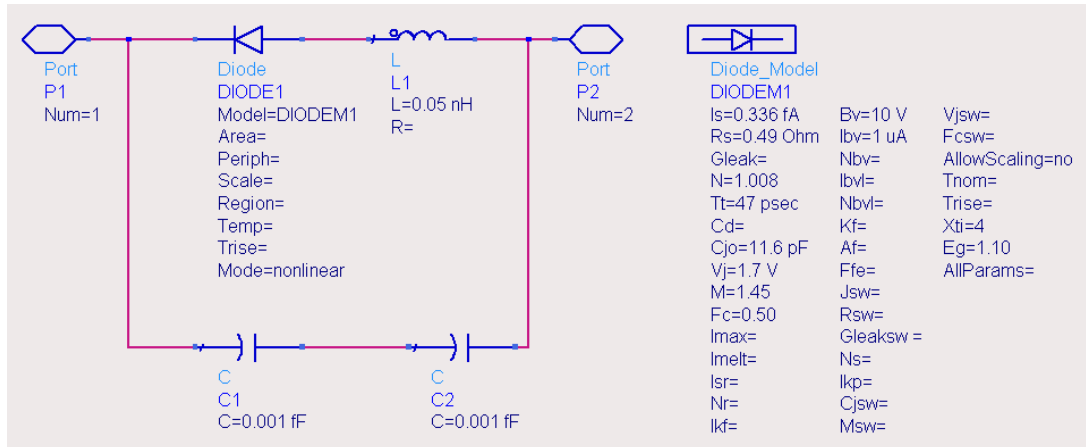


Figure B.1: Model of JDV2S25FS Used in ADS

B.2 Model of JDV2S08FS Varactor Diode

Spice parameters of JDV2S08FS is also provided by its manufacturer [32][33]. Only C_{jo} is changed slightly to fit the simulated and measured capacitance values. The model used is given in Figure B.2.

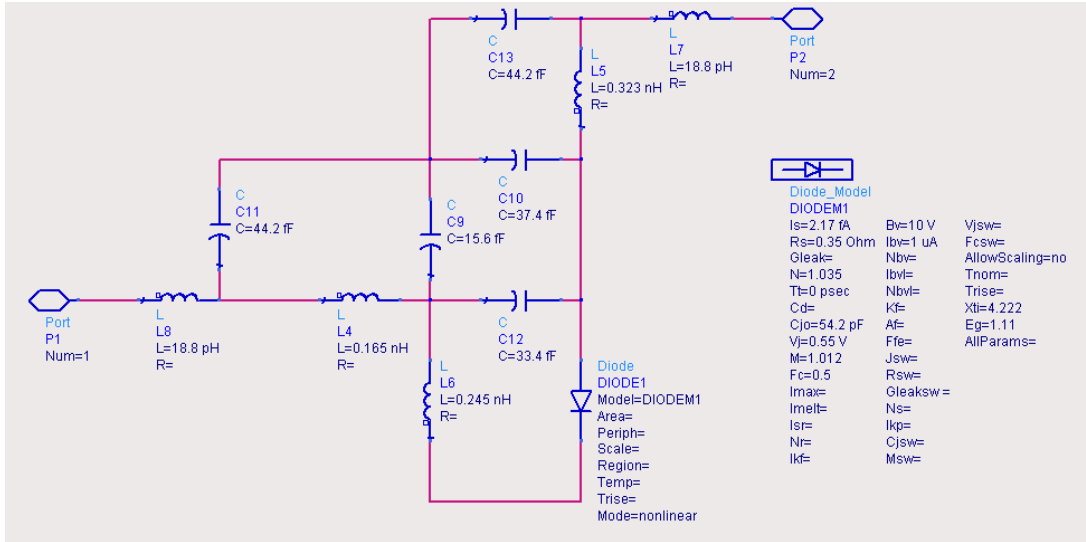


Figure B.2: Model of JDV2S08FS Used in ADS

B.3 Model of JDV2S07S Varactor Diode

Model shown in Figure B.3 is used for JDV2S07S. It is provided by its manufacturer [31] and fits the specifications given in its datasheet [30].

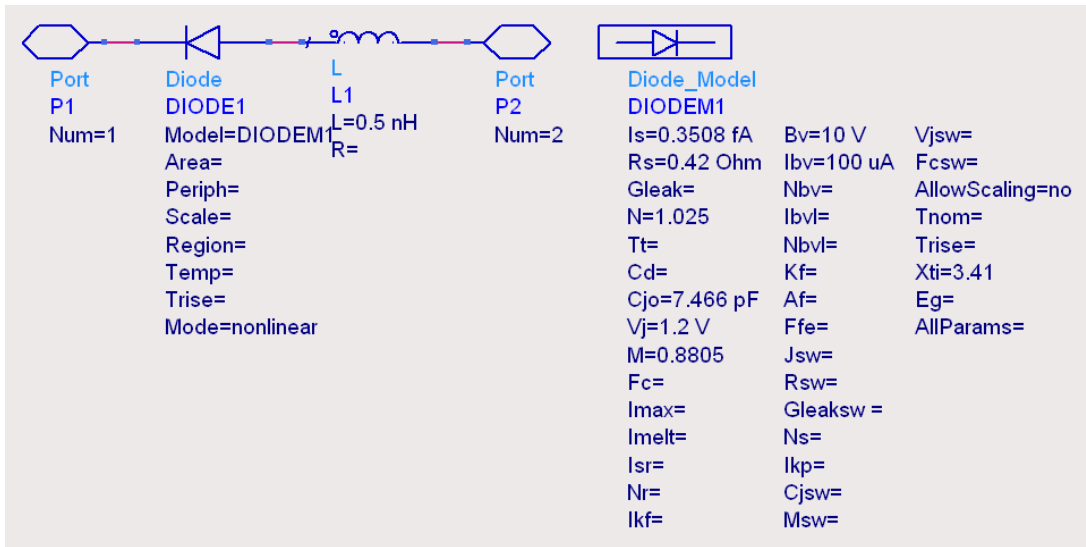


Figure B.3: Model of JDV2S07S Used in ADS

B.4 Model of 1SV325 Varactor Diode

Model of this diode is created using the spice parameters provided by its manufacturer [23][24] as shown in Figure B.4.

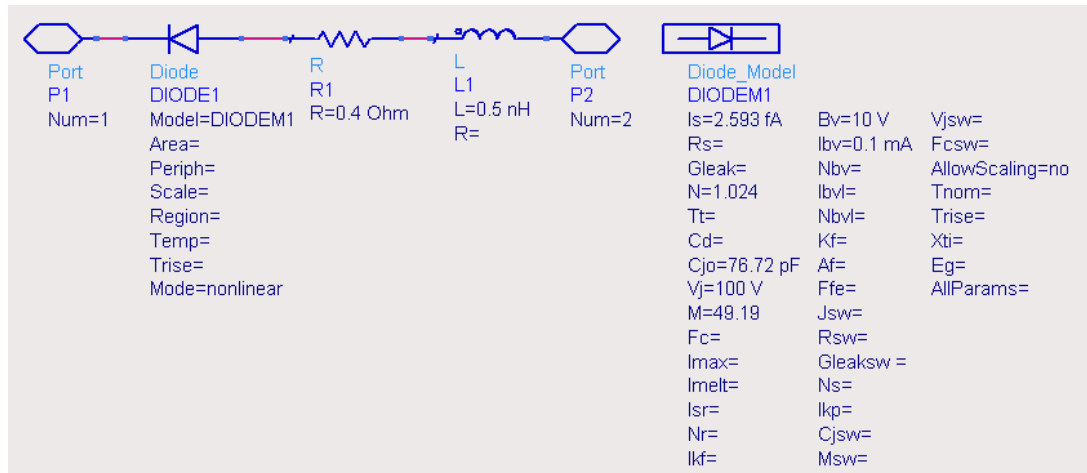


Figure B.4: Model of 1SV325 Used in ADS

B.5 Model of BFR340F Bipolar Junction Transistor

Manufacturer of BFR340F provides its prepared spice model for ADS [34]. The model is given in Figure B.5.

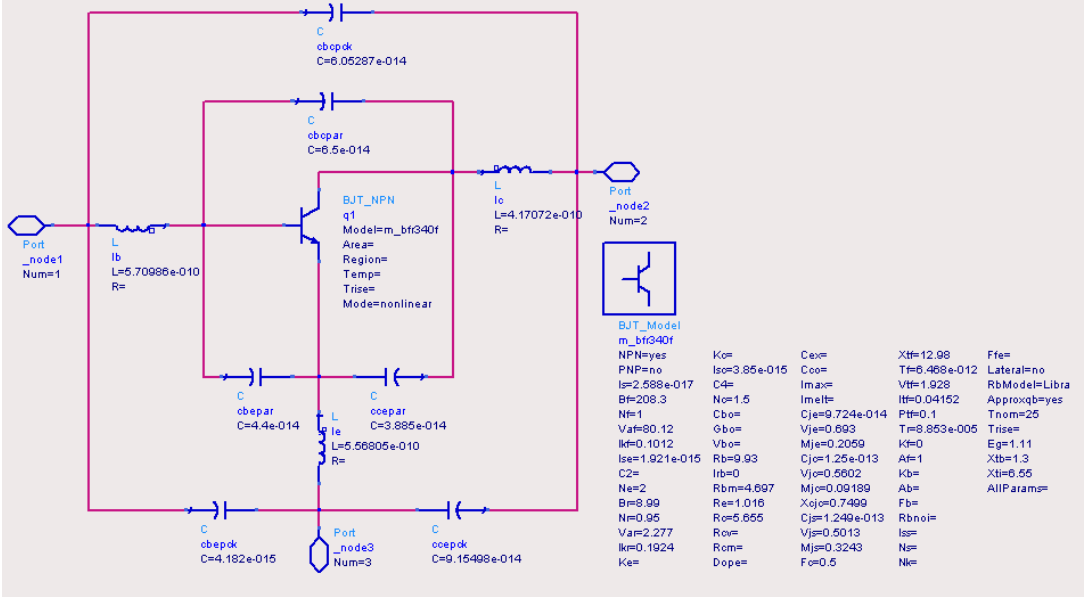


Figure B.5: Model of BFR340F Used in ADS